Title
Developmental expansion of the human neocortex

Permalink
https://escholarship.org/uc/item/81m389qv

Author
Lui, Jan Hsi

Publication Date
2011

Supplemental Material
https://escholarship.org/uc/item/81m389qv#supplemental

Peer reviewed|Thesis/dissertation

Developmental expansion of the human neocortex

by

Jan Hsi Lui

DISSERTATION

Submitted in partial satisfaction of the requirements for the degree of

DOCTOR OF PHILOSOPHY

in

Biomedical Sciences

in the

GRADUATE DIVISION

of the

UNIVERSITY OF CALIFORNIA, SAN FRANCISCO

© Copyright (2011)

by

Jan Hsi Lui

This dissertation is dedicated to Henry Tang, Jerry Hagler, Ravi Palanivelu, and Jochen Mattner,

who took the time to guide my interest in science at different stages of my life.

Acknowledgments

First and foremost, I have to thank my advisor Arnold Kriegstein for his extraordinary mentorship over the past four years. I came to Arnold's lab with no real background in neuroscience or developmental biology, and yet he took a risk in allowing me to join the lab and take on the projects that I was interested in. Over the years, I have learned to appreciate and even thrive on Arnold's mentorship style. Arnold respects the intellectual independence of his trainees above all else. While he ultimately allows you to be in charge of your own work, his door is always open for conversation, providing an overarching big picture vision that guides your independent development. Because of this attitude, I have had the opportunity to figure many things out for myself, and thank Arnold for his trust and patience in me to complete all the work that lead to this dissertation.

I also thank Arnold for being transparent about the inner workings of his own job of managing scientific research away from the bench. It is rare to learn so much about grant writing, funding agencies, the media, paper reviews, journal editors, and competitors at the stage of a graduate student. Although Arnold allows the science in his lab to develop in a free-form manner, I have also been particularly impressed by his more pragmatic side, as he always knows when the time is to transform a fragmented story into a focused, publishable one. By simply interacting with Arnold over the past four years in these capacities, I now feel uniquely prepared towards becoming an independent scientist in the future.

Next, I have to thank my thesis committee members Arturo Alvarez-Buylla and David Rowitch for their continued support. Both Arturo and David run fantastic labs that neighbor us, and have facilitated a collaborative and fun working environment through my entire graduate career. They both serve as scientific role models to the highest degree, and I have learned much from their critical nature during group meetings. I especially have to thank them for finding the time to read

and comment on my manuscript drafts in a way that elevated my work to the next level. More recently, they have also taken the initiative to advise me on my career path, which I am also deeply appreciative of.

One of the most enjoyable parts of being a graduate student is working in close proximity with a wonderful group of people. I have to thank all the members of the Kriegstein Lab, both past and present for their scientific support, but also for being some of the most fun and least professional people I have ever met. We have had too many fun times to list here, and I am deeply grateful for all the strong personal bonds that we have formed. These are of course not limited to the Kriegstein Lab, and I must also extend my thanks to all the members of HSW12 and Pod D for their friendship.

My graduate career would have been very different if it had not been for my close collaboration with David Hansen, or what we call "Team Human". David has the incredible ability to juggle an enormous number of personal responsibilities, while still putting in an absurd number of hours at work and maintaining a sense of humor. Through our many years of working together, I have learned the great benefit of having someone brilliant and trustworthy to discuss ideas with every day. Sharing the joy of discovery with David literally by my side has been the best part of my graduate career. Finally, our friendship extends outside of work, and I am thankful for David's taste in music and for introducing me to the greatest band of all time, *Rush*.

I also have to acknowledge specific members of the Kriegstein Lab for their contribution to my graduate experience. Phil Parker joined the lab as a technician at the same time as I did, and being roughly the same age and with similar interests in Arnold Schwarzenegger movies, our friendship quickly blossomed both in and out of the lab. William Walantus, our lab manager, has been a tremendous friend and provider of technical support in the lab. Corey Harwell and Ashkan Javaherian were responsible for teaching me all the techniques that I know. Doris Wang, Laura

Elias, Tristan Sands, and David Castaneda have served as role models as more senior students in the lab. In more recent years, I have enjoyed the friendship of Caitlyn Gertz and Bridget LaMonica, who I am particularly excited to have continue my work on the human neocortex.

In the last year and a half, I have been fortunate to work in collaboration with a new UCSF fellow, Michael Oldham. Mike has brought a completely new, more quantitative perspective to my understanding of biology. He has shown much patience in teaching me how to analyze and interpret bioinformatic data, but has also given me the freedom to take the data in the directions that I want, for which I am very grateful. Mike's lab manager, Melanie Bedolli, always has a positive presence on our floor, and I thank her for teaching me a lot about molecular biology.

My graduate career would not have run so smoothly without the programmatic support of the BMS and stem cell administrative staff. I especially have to thank Lisa Magargal for everything she has done for the program, and Caroline Rutland and Nathan Jew for always being up for a fun chat in the BMS office. Erica Stidham in the stem cell office has also been a great friend for many years.

I also have to thank my classmates, particularly Michael Patnode, Jen Bando, and Emily Thornton. It has been a joy to mature together as scientists with such an intelligent and fun group of people. I am so excited to see where all our careers go in the future. In addition to my classmates, my numerous other friends at UCSF have also been a huge source of support both in and out of the lab. Jesse Green, April Price, and Collin Melton were students one year ahead of me in the labs that I rotated in. They went out of their way to help navigate my way through the first year. We have formed strong friendships that continue to this day. In more recent years, Rob Judson has been a fantastic friend and partner in eating meat.

Although I am not particularly good at keeping in touch with friends from previous stages of my life, I have remained close with a handful of people: Adrian Liu, Stuart Brown, Betsy England,

Contributions to presented work

All of the work described in this dissertation was done under the direct supervision and guidance of Arnold Kriegstein.

The contents of Chapter 1 and 3 are modified and reproduced from the publication: **Lui, J.H.**, Hansen, D.V., and Kriegstein, A.R. (2011). Development and evolution of the human neocortex. Cell *146*, 18-36.This manuscript is reproduced in accordance with the policies of *Cell Press* and *Elsevier*.

Chapter 1 is an extended introduction derived from the published review article, whereas Chapter 3 is the remainder of the same article, which discusses the implications and future directions of the data in Chapter 2. The ideas and conceptual framework presented in these chapters are the result of much discussion between David Hansen, Arnold Kriegstein, and myself. I wrote the manuscript, which was edited by David Hansen and Arnold Kriegstein. I designed the figure schematics, which were executed by Kenneth Probst using Adobe Illustrator. Stephanie Redmond, a rotation student of mine in 2010, contributed to the observation and quantification of immature neurons present in the OSVZ (Chapter 3, Fig. 1A)

Chapter 2 is reproduced from the publication: Hansen, D.V., **Lui, J.H.**, Parker, P.R., and Kriegstein, A.R. (2010). Neurogenic radial glia in the outer subventricular zone of human neocortex. Nature *464*, 554-561. This manuscript is reproduced in accordance with the policies of *Nature Publishing Group*. This work was guided by Arnold Kriegstein and performed in equal collaboration with David Hansen.

David initially began studying donated human fetal brain tissue for the purpose of understanding the origin and behaviors of GABAergic inhibitory neurons. Because it was relatively difficult to recover the "ventral" neocortical tissue that would address those questions, but relatively possible

to recover "dorsal" neocortical tissue that would address questions of neocortical expansion and generation of excitatory neurons in humans, David and Arnold shifted the focus of the project towards the latter. I joined up at the very early stages of this project to use my expertise in timelapse imaging cortical slice culture to describe the behavior and lineage of progenitor cells in these donated samples. This quickly became a full-blown collaboration, where David and I performed complementary aspects of all the resulting experiments together. Near the end of the project, we analyzed the data, wrote the manuscript, and generated most of the figures together. As a result, we appeared as co-first authors on this manuscript.

Because David and I had no expertise in electrophysiology, we recruited the help of Philip Parker to analyze the resting membrane and firing properties of cells in the fetal human neocortex. Philip performed all the electrophysiology and data analysis in Chapter 2 and is also an author on the manuscript. As an extension to the technical training I had received as a rotation student, Ashkan Javaherian introduced and taught me how to electroporate dyes (Haas et al., 2001) into live slices of human neocortex. This technique was an instrumental part of learning the morphology of progenitor cells in the human neocortex. Towards the same end, Tamily Weissman and Brian Clinton, both former members of the Kriegstein Lab, shared their modified protocol for "DiOlistics" (Gan et al., 2000), which they called "Dustolistics", a method for labeling cells with dye-coated beads.

The manuscripts that form Chapters 1-3 benefitted greatly from the critical reading and insightful comments of Arturo Alvarez-Buylla, David Rowitch, and Daniel Lim (Chapters 1 and 3). In every case, their comments resulted in a much improved restructuring of the manuscript.

The work described in Chapter 4 was originally conceived from discussions between David Hansen, Arnold Kriegstein, and myself. We realized the need for a better molecular characterization of cell types present in the developing human neocortex, but did not have the

necessary tools to delineate different cell types in an unfamiliar tissue, let alone analyze their gene expression patterns. Because of this, we recruited the help of Michael Oldham, a UCSF fellow who, during his graduate career, pioneered a new method for determining and grouping gene co-expression patterns from microarray datasets.

Michael and I took the lead on this project, where we devised a strategy to create a large microarray dataset that would allow us to determine the most significant gene co-expression patterns in the developing human neocortex. My initial role in this project was to perform the hands-on work that would lead to the creation of the data set. This included fetal tissue collection, microdissection, serial sectioning, RNA extraction, and RNA quality control. The microarray analysis itself was performed by the Southern California Genotyping Consortium. Michael guided this process carefully, and upon receiving the data, performed all the bioinformatic quality control to normalize the data and remove batch effects. Michael wrote all of the code that first organized and displayed the raw data in the structure of modules, and then compared the modules to data from published gene sets.

Following this, Michael taught me how to interpret and analyze the bioinformatic data, which we eventually did together. We identified the block structure of the modules and determined candidate genes to place in an anatomical context. Towards this end, I performed all of the immunostaining and Melanie Bedolli, Michael's lab manager, performed the *in situ* hybridization for *CPNE4*. The identification of genes with human-specific evolutionary change present in our module structure was done in collaboration with Alisha Holloway of the Gladstone Bioinformatics Core Facility. I wrote the manuscript for Chapter 4, with edits and insightful comments from Michael Oldham and Arturo Alvarez-Buylla.

Developmental expansion of the human neocortex

By Jan Hsi Lui

ABSTRACT

Many of the extraordinary intellectual capabilities of humans are attributed to the proper development and function of the neocortex. This region of the brain is responsible for higher cognitive functions such as sensory perception, spatial reasoning, and conscious thought, and is distinguished in humans by its large size and extensively folded pattern. However, the developmental events that underlie this structure have mostly been inferred from characterizations of the mouse or rat, whose neocortex is small and not folded.

Here, we directly characterize the progenitor cells present in the developing human neocortex. We find that the developing human neocortex utilizes a proliferative cell population that forms the outer subventricular zone (OSVZ), a region removed from the cerebral ventricles that is not present in the mouse. We further identify an OSVZ progenitor cell type known as an outer radial glial (oRG) cell and demonstrate using real-time imaging that they undergo self-renewing asymmetric divisions to generate neuronal progenitor cells. oRG cells function as neural stem cells and underlie an OSVZ lineage of progenitor cells, which over the course of many cell cycles amplifies neuron number and likely modifies the trajectory of migrating neurons.

Because the establishment of non-ventricular radial glia may have been a critical evolutionary advance underlying increased cortical size and complexity in the human brain, we further discuss the prevalence of oRG cells and OSVZ proliferation in different species throughout evolution. We learn that OSVZ proliferation is present in all superorders of placental mammals, but only in

those species with folded brains are these mechanisms appreciably utilized. To gain insight into the molecular and evolutionary bases for these phenotypic differences, we performed serial microrarray analysis to uncover gene co-expression patterns present in the developing human neocortex. From these data, we identified co-expression modules that correspond to human radial glia and further determined genes within these modules that have undergone human-specific evolutionary changes. This data serves as a molecular substrate for comparisons of radial glia between species and will help elucidate the molecular mechanisms that drive OSVZ proliferation.

TABLE OF CONTENTS

LIST OF FIGURES

Chapter 4

CHAPTER 1

Introduction

The content of this chapter was modified from the following publication:

Lui, J.H., Hansen, D.V., and Kriegstein, A.R. (2011). Development and evolution of the human neocortex. Cell *146*, 18-36.

Evolution of the neocortex in mammals is considered to be a key advance that enabled higher cognitive function. However, neocortices of different mammalian species vary widely in shape, size, and neuron number (reviewed by Herculano-Houzel, 2009). These differences are presumably reflected in the organization, abundance, and behavior of neural progenitor cells during embryonic development. In no other species are these characteristics more significant than the human, since the large size and highly folded structure of the human neocortex is thought to underlie our unique intellectual capabilities. Understanding the developmental events giving rise to the human neocortex is therefore essential, since they are the foundation of our intellectual capacity and the physiological context that is disrupted in neurodevelopmental diseases.

Recent models of neocortical development have largely been based on cellular and molecular studies of the mouse and rat, whose neocortex exhibits many of the key features general to all mammals, including a six-layered organization and regionalization into sensory, motor, and association areas. However, because the rodent neocortex is small and nonfolded (lissencephalic), its ability to model or illuminate the developmental mechanisms of larger and highly folded (gyrencephalic) neocortex, such as that of humans, is inherently limited.

Because the fossil record for soft tissues such as the brain is severely restricted, efforts to understand the evolution of the neocortex at a cellular level have been limited to comparisons of living species—an approach known as evo-devo (Gould, 1977). This approach assumes that related biological systems share inherent functional modularity, such that a small number of evolutionary changes to key regulators of these modules, if heritable and beneficial, can be positively selected and have major consequences for the species. Observed differences in the mechanisms of brain development across species may therefore be evolutionary variations of the same ancestral mechanisms.

The prerequisite for gaining these insights is a characterization of neocortical development in

multiple species, both at the cellular and molecular level. In particular, understanding the characteristics and abundance of neural progenitor cells in the human may give especially important clues to understanding brain evolution. Following some historical perspective and a discussion of previous models of how the neocortex could have expanded in evolution, this dissertation will focus on our work in directly characterizing the cellular mechanisms of human neocortical development. We discover that an expanded population of progenitor cells in the outer subventricular zone (OSVZ) underlies the large volume and surface area of the human neocortex. This characterization provides the physiological context for understanding how large neocortex size could have evolved and provokes a discussion of the generality of these features across different species.

HISTORICAL PERSPECTIVE

Like modern studies, even the earliest observations of cortical morphogenesis over 150 years ago attempted to connect the structure and organization of the mature cortex with the proliferation and morphogenic movements of germinal cells. The manuals of human histology and embryology by Albert von Kolliker (1817-1905) were some of the first evidence of the layered structure of the neocortex and its pseudostratified epithelium of elongated cells lining the cerebral ventricles. However, it was Wilhelm His (1831-1904) who first appreciated the relationship between progenitor cells near the ventricle and their eventual progeny in the mature cortex. From his work in human embryology, His asserted several key principles of cortical development: 1) that germinal cells divide rapidly in the ventricular epithelium, 2) that neuroblasts migrate from inner to outer zones, and 3) that a cell population known as spongioblasts (modern radial glia) forms a syncytium through which the neuroblasts migrate (summarized by Bentivoglio and Mazzarello, 1999). Although these general concepts continue to hold true, the ensuing century was filled with debate over the cell types present in the embryonic germinal zone near the ventricle, both in terms

of whether they produce glial or neuronal lineages, as well as how this region develops in its own right.

His proposed that neurons and glia were produced from specialized and distinct progenitor cell types known as "germinal cells" and "spongioblasts," respectively (Bentivoglio and Mazzarello, 1999). This concept became influential and was perpetuated by Ramon y Cajal, who believed that although in the same location, neuroepithelial cells (the spongioblasts) were a separate population from the neural progenitor cells that formed mitotic figures at the ventricular surface (Cajal, 1911; Bentivoglio and Mazzarello, 1999). Although Sauer eventually showed that neuroepithelial cells underwent interkinetic nuclear migration and descended to the ventricular surface to divide (Sauer, 1935), this was not sufficient proof to suggest that neuroepithelial glial cells were in fact neuronal progenitor cells.

Many influential studies of the role of cells now universally known as radial glia (Rakic, 1971) were performed, under the premise that they were a type of glial scaffolding cell. In particular, the morphology of radial glia (RG) has been an especially important feature for deducing its cellular function. The first descriptions of "radial cells" are attributed to Camillo Golgi who, using his new impregnation technique, found cylindrical cells that originated from the central canal of the chick spinal cord, radiated thin filaments that traversed the entire coronal plane, and inserted into the pia mater in a conical swelling (Bentivoglio and Mazzarello, 1999). Giuseppe Magini further substantiated these observations in the developing neocortex of a variety of mammalian species including humans, by finding a similar arrangement of cells near the ventricular cavity with fibers radiating toward the pial surface. Magini first described that these radial filaments bore numerous varicosities or swellings like "the grains of a rosary," and suggested that these could represent future nerve cells (Bentivoglio and Mazzarello, 1999). The identity of these varicosities was eventually resolved by the work of Pasko Rakic who used electron microscopy and Golgi staining to demonstrate that neurons were intimately apposed to

RG fibers during their migration (Rakic, 1972). These studies have lead to the universal acceptance that radial glial fibers are the physical substrate for neuronal migration.

THE RADIAL UNIT HYPOTHESIS

Studies by Rakic that utilized a wide range of techniques to describe the development of monkey neocortex culminated in the influential concept known as the radial unit hypothesis (Rakic, 1988). This scheme formally integrated a number of key observations, proposing that: (1) the neuronal output of proliferative units (at the ventricle) is translated by the fiber guides of RG to the expanded cortex in the form of ontogenetic columns and (2) the proto-map formed by these proliferative units could be influenced by thalamic inputs and define cortical areas of variable size, cellular composition, and function. This provided a framework for the mechanics of neocortical development in the radial dimension, where neurons of the same ontogeny (progeny of a given ventricular neuronal progenitor) would tend to migrate on a continuous fiber to the cortical plate, form a radial column of cells with related function, and project a ventricular proto-map onto the developing cortex.

NEUROGENESIS BY RADIAL GLIA

The radial unit hypothesis described the events of neocortical development only in general terms and did not assume any lineage relationship between RG and neuronal progenitor cells in the ventricular zone (VZ). This conceptual separation was not resolved until a decade ago, as even modern studies reported that the primate VZ contains a heterogeneous population of progenitor cells of which only some express the glial marker GFAP (Levitt et al., 1981). Although evidence from the neurogenesis of songbirds first suggested and then demonstrated the neurogenic role of RG (Alvarez-Buylla et al., 1988; 1990), this concept was not fully appreciated until cell fate analysis in the developing rodent brain proved that RG cells give rise to neurons (Malatesta et al.,

2000; Miyata et al., 2001; Noctor et al., 2001). Time-lapse imaging of retrovirally labeled clones demonstrated that RG cells generate neurons by multiple rounds of self-renewing, asymmetric division and that newborn neurons often use the parent cell's radial fiber to migrate to the cortical plate (Noctor et al., 2001; Noctor et al., 2004; Noctor et al., 2008).

Further studies showed that, in the rodent, the vast majority of progenitor cells in the VZ have RG morphology and contact both the ventricular (apical) and pial (basal) surfaces of the neocortex (Hartfuss et al., 2001; Noctor et al., 2002). That RG cells were neuronal progenitor cells provided an explanation for the radial organization of the neocortex at a clonal level, with RG cells in the VZ forming an epithelial niche that gives rise to radial clones of excitatory neurons through repeated rounds of asymmetric division. This model also simplified the radial unit hypothesis, as the proliferative units were shown to be the same cells as the glial guides. Importantly, these data further suggested that evolutionary expansion of neocortical surface area could occur through expanding the RG founder population before the onset of neurogenesis (Fig. 1A) (Rakic, 1995; 2009).

TRANSIT AMPLIFICATION BY INTERMEDIATE PROGENITOR CELLS

This model was oversimplified, as more detailed clonal analysis utilizing time-lapse imaging in the rodent showed that daughter cells of ventricular RG were often neuronal progenitor cells in their own right and would migrate superficially into the subventricular zone (SVZ) to divide (Noctor et al., 2004; Haubensak et al., 2004). Furthermore, whereas RG divisions were asymmetric and associated with self-renewal, the daughter progenitor cells (intermediate, or basal, progenitors) usually underwent one terminal symmetric division that produced two neurons and depleted the progenitor cell (Noctor et al., 2004). This partially reconciled the earlier observations of GFAP and non-GFAP expressing progenitor cells in the VZ because, at early

stages prior to formation of a distinct SVZ, intermediate progenitor (IP) cells also divide in the VZ (Englund et al., 2005; Noctor et al., 2008; Kowalczyk et al., 2009). Others have reported that a third class of progenitor cells, termed short neural precursors (SNP), also resides in the VZ and divides at the ventricular surface (Gal et al., 2006; Stancik et al., 2010). These SNP cells are reported to have ventricular contact but only short basal processes that do not extend beyond the SVZ. Whether these are a distinct progenitor cell type or early IP cells that have not yet lost ventricular contact is controversial. At any rate, studies have clearly defined the SVZ as the major site of neurogenesis by IP cells that are the multipolar, nonepithelial daughters of RG (Noctor et al., 2004; Noctor et al., 2008; Haubensak et al., 2004; Miyata et al., 2004). Analysis of RG versus IP cell divisions showed that, although RG cells outnumber IP cells at early stages, the majority of neuron-producing cell divisions are by IP cells during all stages (Kowalczyk et al., 2009), even before the SVZ is a distinct progenitor zone. This implies that a major role of RG cells in rodent neurogenesis is to make neuronally committed IP cells.

The identification of the VZ as a site of asymmetric divisions and the SVZ as a site of symmetric divisions altered hypotheses regarding neocortical expansion. Independently of RG divisions, the number of symmetric IP cell divisions could also affect neuron number and be a determinant of neocortical size. Because IP cell daughters have the same birth date and are predicted to occupy the same laminar position, an increase in their numbers would be more consistent with tangential expansion of neocortical surface area, whereas increasing the number of asymmetric RG cell divisions would be predicted to expand neocortical thickness. Furthermore, expansion of founder cells within the VZ can only account in part for the neuron number observed in gyrencephalic species, as neocortical surface area is disproportionately expanded compared to the ventricular surface area, which remains relatively modest. These observations could be reconciled if SVZ progenitor cells have a greater capacity for transit amplification in gyrencephalic animals, such that they undergo multiple rounds of cell division before generating neurons (Fig. 1B) (Kriegstein

et al., 2006). However, this scheme could exhaust the capacity of RG cells to guide neuronal migration, as the expanded population of immature neurons would greatly outnumber the restricted number of migratory guides.

Indeed, a human genetic study mapped the disease-causing gene in a family exhibiting congenital microcephaly to the homozygous silencing of TBR2 (EOMES) (Baala et al., 2007), a transcription factor shown in rodent studies to be a selective marker for IP cells (Englund et al., 2005) and functionally required for SVZ neurogenesis (Arnold et al., 2008; Sessa et al., 2008). This condition further supports the overall importance of SVZ progenitor cells in the control of neocortical size.

THE EXPANDED PRIMATE SVZ

The effect of progenitor cell expansion on a subsequent increase in neuron number is dependent on the natural counterbalancing relationship between rates of cell proliferation and death. Genetic deletion of key players in the apoptosis pathway in mice results in modest increases to neocortical size and widespread dysregulation of ventricular architecture (reviewed by Kuan et al., 2000). However, even though apoptosis plays a role in normal neocortical development, an evolutionary reduction in cell death during development is unlikely to be a factor that sufficiently explains the great magnitude of neocortical expansion in primates. Although mathematical modeling studies have predicted that cell death rates in developing primate neocortex may be increased compared to rodent (Gohlke et al., 2007), observations of the remarkable size of the primate SVZ region (Smart et al., 2002; Lukaszewicz et al., 2005) imply even greater increases in progenitor cell proliferation. We therefore turn our attention to the direct characterization of progenitor cells in the expanded SVZ of humans to illuminate mechanisms of neocortical expansion.
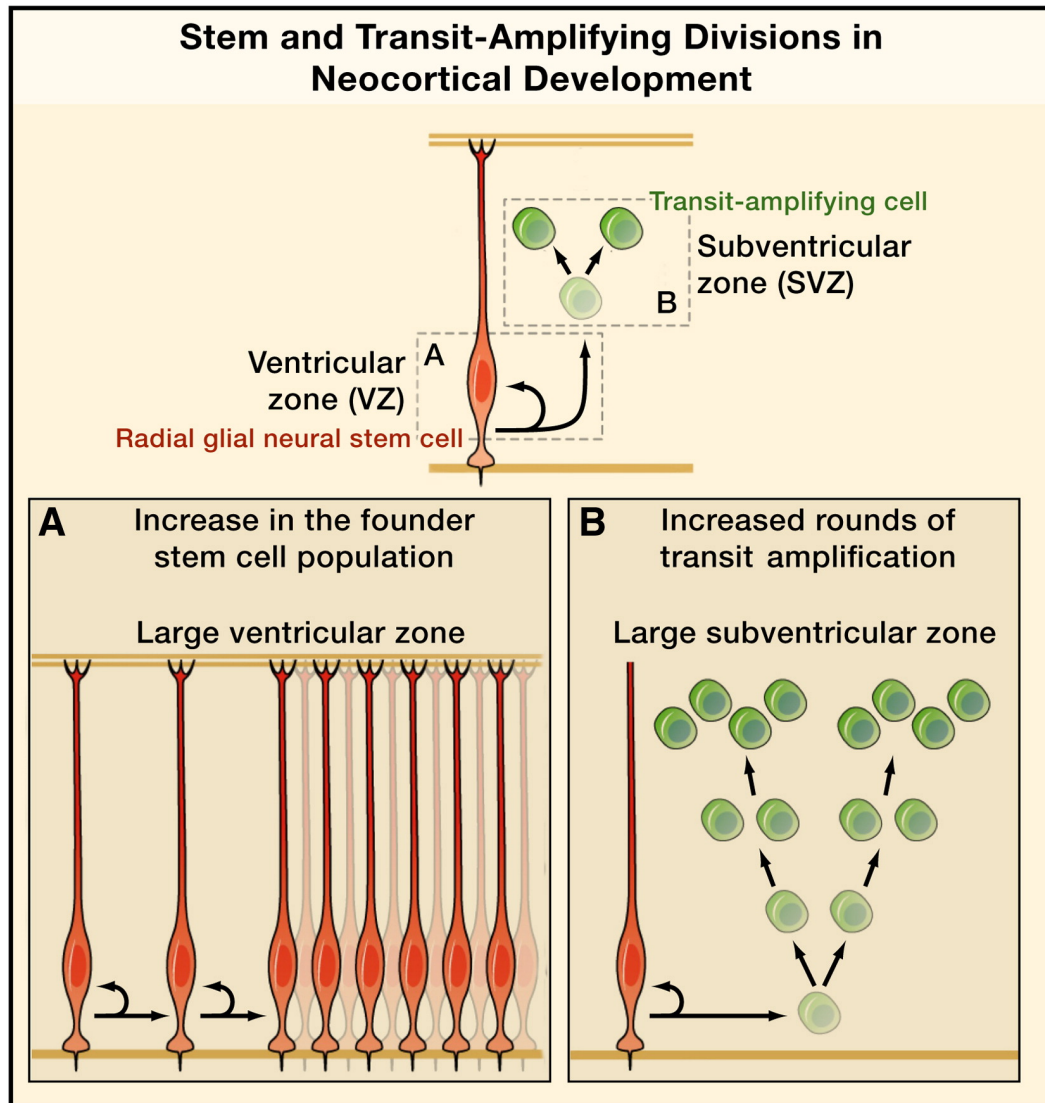
Figure 1. Progenitor cell expansion can underlie neocortical enlargement.

Neuronal number is a key determinant of neocortex size and shape. Neurons are produced from a lineage of radial glia (RG) stem cells (red) and transit-amplifying intermediate progenitor (IP) cells (green). Expansion in one or both cell populations has been proposed as potential mechanisms that underlie neocortical expansion. Expansion of the founder RG cell population prior to the onset of neurogenesis (A) predicts a large ventricular zone (VZ). Expansion in the number of transit-amplifying divisions (B) predicts a large subventricular zone (SVZ).

CHAPTER 2

Neurogenic radial glia in the outer subventricular zone

of human neocortex

SUMMARY

Neurons in the developing rodent cortex are generated from radial glial cells that function as neural stem cells. These epithelial cells line the cerebral ventricles and generate intermediate progenitor cells that migrate into the subventricular zone (SVZ) and proliferate to increase neuronal number. The developing human SVZ has a massively expanded outer region (OSVZ) thought to contribute to cortical size and complexity. However, OSVZ progenitor cell types and their contribution to neurogenesis are not well understood. Here we show that large numbers of radial glia-like cells and intermediate progenitor cells populate the human OSVZ. We find that OSVZ radial glia-like cells have a long basal process but, surprisingly, are non-epithelial as they lack contact with the ventricular surface. Using real-time imaging and clonal analysis, we demonstrate that these cells can undergo proliferative divisions and self-renewing asymmetric divisions to generate neuronal progenitor cells that can proliferate further. We also show that inhibition of Notch signaling in OSVZ progenitor cells induces their neuronal differentiation. The establishment of non-ventricular radial glia-like cells may have been a critical evolutionary advance underlying increased cortical size and complexity in the human brain.

INTRODUCTION

One of the most marked evolutionary changes underlying the unique cognitive abilities of humans is the greatly enlarged cerebral cortex. This change must be reflected in differences in progenitor cell number and/or proliferative output during development. There has been considerable progress in understanding progenitor cell behavior in the developing rodent cortex, where neurogenic cell divisions are confined to a narrow region of proliferative cells near the cerebral ventricles (Smart, 1973). Cortical neurons arise from radial glial (RG) cells, the epithelial stem cells that line these ventricles (Malatesta et al., 2000; Miyata et al., 2001; Noctor et al., 2001). RG cells in the ventricular zone (VZ) generate intermediate progenitor cells that migrate into the SVZ and further proliferate to increase neuronal number (Haubensak et al., 2004; Noctor et al., 2004).

A distinguishing feature of primate corticogenesis is the appearance of the OSVZ during mid-gestation (Smart et al., 2002; Zecevic et al., 2005; Fish et al., 2008). Cell-labeling studies in primates have shown that cell divisions in both the OSVZ and the VZ coincide with the major wave of cortical neurogenesis, suggesting that OSVZ cells produce neurons (Rakic, 1974; Lukaszewicz et al., 2005). However, the progenitor cell types in the OSVZ and the extent to which they participate in neurogenesis have not been characterized. Furthermore, unique features of human cortical development probably underlie neurodevelopmental disorders that affect the cerebral cortex, such as autism and schizophrenia. Here we describe classes of radial glia-like cells and transit-amplifying cells in the human OSVZ that contribute significantly to neurogenesis. OSVZ radial glia-like cells show unusual cell cycle behaviors that further distinguish them from traditional RG cells. These results indicate a new mechanism for cortical expansion outside the ventricular epithelium through the addition of radial columns arising from the OSVZ.

RESULTS

Radial glia-like cells populate the OSVZ

Recent reports have shown that cells expressing the transcription factor PAX6 are found in the OSVZ of human and primate cortex (Fish et al., 2008; Bayatti et al., 2008; Mo and Zecevic, 2008), unlike the rodent where PAX6 is expressed mainly by RG cells in the VZ (Gotz et al., 1998). It has been suggested that PAX6$^+$ cells in the OSVZ include both progenitor cells and postmitotic neurons (Fish et al., 2008; Mo and Zecevic, 2008). We examined sections of fetal cortex and found that most PAX6$^+$ cells (>90%) in the human OSVZ co-expressed the neural stem/progenitor cell marker SOX2, and many also expressed the proliferation marker Ki67 (Supplementary Fig. 1), indicating that most of them are progenitor cells. We sought to characterize the progenitor cells in the human OSVZ further, and determine whether any are RG cells.

RG cells are characterized, in part, by their distinctive morphology, with an apical process extending to the ventricle and a basal process extending to the pia that can guide radial neuronal migration. We examined whether the morphology of OSVZ cells resembled RG cells by focally electroporating dye-conjugated dextran (Haas et al., 2001) in the OSVZ to label cells. We routinely observed OSVZ cells that resembled RG cells by having a long radial process. However, these cells showed only basal and not apical processes (Supplementary Fig. 2). For example, a single electroporation labeled five OSVZ cells that all demonstrated basal but not apical processes. These cells all expressed SOX2, further resembling RG cells (Fig. 1a).

To address whether OSVZ RG-like cells were actively cycling, we infected cortical fragments from gestational week 14 (GW14) with green fluorescent protein (GFP)-retrovirus to label dividing cells, and cultured tissue slices. Many GFP-labeled OSVZ cells had long basal but not

apical processes and expressed PAX6 and SOX2 (Fig. 1b). To quantify the number of progenitor cells with this morphology, we stained for phospho-vimentin, which marks the cytoplasm of neural progenitors in and directly after M-phase of the cell cycle. About half of the SOX2^{+} phospho-vimentin^{+} cells in the OSVZ showed a clear basal but no apical process (141 out of 304, GW15.5), often with varicosities similar to M-phase RG cells (also see Fig. 1c, GW17) (Miyata et al., 2001; Weissman et al., 2003). Phospho-vimentin^{+} cells with this morphology nearly always expressed the RG markers SOX2 (267 out of 272), PAX6 (27 out of 27), nestin (31 out of 31) and GFAP (20 out of 20), but never the early neuronal markers DCX (27 out of 27) or βIII-tubulin (22 out of 22) (Supplementary Fig. 3). On the basis of the number of phospho-vimentin^{+} cells with basal fibers in the OSVZ (145 out of 367) and the strong correlation of these cells with RG markers, we estimate that about 40% of all OSVZ progenitors are RG-like cells.

The radial processes of RG cells in the VZ support neuronal migration and underlie the columnar architecture of the cortex (Rakic, 2003; 1988). The basal processes of OSVZ cells could serve a similar function, particularly if they extend to the pia. We applied DiI-coated beads to the pial surface of fixed cortical tissue (DiOlistics, Gan et al., 2000) to label radial fibers and their corresponding cell bodies. Many OSVZ cells were seen with RG-like morphology but lacking apical processes (Fig. 1d), showing that at least a subset of OSVZ cells contacts the pia. By contrast, ventricular labeling showed only rare OSVZ cells labeled through their apical processes (Supplementary Fig. 4).

To rule out that OSVZ RG-like cells have ventricular processes that escaped labeling with other methods, we examined the ventricular surface to look for evidence of apical endings of OSVZ cells. The centrosomes of OSVZ progenitors reside in the OSVZ where the cells undergo mitosis (Fig. 1c). In contrast, the centrosomes of RG cells in the VZ are anchored at the ventricular surface, to which VZ cell bodies migrate to undergo mitosis (Supplementary Fig. 5a; Chenn et al., 1998). We stained the ventricular surface of whole-mount tissue sections to examine the presence

of centrosomes within the array of RG cell endfeet. An 'en face' view showed that most endfeet (>94%) contained centrosomes and thus originated from ventricular RG cells, confirming that most OSVZ cells do not contact the ventricle (Supplementary Fig. 5b).

Together, these results show that the human OSVZ contains a new class of actively dividing, non-epithelial progenitors that can maintain contact with the pia but not the ventricle. Owing to their radial morphology and expression of nuclear and cytoplasmic markers characteristic of RG cells, we will refer to these cells as oRG (OSVZ radial glia-like) cells to set them apart from traditional RG cells in the ventricular epithelium (vRG cells).

oRG cells self-renew and produce intermediate progenitor cells

An important feature of vRG cells is their ability to undergo several self-renewing divisions. To determine whether oRG cells also do this, we used GFP-expressing adenovirus (adenoGFP) to label cells in cultured slices where the VZ and inner SVZ (ISVZ) had been removed by microdissection, and then sequentially treated with the thymidine analogues BrdU (5-bromodeoxyuridine) and EdU (5-ethynyldeoxyuridine) spaced 36 h apart. This excluded VZ–ISVZ progenitors from the analysis and tested whether OSVZ progenitors go through S-phase more than once. We searched for GFP$^+$ cells with oRG morphology and analyzed them for BrdU and EdU labeling. More than half (13 out of 21) were double-labeled, and 6 out of 21 were single-labeled (Fig. 2a). This suggested that oRG cells could divide and self-renew.

We used real-time imaging to observe the behaviors of oRG cells and their daughters. AdenoGFP-labeled oRG cells frequently divided and exhibited a surprising behavior where the cell soma moved rapidly up the basal fiber before cytokinesis (Fig. 2b and Supplementary Movies 1 and 2). We term this behavior 'mitotic somal translocation'. The duration of translocation was usually <60 min, with distances averaging 57 μm and sometimes exceeding 100 μm (Fig. 2b, c).

Of the hundreds of oRG cell divisions observed, all but three divided with a horizontal cleavage plane with the upper daughter inheriting the basal fiber and maintaining oRG morphology, consistent with asymmetric self-renewing divisions. The lower oRG daughter usually became radially bipolar, with the more prominent process directed towards the ventricle. The mitotic somal translocation of oRG cells contrasts with the interkinetic nuclear migration of RG and neuroepithelial cells, in which the nucleus moves towards the ventricle before mitosis.

We imaged for longer periods and observed oRG cells dividing twice, with two distinct translocations and the upper cell inheriting the radial fiber (Supplementary Movie 3). We also routinely observed the lower daughter of an oRG cell divide again, showing that oRG daughters can also be progenitors (Fig. 2d and Supplementary Movies 2 and 4). Limitations in slice culture viability made it difficult to observe cells for more than two divisions. However, we observed cells resembling bipolar oRG daughters (similar to Fig. 2d at time 37 h 40 min, white arrowhead) that divided twice (Fig. 2e), suggesting that oRG daughters can undergo transit-amplifying divisions. Together, these results support a model in which the OSVZ contains at least two different types of progenitors that can divide multiple times (Fig. 2f).

oRG cells are neurogenic

To test whether OSVZ progenitor cells produce neurons, we dissected OSVZ tissue away from the VZ–ISVZ and cultured dissociated cells with BrdU to label newborn cells. BrdU$^+$ βIII-tubulin$^+$ neurons were present in the VZ–ISVZ and OSVZ but not cortical plate cultures (Supplementary Fig. 6a). About 5% of βIII-tubulin$^+$ neurons from OSVZ cultures (60 out of 1,295) were BrdU$^+$, indicating that OSVZ progenitor cells produced neurons. It has been reported that two-thirds of GABA (γ-aminobutyric acid)-containing inhibitory neurons in the human cortex are generated locally (Letinic et al., 2002). We therefore looked for GABA$^+$ BrdU$^+$ neurons in our VZ–ISVZ and OSVZ cultures. Of the neurons from OSVZ cultures that were

GABA$^+$ (82 out of 1,295), not one was BrdU$^+$ (Supplementary Fig. 6b). Cultured VZ–ISVZ cells

gave similar results, suggesting that cortical progenitors do not produce inhibitory neurons.

Alternatively, our culture conditions may not support their production. In contrast, some cultured

cells expressed TBR2 (also known as EOMES), a transcription factor expressed by intermediate

progenitor cells and newly born neurons of the excitatory lineage (Englund et al., 2005;

Kowalczyk et al., 2009; Petanjek et al., 2009). Nearly all of these (63 out of 65 in OSVZ culture)

were BrdU$^+$ and thus must have originated from SOX2$^+$ or TBR2$^+$ cells, and many of these (25

out of 63) were also βIII-tubulin$^+$, suggesting that excitatory neurons were being generated in the

human OSVZ (Supplementary Fig. 6b).

These results indicated that neurons are produced by OSVZ progenitor cells but did not identify

the cell type of origin. To explore whether oRG cells produce neurons, we monitored oRG cell

divisions in real time and determined daughter cell fate by immunostaining. Early commitment to

a neuronal lineage was indicated by the expression of TBR2 or ASCL1 (a transcription factor

reported to specify GABAergic neuron fate in primate cortical progenitors, Letinic et al., 2002;

Petanjek et al., 2009). Most of the oRG cell divisions analyzed (13 out of 17) showed that both

daughters continued to express SOX2 but not TBR2 or ASCL1, even after another division (Fig.

3a and Supplementary Fig. 7). Occasionally, the non-oRG daughter even extended a basal process

and re-acquired oRG cell morphology (Supplementary Fig. 8). This supports a model of cortical

neurogenesis in which oRG cells produce daughter cells that often proliferate before

differentiation, thus expanding the OSVZ progenitor pool.

We observed six OSVZ cell divisions that gave rise to TBR2$^+$ daughters, three of which

originated from progenitors with oRG morphology (Fig. 3b and Supplementary Fig. 9). In each

case, the cell that inherited the basal process remained SOX2$^+$ TBR2$^-$, whereas the daughter cell

became TBR2$^+$ and in two of three cases divided again. These examples are evidence of

asymmetric oRG cell divisions that yield a self-renewed oRG cell and a neuronally committed

intermediate progenitor cell. Of the four divisions we observed that gave rise to ASCL1$^+$ cells, one was from a progenitor with oRG morphology (Fig. 3c). The oRG cell retained the basal process and expressed only SOX2—a further example of self-renewing, neurogenic oRG cell division.

Our observation that oRG cells can directly produce either TBR2$^+$ or ASCL1$^+$ cells suggested that oRG cells generate neuronal precursors for both excitatory and inhibitory lineages. To determine the relative amounts of these two precursor types, we stained cryosections for TBR2 and ASCL1 along with SOX2. Surprisingly, all ASCL1$^+$ cells co-expressed SOX2 and/or TBR2 (Supplementary Fig. 10), placing cortical ASCL1$^+$ progenitors in the same lineage as TBR2$^+$ cells. We were therefore unable to distinguish distinct precursors for inhibitory neurons because they seem to share a common precursor with excitatory cells. The identification of new markers may help identify subtypes of precursor cells committed to these lineages.

We also examined the membrane properties of oRG cells and compared them to other glial and neuronal cells. In patch-clamp recordings, the input resistances of vRG and oRG cells were comparable (vRG = 557.0 ± 190.4 MΩ (mean ± standard error), n = 3; oRG = 515.4 ± 10.7 MΩ, n = 3), both of which were lower than other OSVZ cells (multipolar = 1,265 ± 217.1 MΩ, bipolar = 1,952.8 ± 357.0 MΩ). However, although vRG cells showed typical passive membrane properties upon depolarization, oRG cells that were seen dividing in time-lapse images showed small, brief, inward, tetrodotoxin (TTX)-sensitive currents (77.9 ± 34.2 pA; Fig. 3d), suggesting mediation by voltage-gated sodium channels. These currents were also seen in oRG cells patched blindly in acute slices (n = 3). Two cells from a symmetrical division of an oRG daughter intermediate progenitor cell also showed similar inward currents that were abolished by TTX (Supplementary Fig. 11). Most multipolar (n = 4 of 7) and bipolar (n = 3 of 4) cells in the OSVZ also showed fast inward sodium currents (multipolar = 101.4 ± 20.5 pA, bipolar = 60.6 ± 11.1 pA), which were small compared with that of a cortical plate neuron (935.7 pA). A survey of active membrane

conductances of OSVZ cells and neurons suggested that these small currents could represent early instances of sodium current underlying action potential firing. In all, the emerging active properties of OSVZ cells are consistent with a neuronal lineage.

OSVZ progenitors outnumber VZ–ISVZ progenitors

A similar lineal relationship exists between RG and intermediate progenitor cells in the OSVZ as in the VZ–ISVZ, but it is unclear how proliferation in these two regions compares throughout human cortical development. Before the OSVZ arises, the periventricular region contains vRG cells and intermediate progenitor cells (Fig. 4d, GW11.5) and resembles the developing rodent cortex (compare mouse embryonic day (E)13, Supplementary Fig. 12). By GW13, an increase in SVZ SOX2$^+$ cells marks the development of the OSVZ, which expands massively in the following gestational month (Fig. 4d). In contrast, the VZ–ISVZ remains fairly constant through GW15.5 and diminishes by GW17, suggesting that the OSVZ becomes the predominant proliferative zone.

We compared Ki67-labeling in the OSVZ versus VZ–ISVZ to quantify actively cycling cells over time (Fig. 4b). At GW13, the OSVZ already accounted for >40% of proliferating cells. This increased to ~60% at GW14 and GW15.5, and >75% by GW17, highlighting the extensive contribution of oRG and intermediate progenitor cells in the OSVZ to human corticogenesis. Using SOX2, TBR2 and Ki67 expression to classify cortical progenitors (see Fig. 4a) showed similar proportions of progenitor cell types between the VZ–ISVZ and OSVZ (Fig. 4c and Supplementary Fig. 13). Thus, the human OSVZ is a duplicated neurogenic zone, similar to the VZ–ISVZ in progenitor cell types and proportions but much greater in size.

Finally, we correlated the SOX2 and TBR2 expression profile of OSVZ progenitors with their morphology by staining for phospho-vimentin (data not shown). Almost all phospho-vimentin$^+$

cells with oRG morphology were SOX2$^+$ TBR2$^-$ (65 out of 70), supporting the idea that oRG cells are undifferentiated progenitors. Notably, one-third of phospho-vimentin$^+$ OSVZ cells without oRG morphology were also SOX2$^+$ TBR2$^-$ (29 out of 81). Thus, cells with oRG morphology account for only a subset of undifferentiated OSVZ progenitors (65 oRGs out of 94 total SOX2$^+$ TBR2$^-$ cells). This corroborates our real-time imaging and fate analysis of oRG cell divisions, in which oRG daughter cells often remained undifferentiated during the ensuing cell division, and underscores the proliferative capacity of OSVZ progenitors.

Notch inhibition induces OSVZ differentiation

It is widely believed that vRG cells must retain certain epithelial properties to maintain progenitor cell status (Fish et al., 2008; Gotz and Huttner, 2005). oRG cells are removed from the VZ epithelium and lack apical processes, raising the question of how they persist as RG-like progenitors. A known mechanism of RG cell maintenance is the Notch pathway (Gaiano et al., 2000; Shimojo et al., 2008). We therefore investigated whether Notch signaling maintains oRG cell identity.

The Notch effector HES1 was expressed almost exclusively in PAX6$^+$ cells (355 out of 356 OSVZ HES1$^+$ cells were PAX6$^+$) (Fig. 5a). In cultured slices, about 80% (45 out of 56) of adenoGFP-labelled PAX6$^+$ SOX2$^+$ cells with oRG morphology also expressed HES1 (Fig. 5b), supporting a role for Notch in oRG cells. Furthermore, more than half of PAX6$^+$ SOX2$^+$ cells without oRG morphology were also HES1$^+$ (98 out of 158), consistent with our observation that some oRG daughter cells continue to proliferate before differentiation. This suggests that Notch signaling contributes to the expansion of the undifferentiated OSVZ progenitor pool.

Although some SOX2$^+$ cells express TBR2 and/or ASCL1, we saw no co-expression of HES1 with either TBR2 or ASCL1 (Fig. 5c), suggesting that Notch restrains neuronal differentiation. To

test the requirement for Notch signaling in OSVZ progenitor cell maintenance, we treated slice cultures with DAPT, a chemical inhibitor of Notch activity. Control slices maintained robust SOX2 expression in the OSVZ and stable ratios of SOX2$^+$, SOX2$^+$ TBR2$^+$, and TBR2$^+$ cells. In contrast, DAPT-treated slices demonstrated an increase in TBR2$^+$ and decrease in SOX2$^+$ cells over time (Fig. 5d). Analyzing ASCL1 expression showed similar trends (Supplementary Fig. 14). That SOX2$^+$ cells undergo widespread neuronal differentiation after Notch inhibition shows their overall neurogenic capacity and further underscores the contribution of OSVZ progenitors to human corticogenesis.

DISCUSSION

An expansion of cortical progenitor cell number during evolution must have contributed to the increase in size of the human brain (Abdel-Mannan et al., 2008). However, it has been unclear whether expansion of cortical progenitor number is specific to stem versus transit-amplifying cell types—both of which could shape the eventual cellular composition of the cerebral cortex. Our results show that progenitor cells with markers and morphology of neural stem and transit-amplifying cells (RG cells and intermediate progenitor cells) are well represented in the human cortex in both the periventricular zone and the OSVZ. Proliferating cells in the OSVZ were observed decades ago, but the types of cells produced were unknown (Rakic and Sidman, 1968). Cells in the OSVZ resembling radial glia had also been observed, but their role in cortical development was not defined (Choi, 1986; Schmechel and Rakic, 1979a; 1979b). We have shown that oRG cells, although distinct from the ventricular epithelium, can self-renew and produce neuronal precursors. They further resemble traditional RG cells in terms of marker expression and dependence on Notch signaling. The production of neurons by oRG cells and their daughters presents a more complex scheme of human neurogenesis (Fig. 5e). Although the origin of this previously unappreciated cell type remains unknown, we infer that oRG cells originate in the VZ and use mitotic somal translocation to migrate away. The stepwise translocation of oRG cells towards the cortical plate in coordination with cell divisions helps explain how the OSVZ expands while accumulating large numbers of oRG and intermediate progenitor cells.

Our finding that OSVZ progenitors undergo expansive proliferative divisions contrasts with observations of the rodent SVZ—in which intermediate progenitor cells usually divide only once—and provides a new cellular basis for understanding the evolutionary expansion of surface area in human cortex (Kriegstein et al., 2006). It will be interesting to study whether the OSVZ

and oRG cells are a general feature of gyrencephalic brain development, especially in non-primate species such as ferret and cat.

The radial unit hypothesis posits that the output of proliferative units (at the ventricle) is translated by glial guides to the expanded cortex in the form of ontogenetic columns (Rakic, 1988). Our results add a layer of complexity to the radial unit model and show that the production of neurons in human cortex occurs simultaneously from primary and secondary progenitor cells in both periventricular and outer subventricular regions—therefore defining two distinct origins for neurons in the mature cortex. Our model suggests that ontogenetic columns can arise from both ventricular and non-ventricular sites during human cortical development. An intriguing future question is whether there are functional differences between neurons generated from these two regions, a feature that would further increase cortical complexity.

ACKNOWLEDGMENTS

Author Contributions

D.V.H. and J.H.L. (listed alphabetically) carried out all the experiments except for the electrophysiology, analyzed the data, and wrote the manuscript. P.R.L.P. performed the electrophysiology and analyzed data. A.R.K., as the principal investigator, provided conceptual and technical guidance for all aspects of the project. All authors discussed the results/experiments and revised/edited the manuscript.
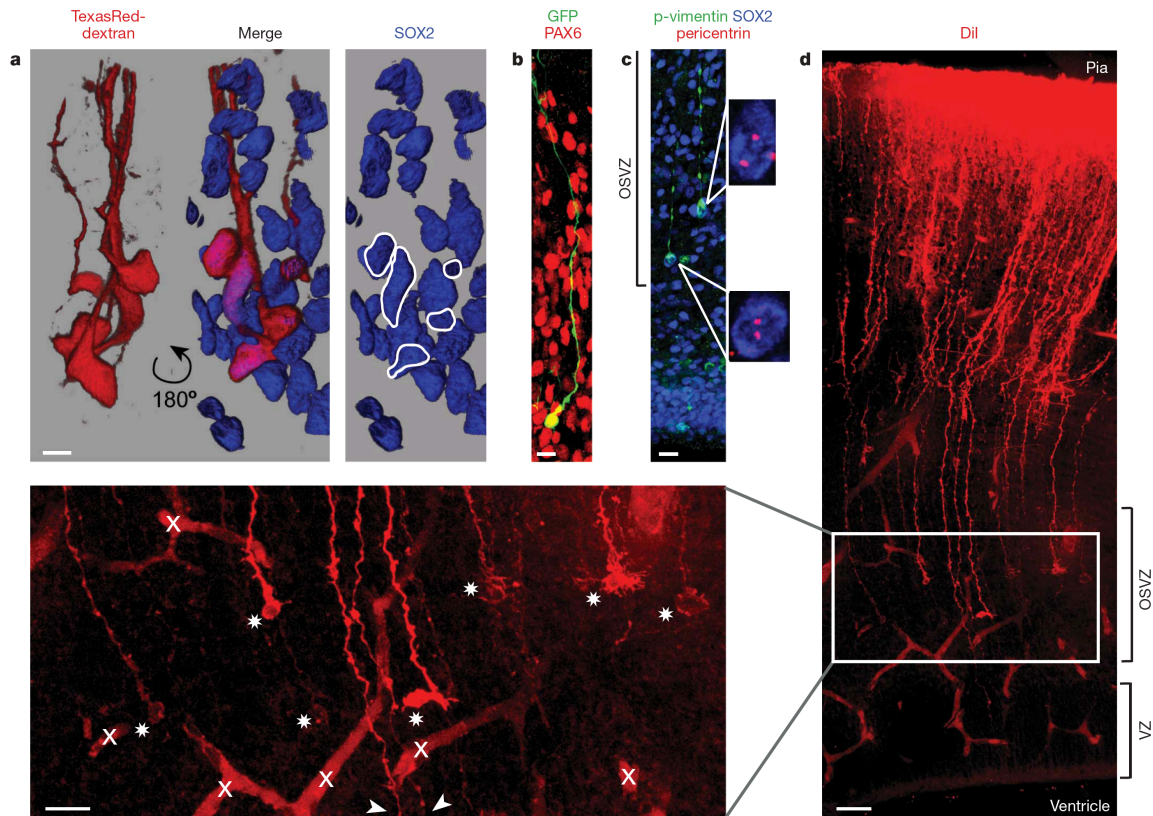
Figure 1. The human OSVZ is populated with non-epithelial radial glia-like cells.

a, Five OSVZ cells in GW15.5 cortex labeled by focal dye electroporation followed by immunostaining for SOX2 (blue). Cell bodies were labeled 100 μm from injection site through their basal processes. Three-dimensional rendering is shown. Nuclei are outlined in white. Scale bar, 5 μm. **b**, Representative GFP-retrovirus-labeled cell co-expressing PAX6 (red) in GW14 OSVZ. Scale bar, 15 μm. **c**, GW17 cortex stained for SOX2 (blue), phospho-vimentin (p-vimentin; green, cytoplasm of M-phase cells), and pericentrin (red, centrosomes), demonstrating morphology and centrosome location of SOX2$^+$ OSVZ cells during mitosis. Scale bar, 15 μm. **d**, Fixed GW15 cortex labeled pially with DiI-coated beads (DiOlistics). Inset demonstrates dye diffusion along radial processes from the pia terminating at distinct cell bodies in the OSVZ (stars) amid coexistent radial fibers that traverse the OSVZ to the ventricle (arrowheads) and autofluorescent blood vessels ('x'). Scale bars, 40 μm (**d**) and 20 μm (inset).
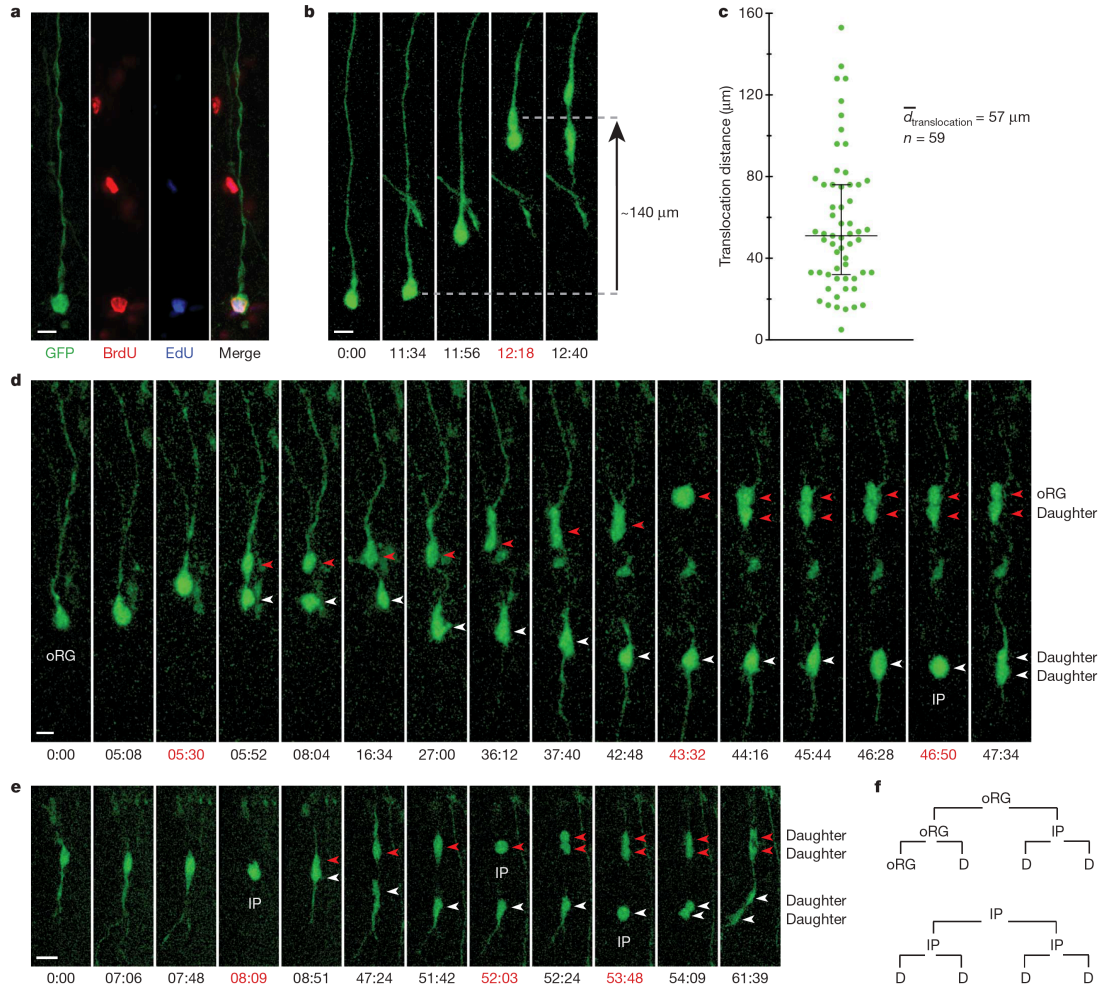
Figure 2. oRG cells self-renew and produce intermediate progenitor daughter cells.

a, AdenoGFP-labelled oRG cell in OSVZ slice culture (GW15), sequentially treated with the thymidine analogues BrdU (red) and EdU (blue) spaced 36 h apart to label cells that passed through S-phase twice (see text for cell counts). Scale bar, 10 μm. **b**, oRG cell undergoes 'mitotic somal translocation' directly before cell division. An adenoGFP-labeled GW15 cortical slice was imaged at 22-min intervals beginning 26 h after infection (see Supplementary Movie 2). Times, h:min (red for mitosis) (for **b**, **d** and **e**). Scale bar, 15 μm. **c**, Quantification of mitotic somal translocation distances of oRG cell divisions from GW15 time-lapse sequences. The median and interquartile range are shown. $n = 59$; mean distance = 57 μm. **d**, oRG cell undergoes two self-renewing divisions followed by division of the initial daughter cell (intermediate progenitor, IP). GW15 cortical slice was imaged as in **b** beginning 40 h after infection (see Supplementary Movie 4). Red and white arrowheads follow the lineages of oRG cell and oRG daughter, respectively. Scale bar, 10 μm. **e**, Bipolar intermediate progenitor cell resembling an oRG daughter undergoes two rounds of proliferative division. Imaging began 42 h after infection at 21-min intervals. Red and white arrowheads follow the lineages of the two intermediate progenitor daughters. Scale bar, 20 μm. **f**, Lineage relationships between cells in **d** and **e**. oRG cells can divide asymmetrically to self-renew and generate an intermediate progenitor cell. Intermediate progenitor cells can also undergo multiple divisions. D, daughter.
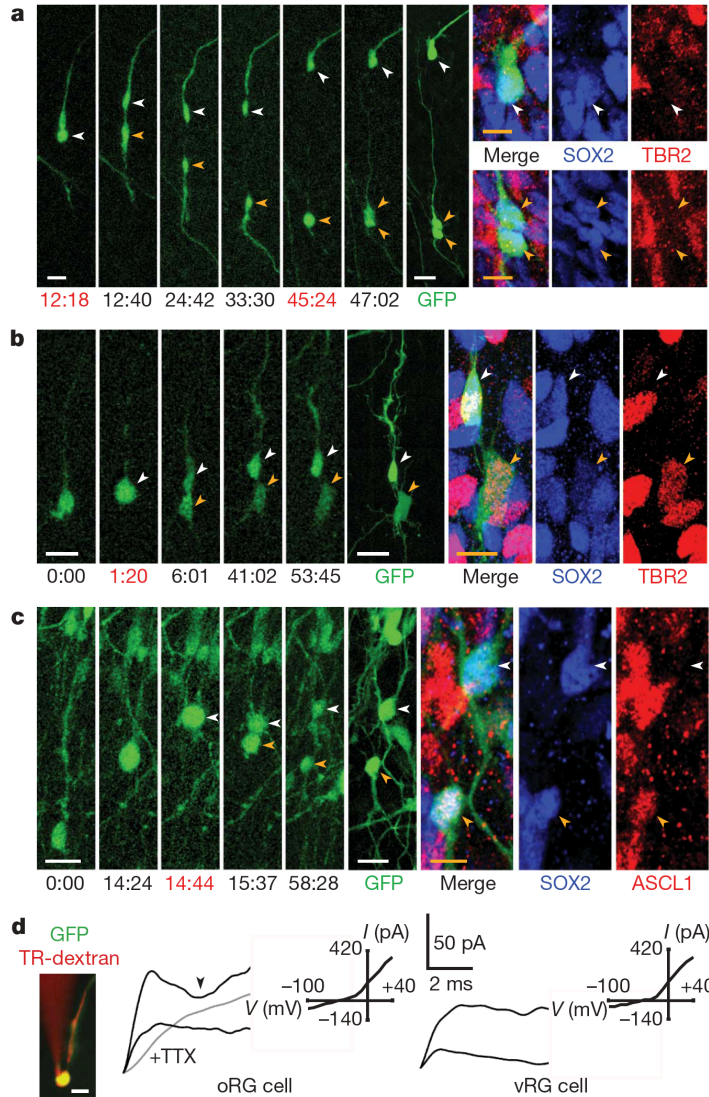
Figure 3. Daughters of oRG cells are neuronal progenitors.

a, Proliferative division of oRG daughter expands progenitor cell number. An adenoGFP-labelled cortical slice was imaged at 22-min intervals (continuation of Fig. 2b), followed by immunostaining to analyze daughter cell fates. Self-renewed oRG cell (white arrowhead) and intermediate progenitor daughter cells (yellow arrowheads) remain undifferentiated (SOX2$^+$ TBR2$^-$). **b**, Asymmetric oRG cell division produces a self-renewed oRG cell (SOX2$^+$ TBR2$^-$, white arrowhead) and a multipolar TBR2$^+$ cell (yellow arrowhead). An adenoGFP-labeled cortical slice (GW15.5) was imaged at 20-min intervals, followed by immunostaining. First image shown (t = 0:00) was 91 h after infection. **c**, Asymmetric oRG cell division produces a self-renewed oRG cell (SOX2$^+$ ASCL1$^-$, white arrowhead) and an ASCL1$^+$ daughter (yellow arrowhead), indicative of neuronal commitment. First image shown (t = 0:00) was 87 h after infection. Times, h:min (red for mitoses). Scale bars (**a–c**), 20 µm (white) and 10 µm (yellow). **d**, Patch-clamp recordings of representative oRG (adenoGFP and TexasRed (TR)-dextran overlay) and vRG cells. Current–voltage relationships and current traces for voltage steps from -60 mV to -40 mV (bottom black) or -10 mV (top black) are shown. A voltage-sensitive inward current (arrowhead) in the oRG cell is abolished by TTX (grey trace, -10 mV). Scale bar, 10 µm.
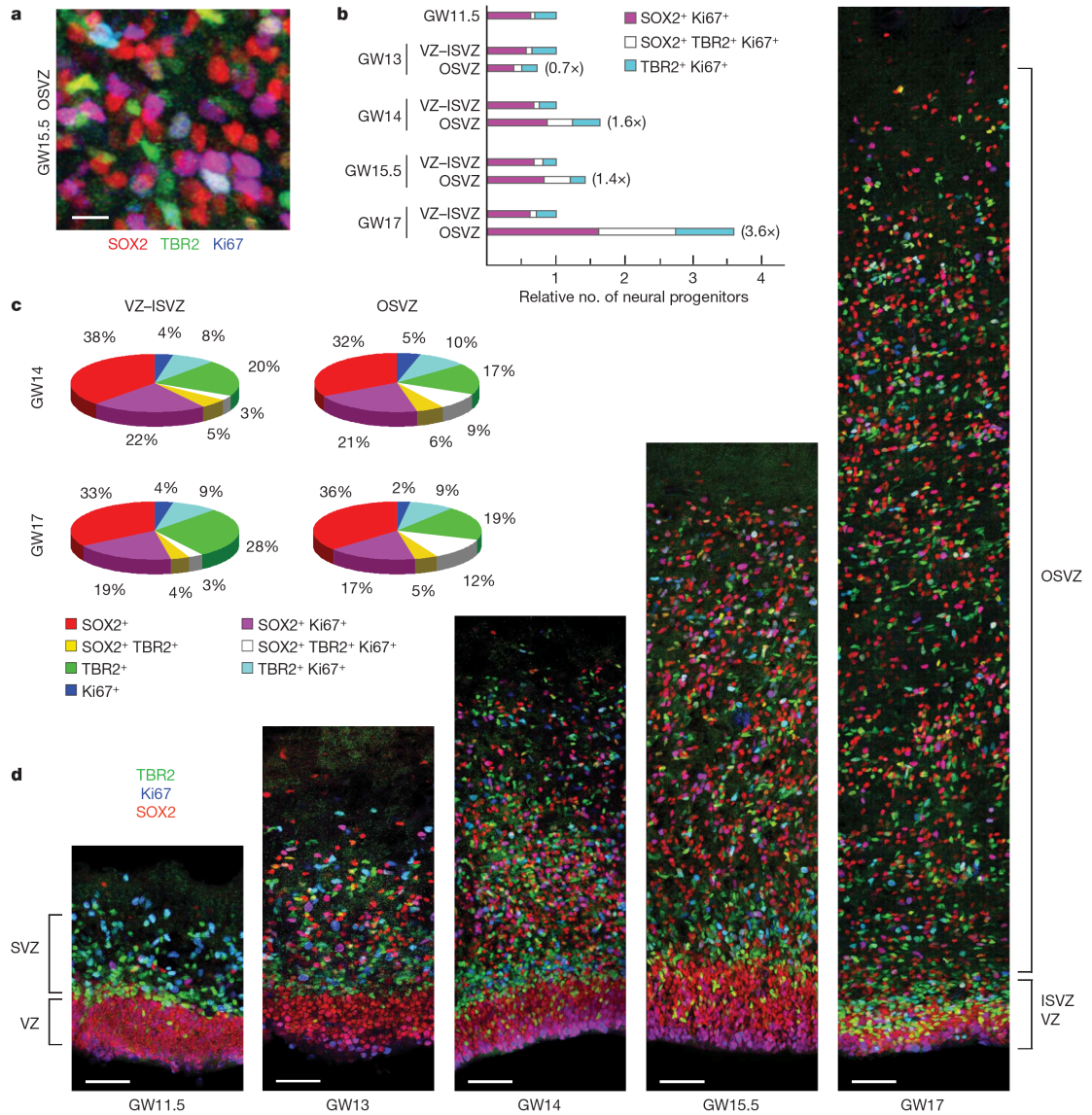
Figure 4. The human OSVZ is the predominant neurogenic zone during mid-gestational cortical development.

a, Image of GW15.5 OSVZ demonstrating the extent of SOX2 (red), TBR2 (green) and Ki67 (blue) co-labeling. Scale bar, 10 μm. **b**, Number of actively cycling OSVZ neural progenitors surpasses the VZ–ISVZ during mid-gestation. Ki67$^+$ cells that co-express SOX2 and/or TBR2 were counted and compared over the same width of OSVZ versus VZ–ISVZ in three representative fields for each age (similar to those in **d**), and averaged. **c**, The OSVZ and VZ–ISVZ contain similar proportions of neural progenitor cell types. Cortical progenitors were counted and classified into seven categories on the basis of SOX2, TBR2 and Ki67 expression. See Supplementary Fig. 13 for graphs of all ages. Only progenitor cells were considered, because roughly half of the OSVZ nuclei (marked by 4′,6-diamidino-2-phenylindole (DAPI), not shown) are SOX2$^-$ TBR2$^-$ Ki67$^-$. **d**, Substantial growth of the OSVZ from GW11.5–17 shown by SOX2, TBR2 and Ki67 staining. Progenitor cells in the inner fiber layer (not labelled) were included in OSVZ counts as they are superficial to the VZ–ISVZ. Scale bars, 50 μm.
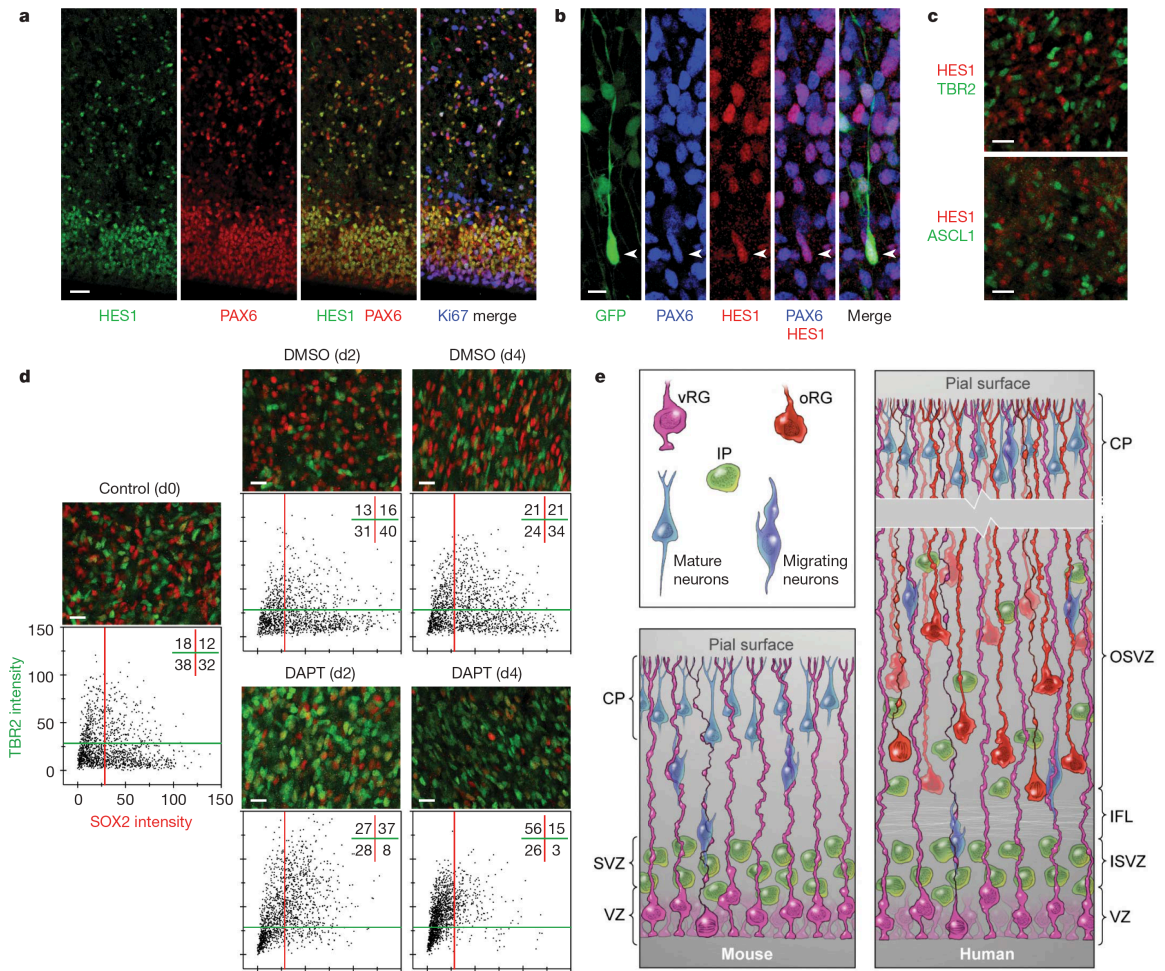
Figure 5. OSVZ progenitors require Notch signaling to remain undifferentiated.

a, Co-expression analysis of the Notch effector HES1 (green), PAX6 (red) and Ki67 (blue) in GW15.5 cryosection. Scale bar, 25 μm. **b**, AdenoGFP-labelled oRG cell (white arrowhead) expressing PAX6 (blue) and HES1 (red) in a GW15.5 cortical slice (see text for cell counts). Scale bar, 10 μm. **c**, The Notch effector HES1 (red) does not co-label with markers of neuronal commitment (TBR2 or ASCL1, green) in GW15.5 OSVZ. Scale bars, 20 μm. **d**, OSVZ cells undergo neuronal differentiation after inhibition of Notch signaling. GW15.5 slices cultured with dimethylsulphoxide (DMSO; control) or 10 μM DAPT to inhibit Notch signaling were stained for SOX2 (red) and TBR2 (green) to identify primary versus committed progenitors. Fluorescence intensity of SOX2 versus TBR2 in OSVZ cell nuclei was quantified, plotted, and defined into quadrants using day 0 (d0) as a reference for positive and negative cells. The percentages in each quadrant are shown in the top right. Day 4 percentages are averages of two experiments. Scale bars, 20 μm. **e**, Model of human cortical development in comparison to the mouse. A second set of primary and secondary neural progenitors proliferates extensively in the human OSVZ in addition to periventricular progenitors. CP, cortical plate; IFL, inner fiber layer.
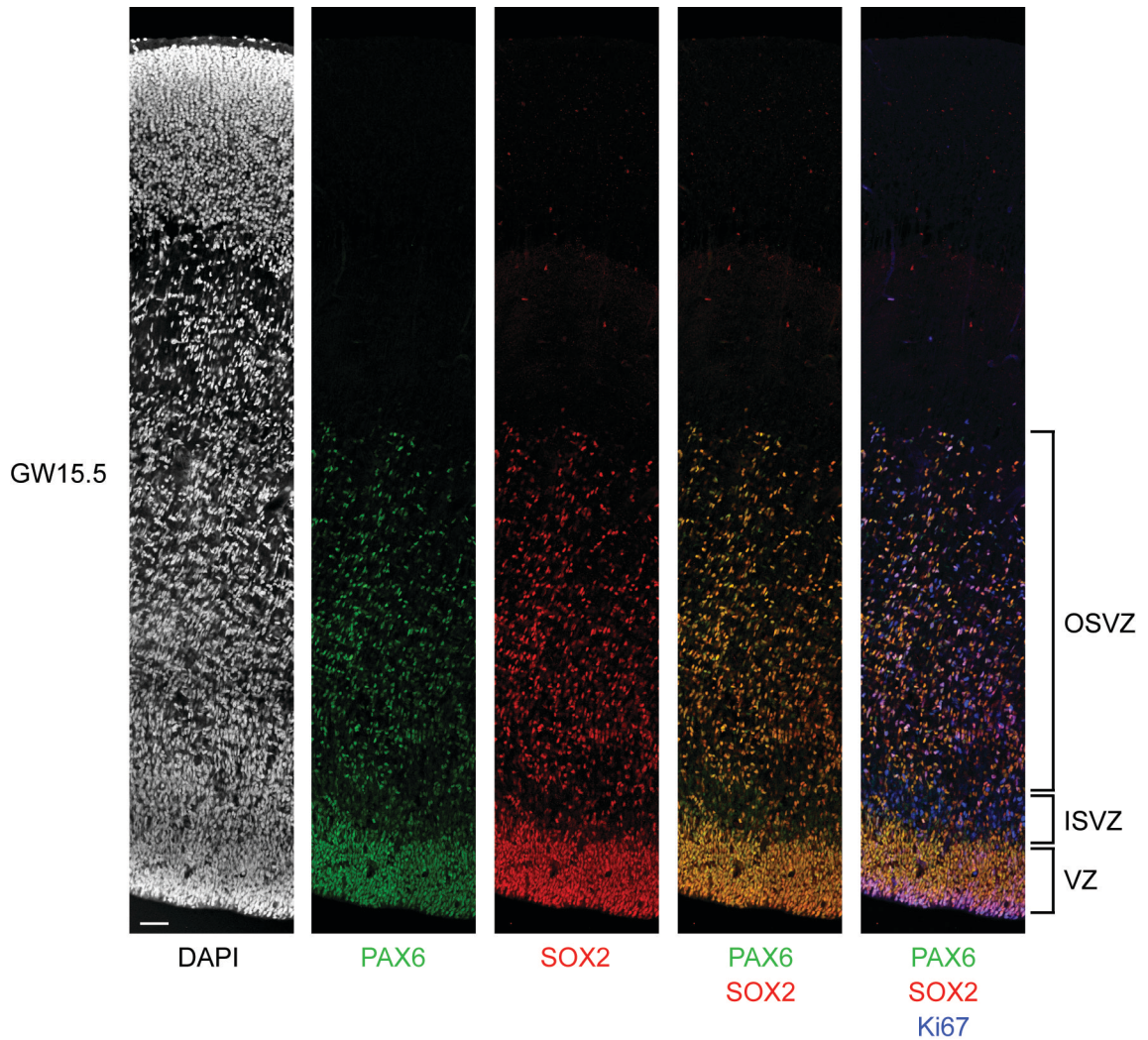
Supplementary Figure 1. Comparison of PAX6, SOX2 and Ki67 localization in the developing human cortex.

Human fetal cortical sections from GW15.5 were triple-immunostained for PAX6, SOX2 and Ki67, visualized by confocal microscopy, and analyzed for co-localization of markers. SOX2 and PAX6 co-localized in the VZ-ISVZ and OSVZ but not in upper layers. In the OSVZ, 93% (746 out of 803) of PAX6^{+} cells coexpressed SOX2, and 51% of these (381 out of 746) were Ki67^{+}. Similar proportions were observed in OSVZ cell counts from other gestational ages. Scale bar, 50 μm.
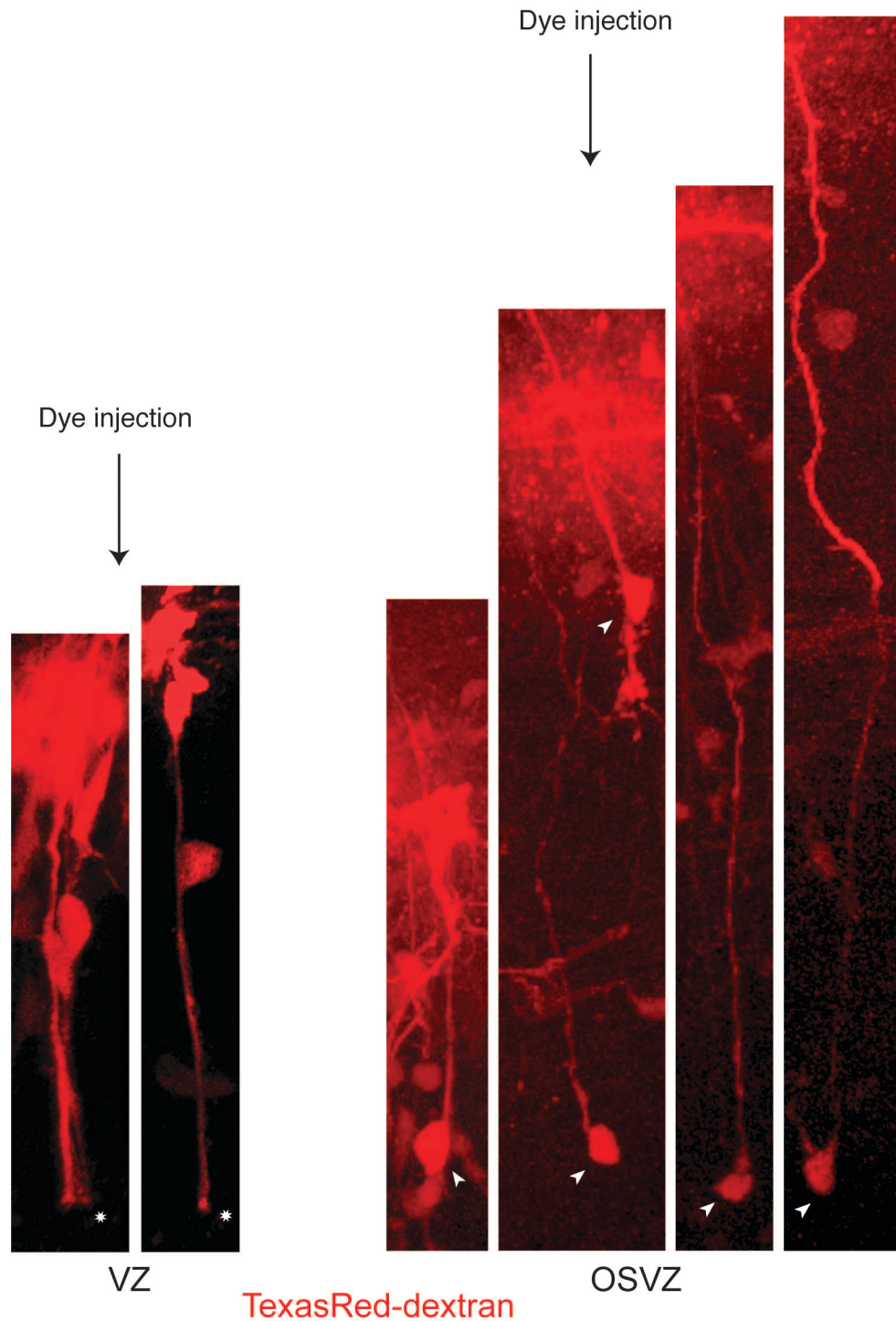
Supplementary Figure 2. Examples of dye electroporation into VZ and OSVZ cells.

Comparison of cell morphology in GW15.5 VZ versus OSVZ by dye electroporation. Labeled VZ cells demonstrated ventricular endfeet (stars) typical of radial glial cells. OSVZ cells were routinely labeled by injected dye that diffused down through their radial processes to the cell body (arrowheads) but no further.
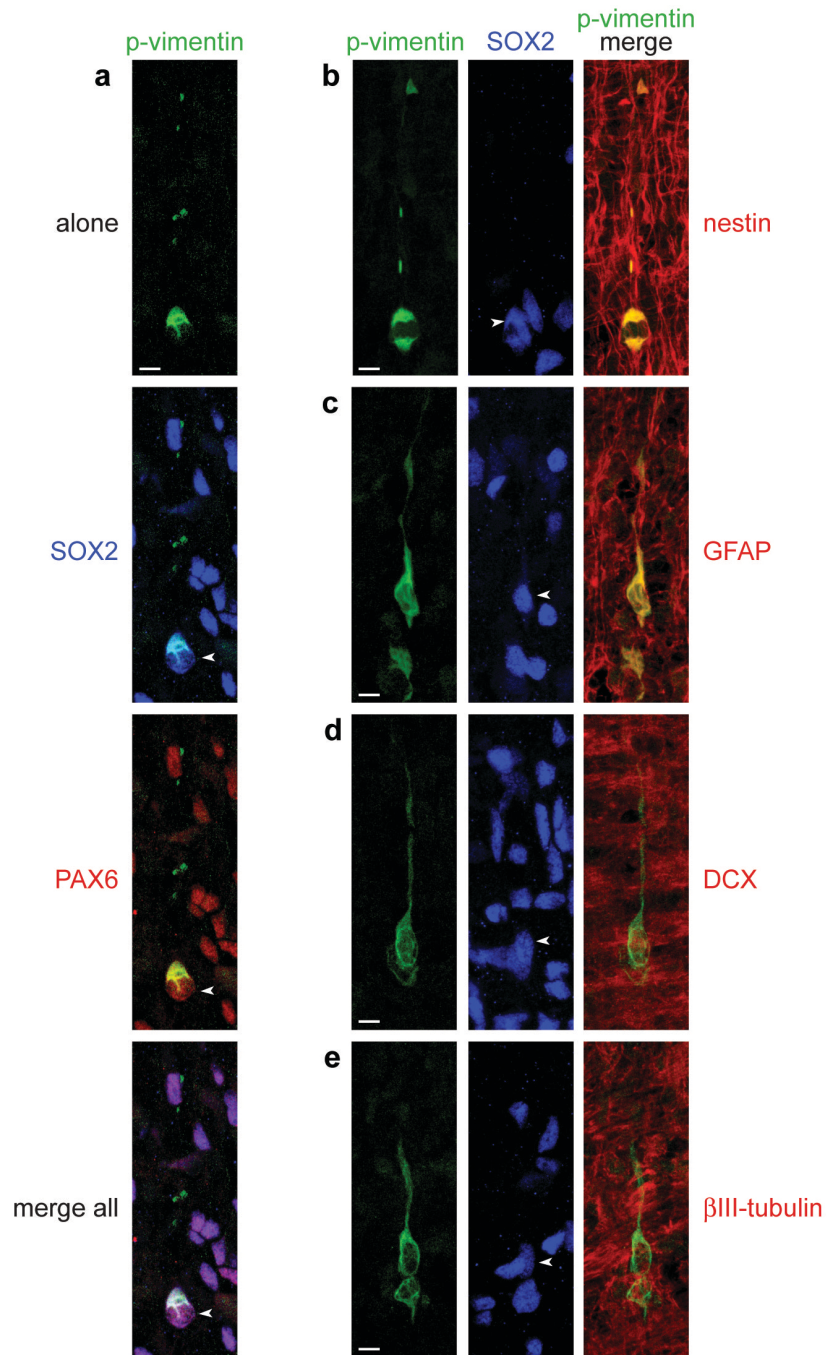
Supplementary Figure 3. Mitotic OSVZ cells with long basal processes express radial glial but not neuronal markers.

Phospho-vimentin[+] mitotic OSVZ cells (GW15) with long basal but not apical processes co-labelled with the radial glial cell markers SOX2 (267 out of 272), PAX6 (**a**, 27 out of 27), nestin (**b**, 31 out of 31), GFAP (**c**, 20 out of 20), but never with the early neuronal markers DCX (**d**, 27 out of 27) βIII-tubulin (**e**, 22 out of 22). Representative images are shown with white arrowheads indicating the nucleus of the phospho-vimentin[+] cell in question. Scale bars, 5 μm.
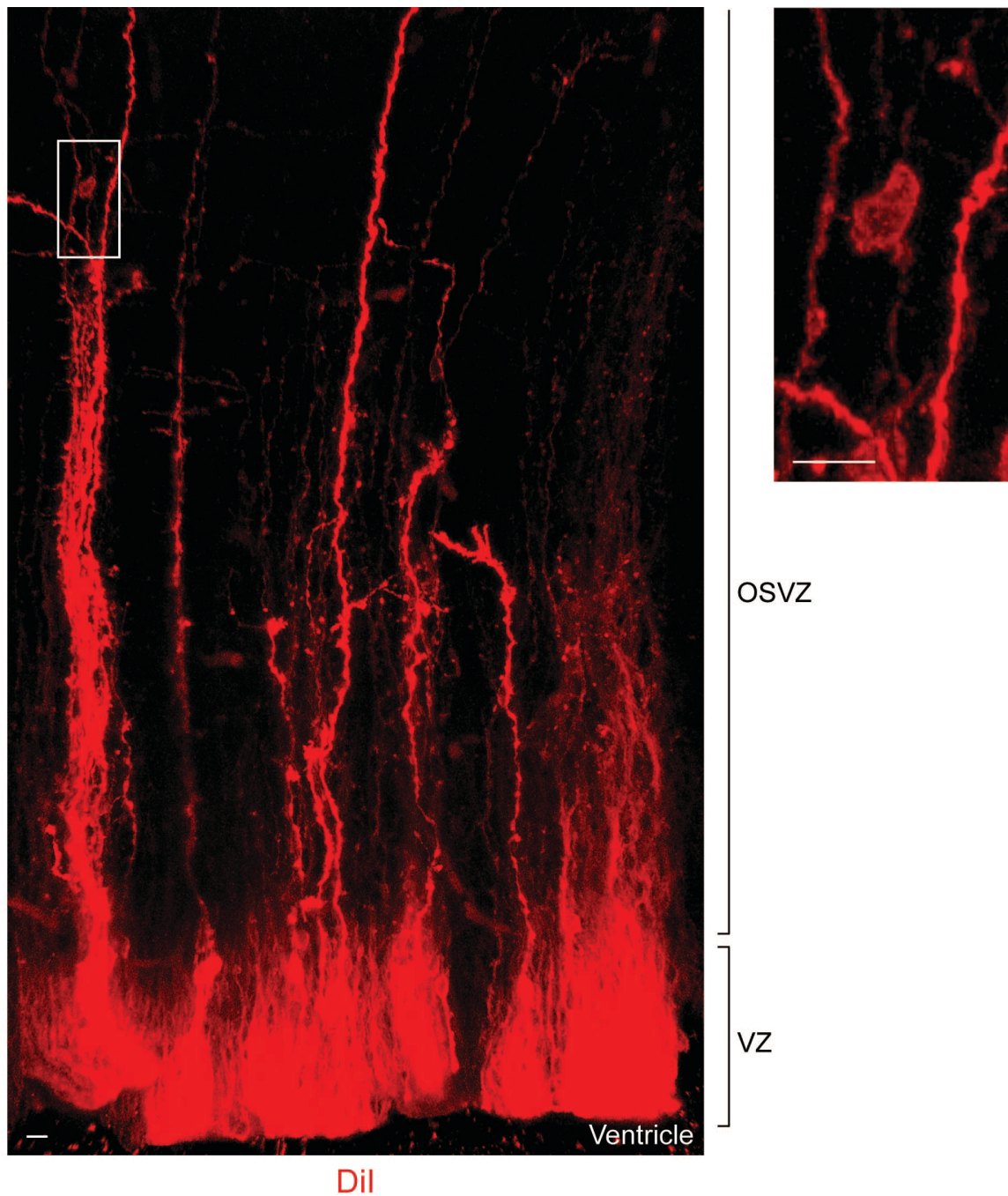
Supplementary Figure 4. DiOlistics labeling from the ventricular surface of GW15 human cortex.

Fixed GW15 cortex labeled from the ventricular surface with DiI-coated 1-μm beads (DiOlistics). DiI fully diffused throughout the membranes of cells for 3.5 weeks and then tissue was re-fixed. Inset demonstrates a rare example of an OSVZ cell labeled by diffusion from the ventricular surface, implying that the cell has ventricular contact. Scale bars, 10 μm.
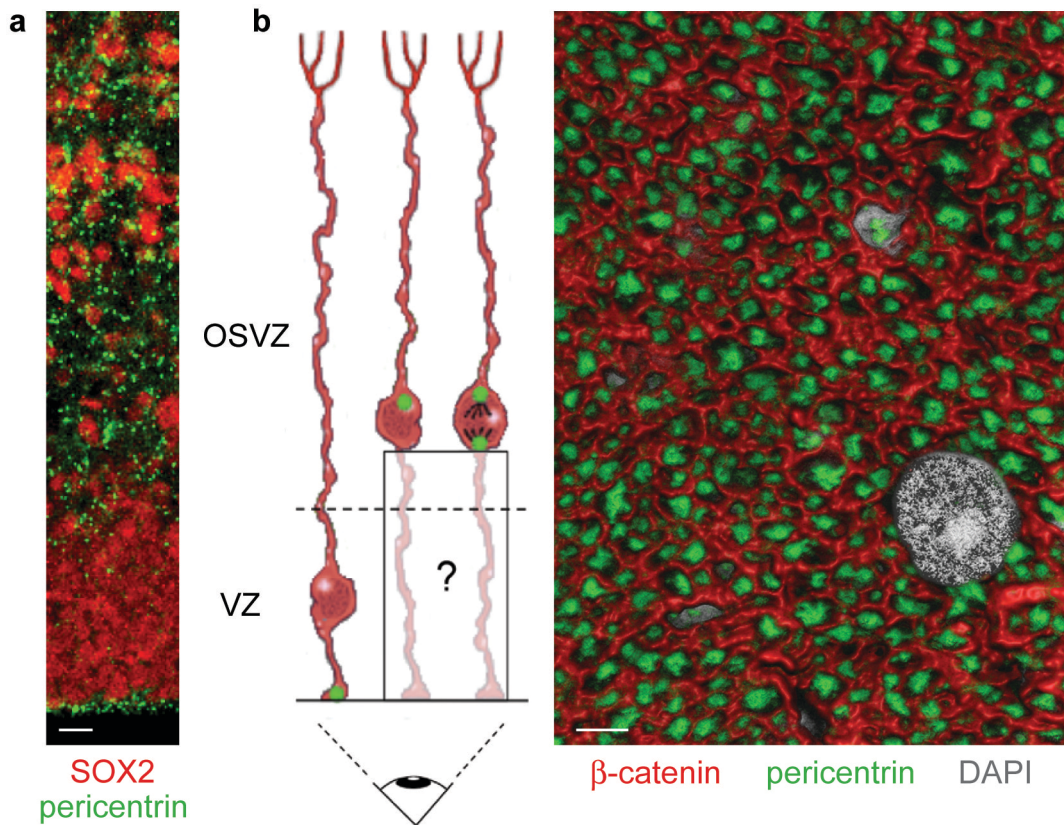
Supplementary Figure 5. Ventricular endfeet do not originate from OSVZ cells as nearly all endfeet are occupied by a centrosome.

a, SOX2 (red) and pericentrin (green) staining of GW15.5 cortex shows restriction of centrosomes in VZ cells to the ventricular surface. Scale bar, 15 μm. **b**, (left) Schematic depicting that ventricular endfeet originating from OSVZ radial glial cells would lack centrosomes since their centrosomes reside in the cell body (see Fig. 1c). (right) Confocal imaging and three-dimensional rendering of an 'en face' view of GW15.5 ventricular surface. Whole-mount section stained for β-catenin (adherens junctions, red) and pericentrin (centrosomes, green) shows the distribution of centrosomes in ventricular endfeet. DAPI counterstain (grey) reveals occasional mitotic nuclei at the ventricular surface. At least 94% of 649 counted endfeet were occupied with centrosomal staining (5 fields of view counted). Scale bar, 3 μm.
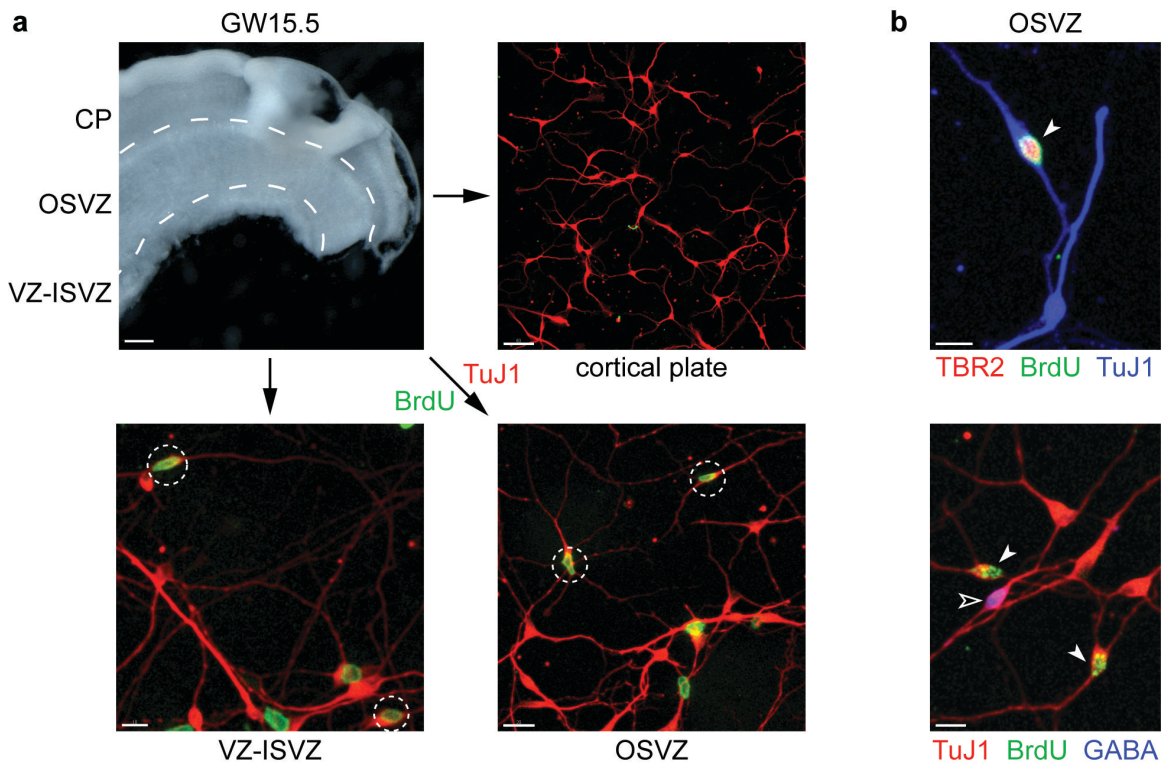
Supplementary Figure 6. OSVZ progenitor cells generate neurons of the excitatory lineage.

a, GW15.5 cortical slices were microdissected (dotted lines) to separate the OSVZ from the VZ-ISVZ and cortical plate (CP). Cells from each region were dissociated and cultured *in vitro* with BrdU to label proliferating cells. After 7 days, cells were fixed and stained for BrdU and the neuronal marker βIII-tubulin (TuJ1 antibody). Newborn neurons (circled) were observed in VZ-ISVZ and OSVZ but not CP cultures. Scale bars: 250 μm (brightfield), 50 μm (CP), 20 μm (OSVZ), 10 μm (VZ-ISVZ). **b**, OSVZ cells dissociated and cultured with BrdU as in (**a**) were immunostained for markers of excitatory or inhibitory neurons (TBR2 or GABA, respectively). Top: arrowhead shows newborn TBR2$^+$ neuron. Bottom: white arrowheads show newborn BrdU$^+$ TuJ1$^+$ GABA$^-$ neurons; clear arrowhead shows BrdU$^-$ TuJ1$^+$ GABA$^+$ neuron. Scale bars, 10 μm.
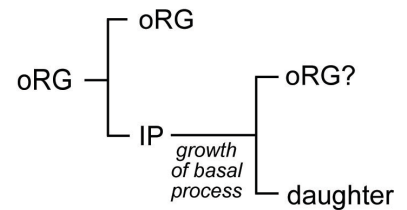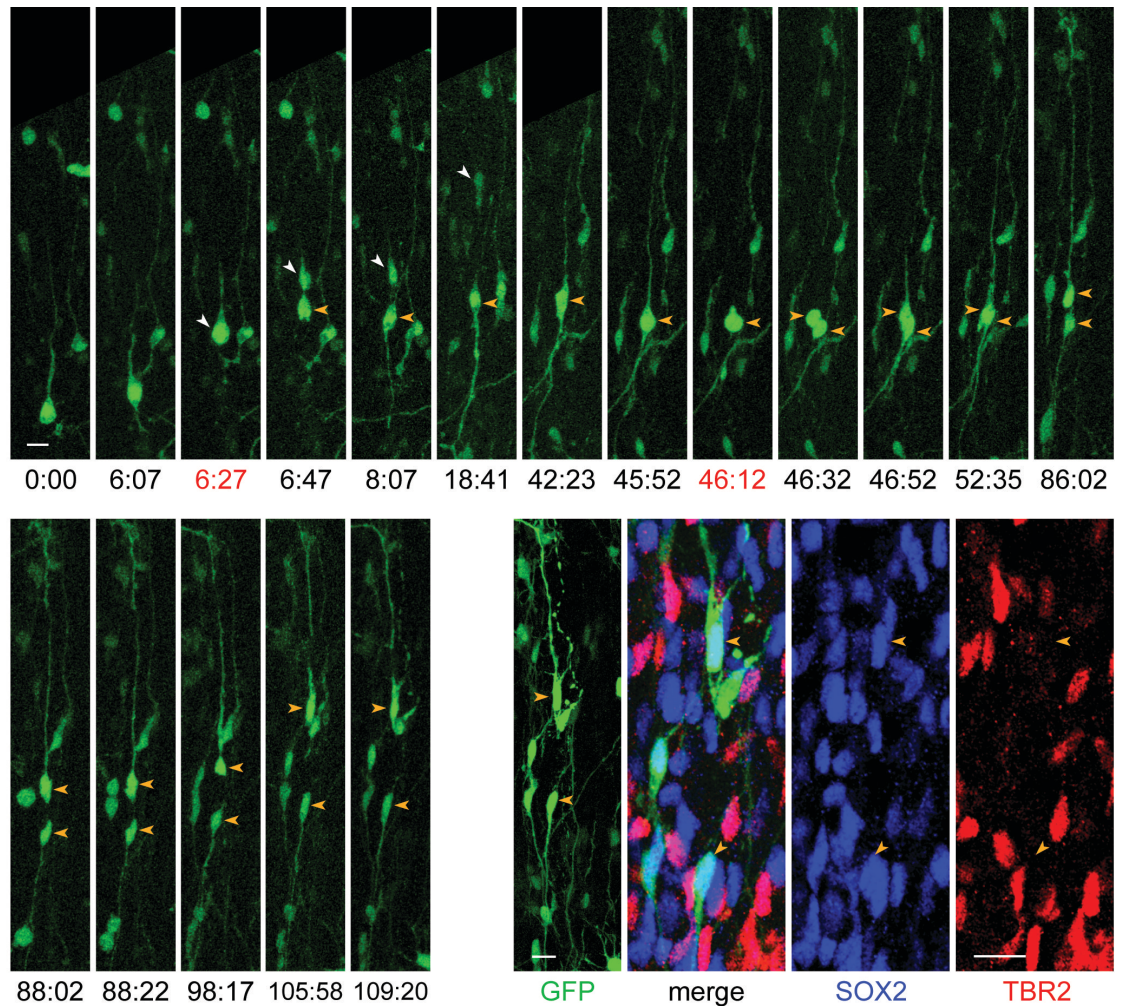
Supplementary Figure 7. OSVZ progenitor cell expansion: undifferentiated oRG daughter cell undergoes proliferative division and regains oRG morphology.

GW15.5 cortical slice was infected with GFP-adenovirus. 24 h later, oRG cell was identified by morphology and imaged at 20-min intervals. After first cell division, we followed the fate of the daughter intermediate progenitor (IP) cell (yellow arrowhead). The self-renewed oRG cell (white arrowhead) left the field of view. oRG daughter cell became bipolar and divided again, with the more basal daughter adopting oRG-like morphology. Both daughters of the IP cell remained SOX2$^+$ TBR2$^-$. First image shown (t=0:00) was 36 h after infection. Time, h:min (red for mitoses). Scale bars, 15 μm.
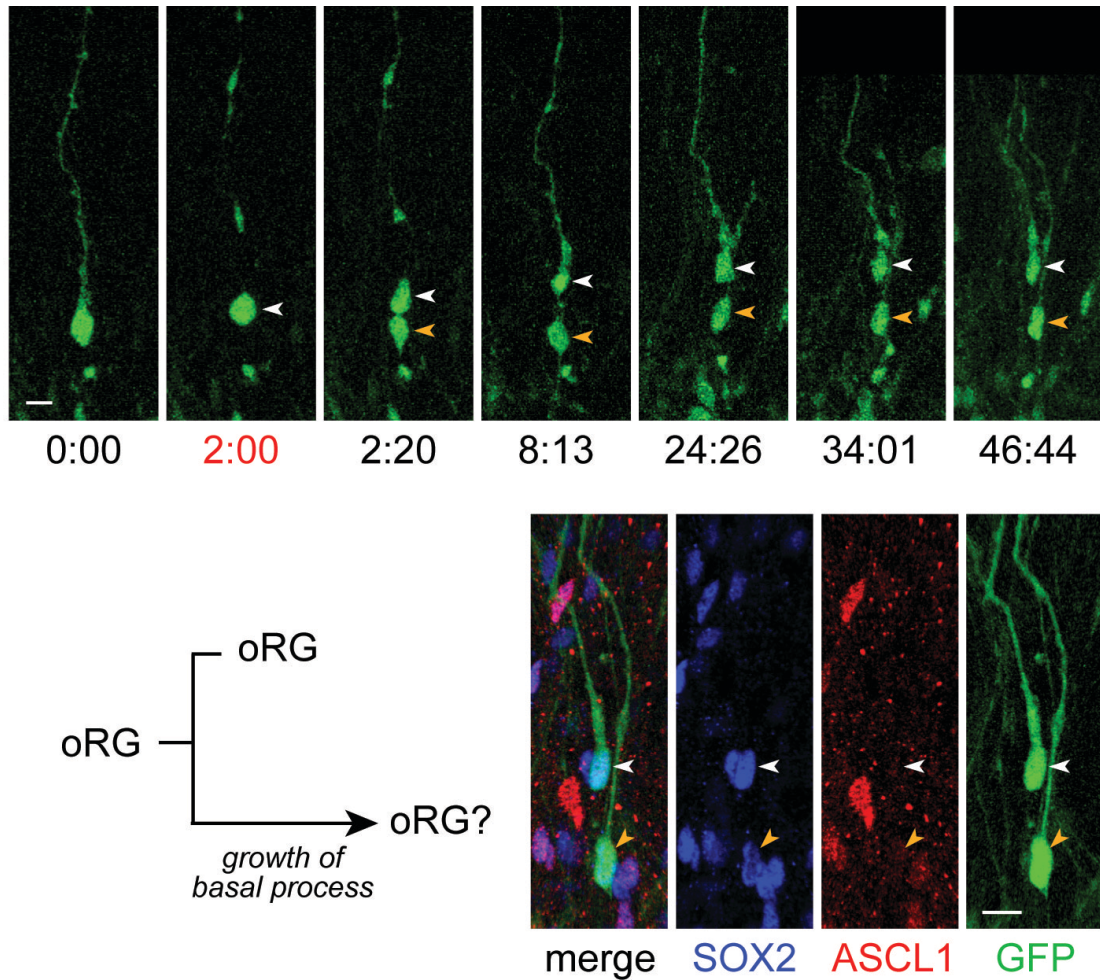
Supplementary Figure 8. OSVZ progenitor cell expansion: undifferentiated oRG daughter cell grows a new basal process and regains oRG cell morphology.

GW15.5 cortical slice was infected with GFP-adenovirus. 24 h later, oRG cell was identified by morphology and imaged at 20-min intervals. After self-renewing division of oRG cell (white arrowhead), the oRG daughter (yellow arrowhead) that did not inherit the basal process grew a new one and adopted oRG-like morphology. Both oRG and daughter cell remained SOX2^{+} ASCL1^{-}. First image shown (t=0:00) was 98 h after infection. Time, h:min (red for mitosis). Scale bars, 10 μm.
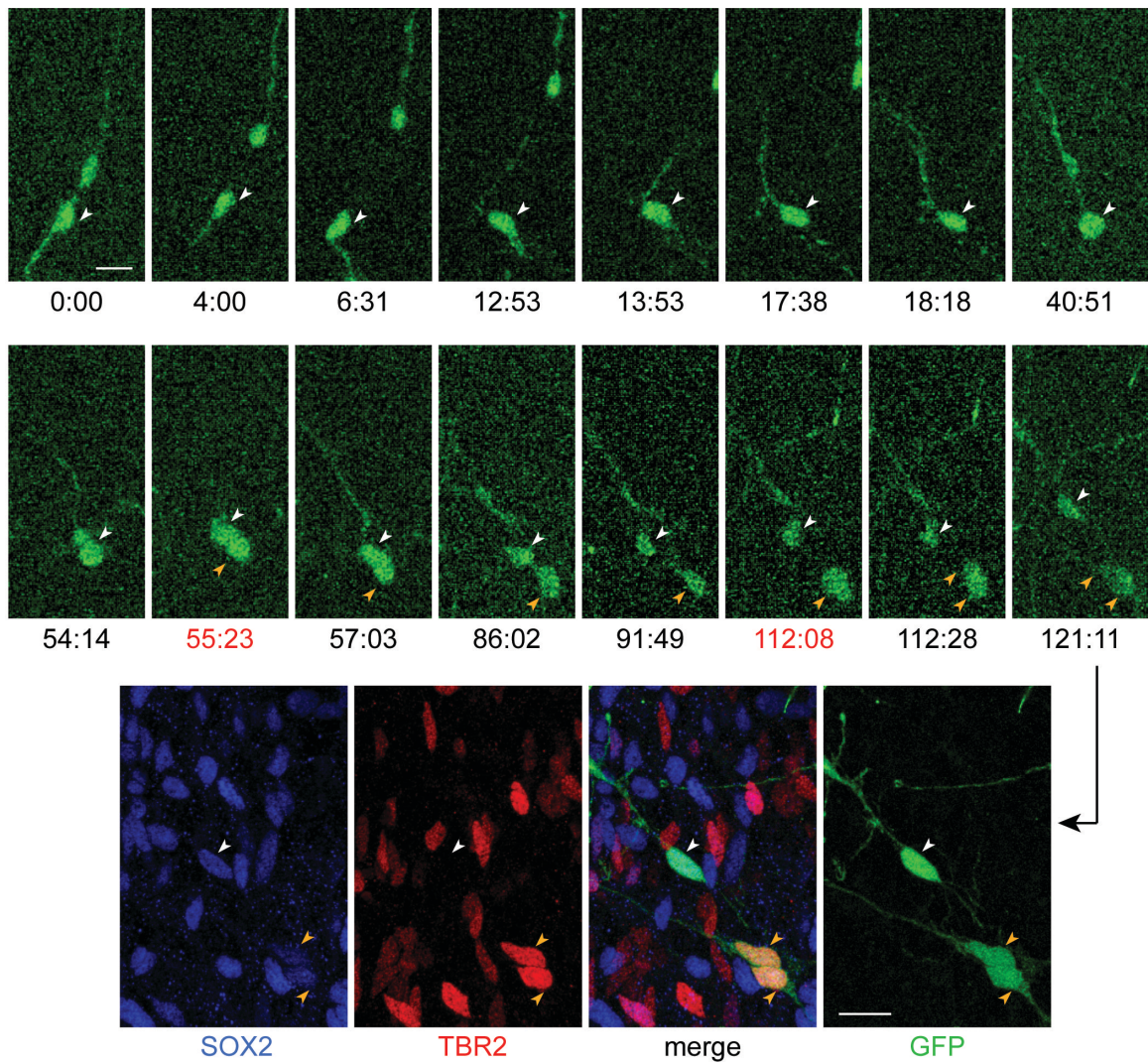
Supplementary Figure 9. Asymmetric division of oRG daughter cell yields one undifferentiated cell and one neuronal intermediate progenitor (IP) cell.

GW15.5 cortical slice was infected with GFP-adenovirus. 24 h later, oRG cell and daughter were identified by morphology and imaged at 20-min intervals. Original oRG cell left the field of view. oRG daughter cell (white arrowhead) grew a basal process and underwent self-renewing division, remaining SOX2$^+$ TBR2$^-$ while giving rise to a neuronal IP cell (yellow arrowhead) that divided again, yielding two TBR2$^+$ cells. First image shown (t=0:00) was 24 h after infection. Time, h:min (red for mitoses). Scale bars, 15 μm. D, daughter.
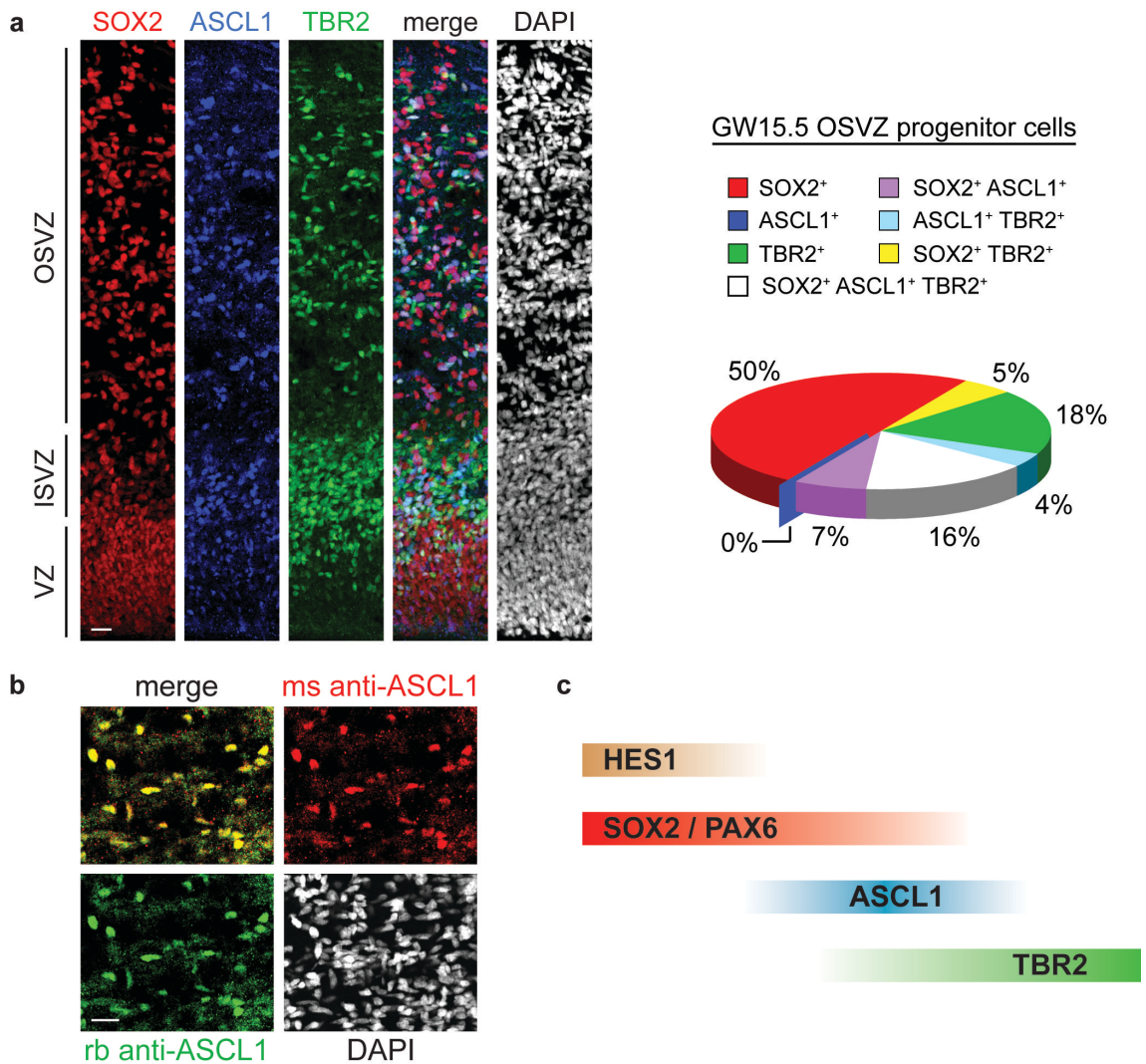
Supplementary Figure 10. ASCL1 expression in GW15.5 cortical progenitor cells.

a, Immunostaining for SOX2 (red), ASCL1 (blue), and TBR2 (green) in GW15.5 cryosections. Cell counting showed that every ASCL1^{+} cell also expresses SOX2 and/or TBR2, consistent with a role for ASCL1 in neuronal commitment. Scale bar, 25 μm. **b**, Perfect co-labeling of two anti-ASCL1 antibodies (rabbit antibody used for fate analysis and DAPT-treated slice cultures; mouse antibody used for testing co-expression with TBR2 in the current figure) confirms staining specificity for the same cells in the OSVZ. Scale bar, 25 μm. **c**, Schematic depicting sequence of transcription factor expression during human cortical neuronal differentiation. Co-labeling in panel (**a**) demonstrated ASCL1 expression in SOX2^{+} and TBR2^{+} cells, surprisingly placing ASCL1 in the same lineage as excitatory neuronal precursors. The Notch effector HES1 co-labels with PAX6 but not ASCL1 or TBR2 (see Fig. 5), consistent with its role in maintaining the undifferentiated state of neural progenitor cells.
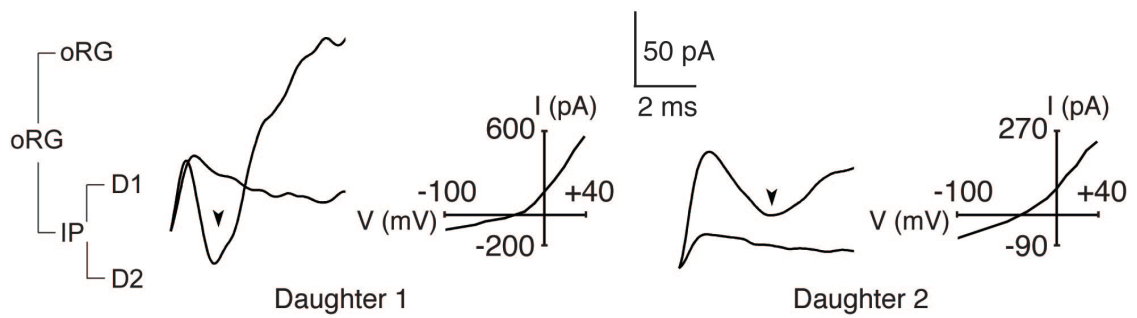
Supplementary Figure 11. Similar electrophysiological properties in daughter cells of an oRG cell-derived intermediate progenitor (IP) cell.

Patch-clamp recordings of sister cells from division of an oRG-derived IP cell after real-time imaging (see schematic, 5 days in culture). Current-voltage relationships and current traces for voltage steps from -60mV to -40mV (lower trace) or -10mV (upper trace) are shown. Note the inward currents (arrowheads) in both sisters, which were abolished by TTX (not shown). D, daughter.

TBR2
Ki67
SOX2

SVZ

VZ

mouse E13   human GW11.5
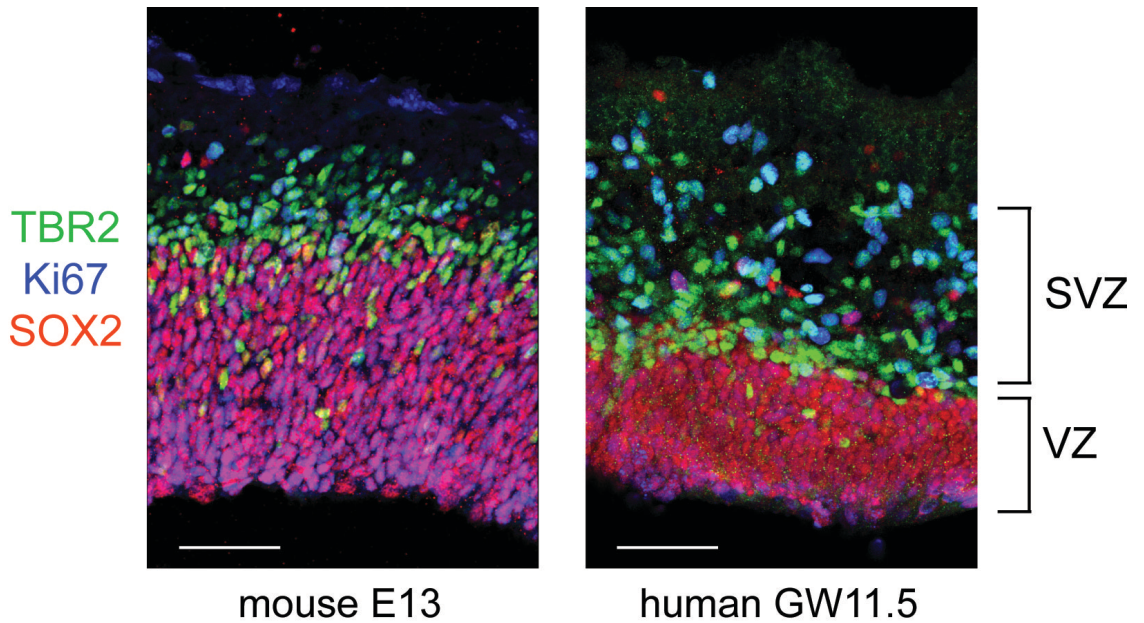
Supplementary Figure 12. Progenitor zone organization in GW11.5 human cortex resembles that of E13 mouse.

Triple-immunostaining of fixed cortical sections from embryonic day 13 (E13) mouse and gestational week 11.5 (GW11.5) human showing overlay of SOX2 (red), a RG stem cell marker; TBR2 (green), an intermediate progenitor cell marker; and Ki67 (blue), a proliferation marker. Scale bars, 50 μm.
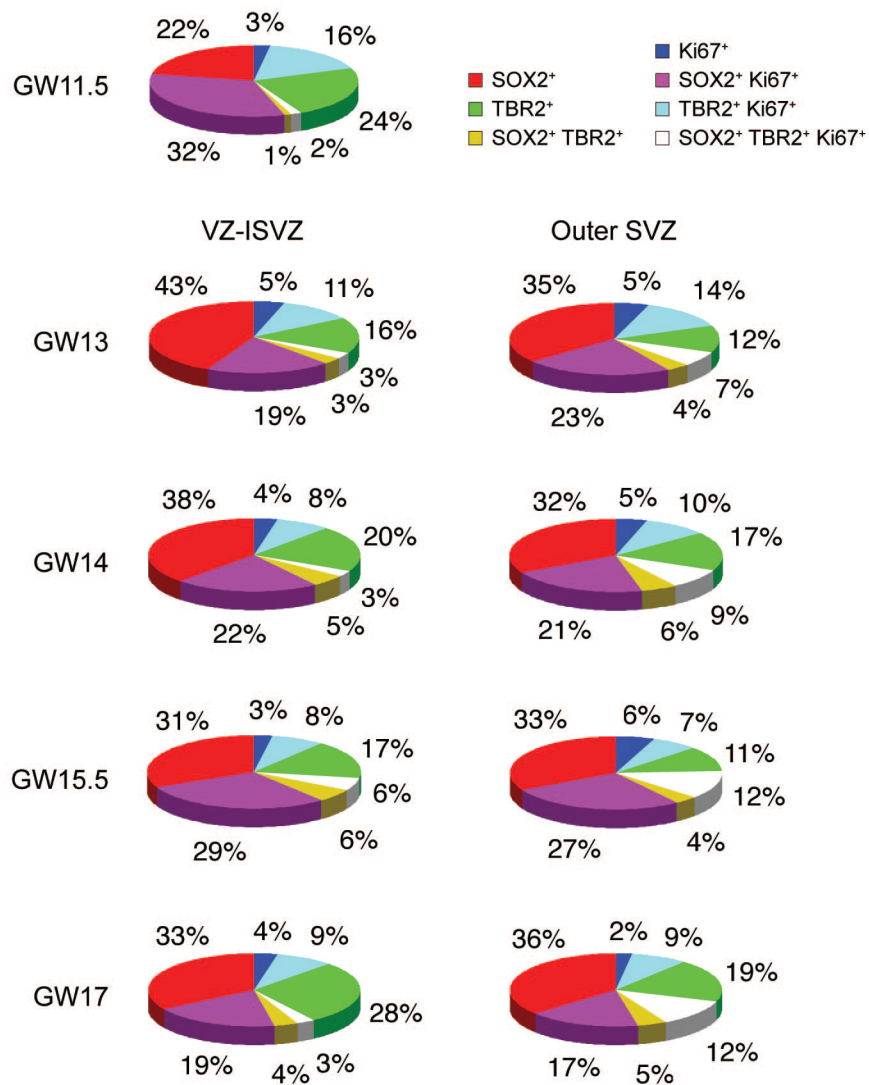
Supplementary Figure 13. The human OSVZ is a duplicated neurogenic zone, containing the same progenitor cell types as the VZ-ISVZ and in similar proportions.

Human fetal cortical sections were triple-immunostained for SOX2, TBR2, and Ki67, visualized by confocal microscopy, analyzed for co-localization, and cells categorized into one of seven progenitor classes. Relative sizes of these seven classes were compared between VZ-ISVZ and OSVZ of the same age and across ages (GW11.5-17, see Fig. 4d).
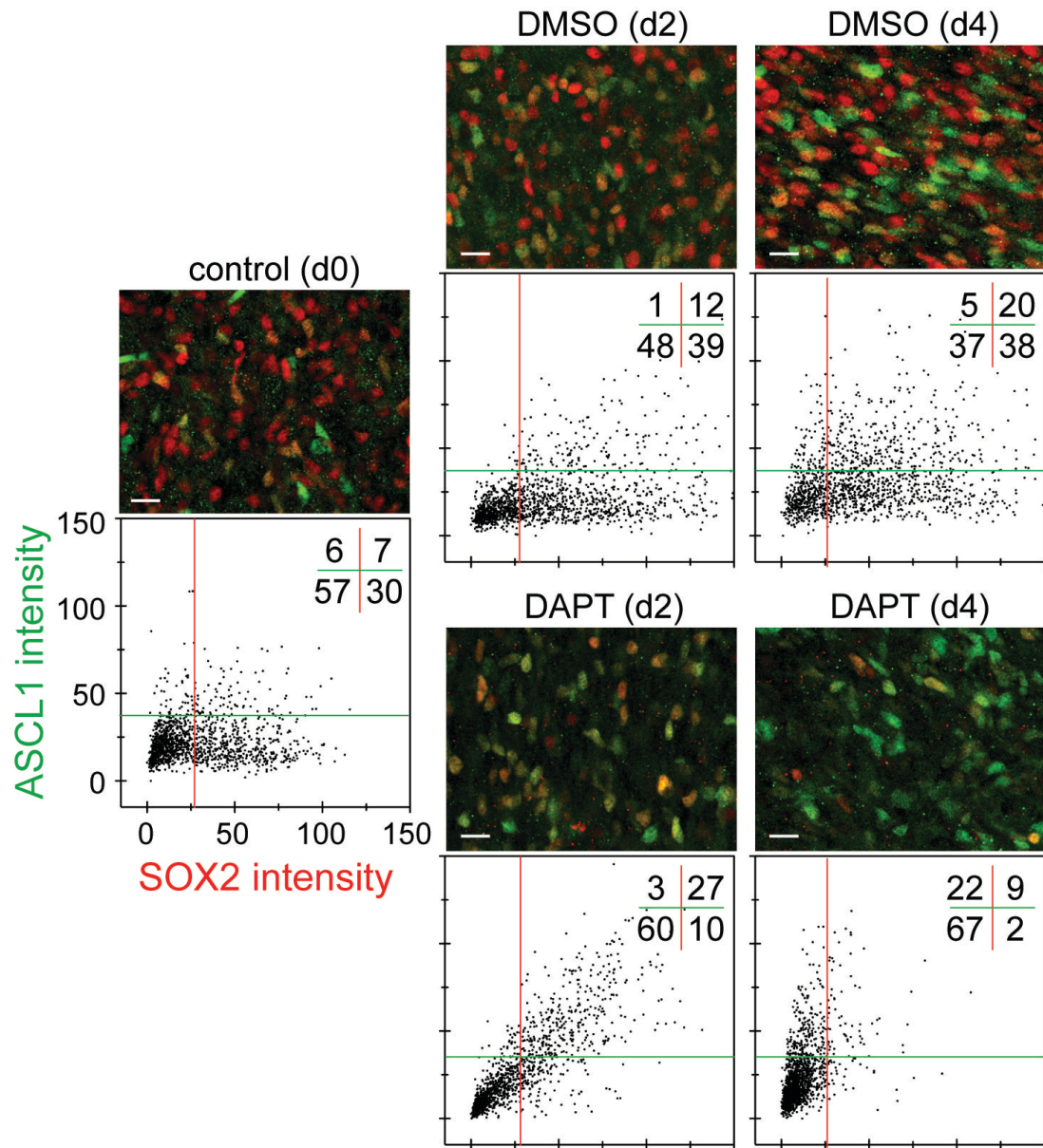
Supplementary Figure 14. Neuronal differentiation of SOX2$^+$ OSVZ progenitor cells upon inhibition of Notch signaling.

GW15.5 cortical slices were cultured in the presence of DMSO (control) or 10 μM DAPT to inhibit Notch signaling. Slices were fixed after 0, 2, or 4 days and immunostained for SOX2 (red) or ASCL1 (green) to identify primary vs. neuronally committed progenitor cells. Expression of SOX2 and ASCL1 in individual OSVZ cell nuclei was quantified by measuring fluorescence intensity and plotted with each dot representing one cell. Two fields were analyzed for each condition. Plots were defined into quadrants using day 0 (d0) as a control for positive and negative cells. Percentages of cells in each quadrant are shown in upper right of each plot. Day 4 percentages are averages of two experiments. Scale bars, 20 μm.

Supplementary Movie 1. Multiple examples of mitotic somal translocation and oRG cell division.

This movie can be accessed online at:

http://www.nature.com/nature/journal/v464/n7288/extref/nature08845-s2.mov

A field of densely labeled adenoGFP$^+$ OSVZ cells from gestational week 15 (GW15) is shown over the course of ~20 h in 20-min intervals to illustrate the frequency and characteristic behavior of oRG (outer radial glia-like) cell divisions (8 examples). oRG cells remain relatively stationary during interphase but undergo a rapid translocation along their basal fiber directly prior to division and cytokinesis. oRG cell divisions exhibit a horizontal cleavage plane with respect to the ventricular surface.

Supplementary Movie 2. oRG cell division highlighting mitotic somal translocation, followed by division of intermediate progenitor (IP) daughter.

This movie can be accessed online at:

http://www.nature.com/nature/journal/v464/n7288/extref/nature08845-s3.mov

An oRG cell (GW15 OSVZ, 22 minutes per frame) undergoes mitotic somal translocation of ~140 μm in distance and divides (t=12:18, see Fig. 2b). The upper cell inherits the basal fiber whereas the lower cell rapidly extends a prominent process toward the ventricle. The lower daughter adopts bipolar morphology near the end of the sequence and divides one more time (t=45:46), revealing that it is an intermediate progenitor cell. Fate analysis shows that all three resultant cells are SOX2$^+$ TBR2$^-$ (see Fig. 3a), suggesting that these are proliferative divisions of undifferentiated progenitors. The upper daughter of the second division appears to adopt oRG cell morphology.

Supplementary Movie 3. oRG cell divides and self-renews twice.

This movie can be accessed online at:

http://www.nature.com/nature/journal/v464/n7288/extref/nature08845-s4.mov

An oRG cell (GW15 OSVZ, 22 minutes per frame) undergoes two self-renewing divisions (t=0:44 and t=44:38) each with mitotic somal translocation and inheritance of the basal fiber, as well as generation of a daughter cell.

Supplementary Movie 4. Two self-renewing oRG cell divisions followed by an intermediate progenitor (IP) daughter cell division.

This movie can be accessed online at:

http://www.nature.com/nature/journal/v464/n7288/extref/nature08845-s5.mov

An oRG cell (GW15 OSVZ, 22 minutes per frame) undergoes two self-renewing divisions (t=5:30, t=43:32). The daughter from the first division adopts a bipolar morphology and also divides (t=46:50). This sequence shows that oRG cells can undergo multiple rounds of self-renewing division and generate intermediate progenitor daughter cells.

METHODS

Summary

Fetal cortical tissue was collected from elective pregnancy termination specimens at San Francisco General Hospital, usually within 2 h of the procedure. Tissues were examined only with previous patient consent and in strict observance of legal and institutional ethical regulations. Research protocols were approved by the Committee on Human Research (institutional review board) at University of California, San Francisco. Immunohistochemistry was performed on paraformaldehyde (PFA)-fixed tissue using standard protocols. Dye electroporation was performed on vibratome sections as described (Haas et al., 2001). DiOlistics (Gan et al., 2000) was performed on fixed tissue using fixable CM-DiI (Molecular Probes). Whole-cell patch-clamp electrophysiology was performed using standard protocols. Cortical slice culture was performed as described (Noctor et al., 2004), with some modifications, using GFP-retrovirus or -adenovirus to label cells. Time-lapse and still confocal imaging was performed using a TCS SP5 confocal microscope (Leica). Image analysis, three-dimensional rendering, and cell counting were done in Imaris (Bitplane) and Photoshop (Adobe). Co-localization was calculated using Matlab (Mathworks) and ImarisXT (Bitplane).

Fetal tissue collection

Fetal cortical tissue was collected from elective pregnancy termination specimens at San Francisco General Hospital, usually within 2 h of the procedure. Tissues were examined only with previous patient consent and in strict observance of legal and institutional ethical regulations. Research protocols were approved by the Committee on Human Research (institutional review board) at University of California, San Francisco. Gestational age was

determined using fetal foot length. Brain tissue was transported in L-15 medium on ice to the laboratory for further processing.

Immunohistochemistry and confocal imaging

Brain tissue was fixed in 4% PFA in PBS at 4 °C for 3 days, dehydrated in 30% sucrose in PBS, embedded and frozen at -80 °C in O.C.T. compound (Tissue-Tek), sectioned on a Leica CM3050S (50 or 20 μm) and stored at -80 °C. Cryosections were subjected to heat/citrate-based antigen retrieval for 5 min and permeabilized and blocked overnight in PBS plus 0.1% Triton X-100, 10% serum, 0.2% gelatin. Primary incubations were 3 h at room temperature or 4 °C overnight. Washes and secondary incubations were standard procedures. Vibratome-sliced sections (using Leica VT1200S at 250 or 300 μm) were not dehydrated but stained similarly except with longer antigen retrieval (15 min), antibody incubations (48 h primary, 24 h secondary at 4 °C, 0.5% Triton X-100), and washing periods. For the whole-mount stain in Supplementary Fig. 5b, the sliver ~200 μm proximal to the ventricular surface from a slab of fixed tissue was carefully microdissected and stained as if a vibratome section. Images were acquired on a Leica TCS SP5 broadband laser confocal microscope. Composite images, such as those in Fig. 4d, were automatically stitched upon acquisition using 'Tilescan' mode of Leica software. Other than Fig. 1a and Supplementary Fig. 5b, images with morphological information are maximum intensity projections collected with at least 1-μm *z*-step size. Images with nuclear staining for counting were either single optical planes or maximum intensity projections with the same number of planes and depth across compared samples. Images from Fig. 1a and Supplementary Fig. 5b were taken with a ×100 objective at 0.3-μm step size and three-dimensional-rendered using Imaris imaging software (Bitplane).

Primary antibodies were: goat anti-SOX2 (Santa Cruz sc-17320, 1:250), rabbit anti-TBR2 (Millipore AB9618 or Abcam ab23345, 1:400), mouse anti-Ki67 (Dako F7268, 1:150 for human

tissue; BD Pharmingen 550609, 1:200 for mouse), rabbit anti-PAX6 (Covance PRB-278P, 1:200), mouse anti-βIII-tubulin (TuJ1, Covance MMS-435P, 1:250), rabbit anti-GABA (Sigma A2052, 1:1,000), rat anti-BrdU (Abcam ab6326, 1:100), chicken anti-GFP (Aves Labs GFP-1020, 1:1,000), mouse anti-phospho-vimentin (MBL International D076-3S (Ser 55), or D095-3 (Ser82), 1:500), rabbit anti-pericentrin (Abcam ab4448, 1:1,000), mouse anti-β-catenin (BD Transduction Labs 610153, 1:500), rabbit anti-nestin (Abcam ab5968, 1:200), rabbit anti-GFAP (Sigma G9269, 1:300), rabbit anti-DCX (Cell Signaling 4604, 1:200), rabbit anti-βIII-tubulin (Covance PRB-435P, 1:300), rabbit anti-hASH1/ASCL1 (CosmoBio SK-T01-003, 1:2,000), mouse anti-Mash1/ASCL1 (BD Pharmingen 556604, 1:500), and guinea-pig anti-HES1 (a gift from R. Kageyama, Baek et al., 2006, 1:250). Secondary antibodies were: AlexaFluor 488 (1:1,000), 546 (1:500), or 647 (1:500)-conjugated donkey anti-goat, -rabbit or -mouse IgG, or goat anti-chicken IgY (Invitrogen).

Cell counting

Confocal images (stack of ten images, 1 μm apart) were collected from sections stained for SOX2, TBR2 and Ki67. Three representative images (similar to Fig. 4d) were collected for each age. Each 'age' has $n = 1$, because recovery of usable tissue was limited. Fluorescence signal from nuclear immunoreactivity of SOX2, TBR2 and Ki67 was first counted individually using the 'spots' function in Imaris imaging software (Bitplane). A threshold for intensity mean was set to find fluorescent spots sized at 5-μm diameter from each channel as a representation of the number of actual cells. The preliminary sets of positive cells were then manually edited to correct software error. Double and triple co-localized spots were then calculated by Matlab (Mathworks) and the ImarisXT (Bitplane) module, and further edited to correct software errors. The numbers of total and co-localized spots were recorded and subtracted from each other to determine the number of single-, double- and triple-labeled cells. Counts from VZ–ISVZ and OSVZ were separated by a line defined by the outer limit of dense TBR2^{+} staining in the ISVZ. Percentages

were calculated within each sample and then averaged across the three images. OSVZ cell counts from Fig. 5a and Supplementary Figs 1 and 10 were done similarly.

Counts using oRG cell morphology as an initial measure (cells with phospho-vimentin[+] basal fibres, adenoGFP^{+} cells in HES1, BrdU and EdU labeling) were done by first identifying OSVZ cells that had long basal but not apical processes, and then examining their co-localization with markers in the other channels.

Co-localization of BrdU, TBR2 and GABA with βIII-tubulin in dissociated cells was counted manually in 25 fields of vision. Centrosome occupation of RG endfeet was counted in five fields of more than 100 endfeet by first identifying clear endfeet (areas outlined by β-catenin—while blinded to pericentrin), and then subtracting the number of endfeet that did not contain pericentrin.

In the Notch-inhibition experiments, the nuclear fluorescence of SOX2 and either TBR2 or ASCL1 was calculated by first finding 5-μm diameter spheres from the DAPI channel (as a volumetric representation of the nuclei) in two fields of OSVZ cells (cell number >1,200) for each condition using Imaris Spots, and then calculating fluorescence intensity mean values in each spot volume for the other two channels. Background (the lowest recorded intensity mean for each channel) was subtracted from the paired values and then shown as scatter plots (Fig. 5d and Supplementary Fig. 14).

Dissociated cortical cell culture and immunocytochemistry

GW15.5 cortex was vibratome-sliced at 300-μm thickness. Each slice was individually microdissected into three portions (VZ–ISVZ, OSVZ and CP) based on the columnar or stratified appearance of different regions that could be visualized under the dissecting microscope. We purposely erred towards the pial surface for both cuts to avoid contamination of OSVZ with VZ–

ISVZ cells, and to avoid contamination of CP with OSVZ cells. VZ–ISVZ, OSVZ and CP from

seven individual slices were pooled and dissociated using papain (Worthington Biochemical

Corporation) at 37 °C for 20 min and then trituration. Cells were pelleted by centrifugation,

resuspended, passed through cell-strainer caps, repelleted and resuspended. Cells were plated at

120,000 cells per well on 4-well Nunclon Δ multidishes (Sigma) coated with poly-l-ornithine

(Sigma) and laminin (Invitrogen) in RHB-A medium (Stem Cell Sciences) plus BrdU (Sigma,

15 μg ml^{-1}) and cultured at 37 °C, 5% CO_2 for 1 week with medium exchanged every 2 days. Cells

were fixed in 4% PFA for 20 min and processed for immunofluorescence microscopy as

described earlier with some exceptions. GABA stains were performed before antigen retrieval

and in the absence of detergent, followed by another PFA fixation, antigen retrieval and normal

staining for other antigens. For BrdU detection, all other antigens were stained first and fixed

with PFA, followed by 20 min in 2 N HCl, several rinses with buffer, and finally BrdU

immunostaining.

Dye electroporation

Lysine-fixable TexasRed-dextran (Molecular Probes) was focally electroporated into the OSVZ

of 250-μm vibratome slices from GW15.5 cortex (for Fig. 1a) and GW14 (Supplementary Fig. 2)

using similar methods as previously described (Haas et al., 2001). A P-97 micropipette puller

(Sutter) was used to generate pipettes of 0.6–1.0-μm tip width. Electrical stimulation was

generated by the Grass S48 Stimulator (5 pulses per second for 1 second at a time, pulse duration

of 2 ms, voltage of 30–100 V). Dye was allowed to diffuse for 30 min before fixation and

immunostaining.

DiOlistics labeling

GW15 cortical slabs were fixed in 4% PFA in PBS for 24 h. After soaking the fixed tissue

overnight in PBS plus 0.4% EDTA, we used the published 'DiOlistics' gene gun protocol (Gan et

al., 2000) to apply DiI-coated beads to either the pial or ventricular surface, with the following

modifications: 1.1-µm tungsten microcarriers (Bio-Rad) were coated with fixable CellTracker

CM-DiI (Molecular Probes). The Bio-Rad Helios Gene Gun System was substituted with a

common air duster (Fellowes). The beads were shot through 3.0-µm pore size filters from

Transwell Permeable Supports (Costar). CM-DiI was allowed to diffuse throughout the tissue in

0.4% EDTA in PBS for 3.5 weeks and then fixed in 4% PFA and vibratome-sliced for imaging

analysis.

Viral infection, cortical slice culture and real-time imaging

For Fig. 1b, replication-incompetent enhanced-GFP-expressing retrovirus (1×10^6 colony

forming units (c.f.u.)) was applied to a cortical slab for 1 h at room temperature in a minimal

volume of artificial cerebrospinal fluid (ACSF; 125 mM NaCl, 2.5 mM KCl, 1 mM $MgCl_2$, 2 mM

$CaCl_2$, 1.25 mM NaH_2PO_4, 25 mM $NaHCO_3$, 25 mM d-(+)-glucose, bubbled with 95% O_2/5%

CO_2). Tissue was then embedded in 4% low melting point agarose in ACSF, and vibratome-sliced

at 250 µm in ice-chilled ACSF. Slices were transferred to and suspended on Millicell-CM slice

culture inserts (Millipore) over culture medium in culture well plates and incubated at 37 °C, 5%

CO_2.

For all time-lapse imaging, as well as the BrdU, EdU and Notch experiments, 250–300-µm

vibratome slices were generated and suspended in culture medium as described earlier, and

CMV-GFP adenovirus (Vector Biolabs, 1×10^6 c.f.u.) was injected focally into the cortical plate

all along the slice to achieve sparse labeling in the OSVZ. Slices were first cultured at 37 °C, 5%

CO_2, 8% O_2 for ~24 h. Cultures were then transferred to an inverted Leica TCS SP5 with an on-stage incubator (while streaming 5% CO_2, 5% O_2, balance N_2 into the chamber), and imaged using a ×40 air objective at 20–22-min intervals (as specified) for up to 6 days with intermittent repositioning of the focal planes. Maximum intensity projections of the collected stacks (~30 μm at ~2.5-μm step size) were compiled and generated into movies. Mitotic somal translocation distances were measured using Imaris. Only mitotic cells that had long basal processes and no apical ones were considered as oRG cells.

All slice cultures other than those in Fig. 5 were cultured in 66% BME, 25% Hanks, 5% FBS, 1% N-2, 1% penicillin, streptomycin and glutamine (all Invitrogen) and 0.66% d-(+)-glucose (Sigma). For Fig. 2a, BrdU (Sigma, 15 μg ml^{-1}) was added at the beginning of slice culture and washed out after 12 h. EdU (Invitrogen, 15 μg ml^{-1}) was added 36 h after the initial pulse of BrdU and then fixed 48 h later. Slices were stained using EdU Click-iT (Invitrogen) and standard procedures. For Fig. 5d and Supplementary Fig. 14, slices were cultured in RHB-A medium plus 10 μM DAPT (Biomol International) or DMSO (control).

Electrophysiology

GW15 (time-lapse slices) and GW17 (blind acute recordings) cortical slices were prepared as earlier, or after time-lapse imaging, and held in room temperature ACSF until being moved to a 32 °C submersion-type chamber for recordings. Cells were targeted for recording by differential interference contrast (DIC) imaging or GFP immunofluorescence in slices that were previously time-lapse imaged. Patch pipettes were made from 1.5-mm outer diameter (OD)/0.86-mm inner diameter (ID) glass (Corning) and filled with (in mM) 130 K-gluconate, 4 KCl, 2 NaCl, 10 HEPES, 0.2 EGTA, 4 ATP-Mg, 0.3 GTP-disodium, 14 phosphocreatine-dipotassium (pH 7.25, 280–290 mOsm). For morphological reconstruction, 50 μM TexasRed-dextran (Molecular Probes) was included in the recording solution. Tetrodotoxin (TTX, 0.5 μM, Calbiochem) was

perfused onto cells locally using an Octaflow drug application system (ALA Scientific Instruments). Series resistances were typically between 5 and 15 MΩ and were continually monitored and compensated for throughout the recording sessions. Recordings were performed with a MultiClamp 700B amplifier (Axon Instruments) under infrared-differential interference contrast visualization using an Olympus BX50WI and a CCD camera (MTI). Recordings were acquired and analyzed using pClamp version 10 (Axon Instruments) and data were further analyzed in Excel (Microsoft). Input resistance was calculated from small (3–5 mV) 600-ms voltage deflections induced by square hyperpolarizing current injections (averages of 20–40 deflections) in current clamp. Sodium currents were measured in voltage clamp. All averages reported are mean ± standard error.

CHAPTER 3

Development and evolution of the human neocortex

SUMMARY

The size and surface area of the mammalian brain are thought to be critical determinants of intellectual ability. Recent studies show that development of the gyrated human neocortex involves a lineage of neural stem and transit-amplifying cells that forms the outer subventricular zone (OSVZ), a proliferative region outside the ventricular epithelium. We discuss how proliferation of cells within the OSVZ expands the neocortex by increasing neuron number and modifying the trajectory of migrating neurons. Relating these features to other mammalian species and known molecular regulators of the mouse neocortex suggests how this developmental process could have emerged in evolution.

This chapter is an extended discussion of the results in Chapter 2, arguing that the observed proliferation of stem and transit-amplifying cells in the OSVZ functions to increase neuronal number and surface area of the neocortex. We hypothesize that OSVZ proliferation is contingent on evolutionary changes that permit the generation and maintenance of neural progenitor cells outside of the ventricular epithelium and look toward molecular studies of the rodent to understand how the intracellular signaling state of neural progenitor cells could be recapitulated in the OSVZ. We will further compare OSVZ proliferation in different species and explore how the degree of OSVZ proliferation may be tuned to give rise to diversity in brain size and shape.

FEATURES OF HUMAN NEOCORTICAL DEVELOPMENT

In the rodent, the great majority of RG are epithelial cells that reside in the VZ and make full apical-basal contacts (Noctor et al., 2002). However, it is becoming clear that RG are organized differently in the developing neocortex of other species. In developing monkey and human neocortex, cells with similar morphology to RG, but not necessarily spanning ventricle to pia, are found outside of the VZ. However, these cells were historically considered to be translocating RG transforming into astrocytes (Rakic, 1972; Schmechel and Rakic, 1979a; Choi, 1986). Because RG were not yet appreciated to be neurogenic, nonventricular RG-like cells were also not considered to be neuron-producing cells.

Primate corticogenesis is distinguished by the appearance of a large SVZ that has an inner (ISVZ) and outer region (OSVZ), often split by a thin fiber layer (Smart et al., 2002; Zecevic et al., 2005; Fish et al., 2008). Furthermore, thymidine-labeling studies in primates collectively indicate that proliferation of cells within the OSVZ coincides with the major wave of cortical neurogenesis (Rakic, 1974; Lukaszewicz et al., 2005), suggesting that the OSVZ contributes to neuron production. In addition, cells in the OSVZ express RG markers such as nestin (NES), vimentin (VIM), PAX6, and GFAP, as well as the IP cell marker TBR2 (EOMES) (Zecevic et al., 2005;

Bayatti et al., 2008; Mo and Zecevic, 2008). But how OSVZ cells expressing RG or IP cell markers related to the known progenitor cell types near the ventricle was not understood. It was hypothesized that the OSVZ contained progenitor cells that were either epithelial cells resembling RG (Fish et al., 2008) or transit-amplifying cells resembling IP cells (Kriegstein et al., 2006). Recent studies have begun to resolve these questions by demonstrating the cellular heterogeneity of the OSVZ, which includes both RG and IP cell types, and have highlighted their importance for neuron production during human fetal development.

Extending the radial glia founder population into the OSVZ

At the height of human OSVZ proliferation, the OSVZ contains roughly similar proportions of progenitor cells and postmitotic neurons (Fig. 1A). The progenitor cell population is diverse in terms of morphology and marker expression. In particular, ~40% of OSVZ progenitor cells express nuclear and cytoplasmic markers typical of RG and also possess radial fibers. However, unlike RG in the ventricular zone (vRG cells), which are bipolar, the OSVZ radial glia-like cells (oRG cells) are unipolar, with a basal fiber that ascends toward the pia but without an apical fiber that descends toward the ventricle (Hansen et al., 2010; Fietz et al., 2010). Because some oRG cells contact the basal lamina, they can be classified as epithelial cells (Fawcett and Jensh, 2002). However, oRG cells lack key features of epithelial (apical-basal) polarity, as they are removed from the ventricular epithelium and do not express apically localized membrane constituents such as CD133 (PROM1), Par3 (PARD3), or aPKCλ (PRKCI) (Fietz et al., 2010). Immunostaining for mitosis-specific cytoplasmic markers such as phosphorylated-vimentin demonstrates that oRG cells retain the basal fiber throughout the duration of M phase (Hansen et al., 2010), similar to vRG cells.

Dynamic imaging of oRG cell divisions in cultured slices of fetal neocortex shows that oRG cells exhibit a distinctive behavior whereby the cell soma rapidly ascends along the radial fiber during

the hour preceding cell division, a process termed mitotic somal translocation (Fig. 1B) (Hansen et al., 2010). This is in contrast to vRG cells, which undergo interkinetic nuclear migration and descend to the ventricle to undergo mitosis. oRG cells, upon completing mitotic somal translocation, typically divide with a horizontal cleavage plane, with the more basal daughter cell always inheriting the basal fiber. oRG cells were observed to undergo multiple rounds of such divisions, suggesting that these divisions are self-renewing and asymmetric and push the boundary of the OSVZ outward. Cell fate analysis of oRG cell clones confirmed that self-renewed oRG cells remain undifferentiated, whereas oRG cell daughters continue to proliferate and sometimes express markers of neuronal commitment such as TBR2 or ASCL1 (Fig. 1B). Although there is not yet formal evidence for oRG cells exhibiting long-term multipotency for different neural lineages, they can be considered neural stem cells based on their multiple rounds of self-renewing asymmetric division, which functionally define them as the building blocks for OSVZ-derived neurons and progenitor cells.

Although cortical neuron production begins by gestational week (GW) 6, the OSVZ does not arise until GW11. Over the following 6 weeks, the OSVZ expands dramatically to become the predominant germinal region in the neocortex. Importantly, the initial phase of OSVZ expansion does not occur at the expense of progenitor cells in the VZ/ISVZ, implying that the OSVZ is generated by proliferation rather than by delamination and migration of VZ progenitor cells. In cultured slices, oRG cells were sometimes observed to divide and produce another oRG cell (Fig. 1C) (Hansen et al., 2010), suggesting that, though oRG cells likely originate from the VZ, they can also expand their numbers within the OSVZ.

The coexistence of oRG cells with vRG cells demonstrates that human RG consist of two major subclasses, each functioning as neural stem cells in their respective locations. Expanding the population of RG in a distinct germinal zone is a mechanism for increased neuron production that could be highly relevant for building a larger brain.

Enhanced transit amplification in oRG daughter cells

Although we have so far focused on oRG cells, they account for only ~40% of progenitor cells in the human OSVZ. oRG cells most commonly divide asymmetrically to self-renew and generate daughter cells that are bipolar. These bipolar cells tend to remain undifferentiated over additional transit-amplifying cell cycles and typically do not express markers of neuronal commitment, such as TBR2 (Sessa et al., 2008), until days after generation from an oRG cell (Hansen et al., 2010). Therefore, it is likely that each oRG cell functions as a founder cell for an extended lineage of transit-amplifying cells that lose SOX2 expression and gain TBR2 expression at some point during the ensuing cell cycles (Fig. 1B, 1D, and 1E). This subset forms ~60% of the OSVZ progenitor cell population. In contrast, RG daughter cells in the rodent express TBR2 within hours after RG cell division (Noctor et al., 2008; Ochiai et al., 2009) and usually divide only once to produce two postmitotic neurons (Noctor et al., 2004; Noctor et al., 2008). These observations suggest that increased transit amplification is highly relevant in human neocortical expansion. (For discussion of how the rates of neuron accumulation are impacted by different modes of progenitor cell division, see Fig. 2.)

Gyrencephaly in the ferret neocortex

Gyrencephalic brain development is, of course, not limited to primates. Recent studies have examined whether oRG cells and OSVZ proliferation are shared features with ferrets (*Mustela putorius furo*) (Fietz et al., 2010; Reillo et al., 2010), which also exhibit gyrencephaly and have a disproportionate increase in cortical versus ventricular surface area (Smart and McSherry, 1986a; 1986b). Although cells in the ferret SVZ with oRG cell morphology had been reported previously, they were suggested to be translocating astrocytes (Voigt, 1989) or immature neurons undergoing somal translocation (Borrell et al., 2006). Immunolabeling for RG and IP cell markers showed that the ferret SVZ contained both types of progenitor cells, with many PAX6-positive

cells also exhibiting oRG cell morphology (Fietz et al., 2010; Reillo et al., 2010). Thus, oRG cells (also called intermediate radial glial cells/IRGCs in ferret) and an enlarged SVZ (OSVZ) are not primate-specific features but are also present in carnivores.

The ideas that oRG cells expand in number within the OSVZ and that OSVZ proliferation correlates with gyrus formation are substantiated by experimental evidence in the ferret (Reillo et al., 2010). Green fluorescent protein (GFP)-expressing retrovirus was delivered to the OSVZ of early postnatal ferret kits by stereotactic injection, followed by morphological analysis of labeled cells 2 days later. Because retrovirus labels only one of the two daughter cells following the initial cell division and because more than half of the labeled cells were reported to have oRG cell morphology, this ratio suggested a predominance of divisions in the OSVZ that result in two oRG cells (Reillo et al., 2010). This is partially consistent with observations of oRG cell divisions in human tissue slices in which the oRG daughter cell that did not inherit the basal fiber occasionally remained unipolar and extended a new basal fiber of its own (Hansen et al., 2010). Together, these findings support the notion that oRG cells expand in number in the OSVZ (Fig. 1C).

It had previously been proposed that regions of high and low amounts of SVZ proliferation would predict the future locations of gyri and sulci, respectively (Kriegstein et al., 2006). This connection between progenitor cell behavior during development and shape of the adult brain has recently been examined in ferret, cat, and human neocortex (Reillo et al., 2010). Indeed, regions of future gyral formation contain more proliferating cells in the SVZ during development, and in these areas, proliferation is more pronounced in the OSVZ than in the VZ or ISVZ. The authors of this study experimentally manipulated OSVZ proliferation in the ferret visual cortex by removing thalamic inputs, which resulted in local reduction in neocortical surface area. These findings confirm the importance of oRG cell proliferation in the tangential expansion of gyrencephalic neocortex and lead us to consider the mechanisms by which this occurs.

Addition of radial units and a remodeled migration scaffold

The divisions of oRG cells coupled with mitotic somal translocation begin to explain the radial growth of the OSVZ, as we can infer that oRG cells originate from the VZ, pass through the ISVZ, and leave a trail of daughter progenitor cells as they translocate basally. Furthermore, the substantial addition of RG-like cells in a subventricular location increases the number of ontogenetic units active in generating neuronal clones at a given time. In addition to clear changes to the amount of neurogenesis, adding RG-like cells in the OSVZ must have been accompanied by complex rearrangements in the radial scaffold of the neocortex. That oRG cells continue to translocate toward the pial surface while their daughter cells undergo transit amplification makes it unlikely for an OSVZ-derived neuron to begin migration using the basal fiber of its parent oRG cell. However, the fibers provided by oRG cells are presumably still an important part of the scaffold for migrating neurons, functioning to guide cells part of the way toward the cortical plate.

The degree to which the basal fibers of oRG cells and vRG cells actually reach the pial surface and contact the basal lamina is unresolved. Dyes applied to the pial surface can diffuse into a proportion of oRG cells in the OSVZ through their basal fibers (Hansen et al., 2010). However, oRG cell fibers labeled from the OSVZ may not all reach the pia because cells born locally are unlikely to grow basal fibers that traverse such a great distance. The same may be true of vRG cells that initially gave rise to oRG cells but did not inherit the basal fiber. Dye and genetic labeling studies in the ferret have recently shown that radial fibers originating in the VZ diverge and form a fanned array by the time that they reach the pial surface. Because the density of fibers did not decrease at the same rate as the fibers were diverging, it was inferred that new fibers are added in basal locations, a property that is likely achieved by the expansion of oRG cells (Reillo et al., 2010). Although neuronal migration on oRG cell fibers has not been directly observed in either ferret or human, the addition of radial fibers by oRG cells is suggested to solve a

topological problem—they provide guides for the migration of neurons that can then spread over a greater tangential surface.

Updated views of corticogenesis

Recent discoveries concerning the progenitor cell subtypes present in the OSVZ provide an updated view of neurogenesis, neuronal migration, and tangential expansion that revises the radial unit hypothesis and other previous models of human neocortical development (Fig. 3).

Neuronal migration and tangential expansion

In contrast to the columnar organization of neuronal clones proposed by the radial unit hypothesis, several studies have shown considerable lateral dispersion of clonally related neurons in rodents (Walsh and Cepko, 1988; Austin and Cepko, 1990; Tan and Breen, 1993), ferrets (Ware et al., 1999; Reid et al., 1997), and primates (Kornack and Rakic, 1995). Though in rodents, this dispersion is relatively modest and regulated by EphA/ephrin-A signaling (Torii et al., 2009), the OSVZ-based radial scaffold may further contribute to the dispersion of neuronal clones in ferrets and primates. As a result of neuron production in the OSVZ, many newborn neurons begin migration in the OSVZ rather than the VZ. Instead of following the trajectory of a single radial glial fiber, neurons may follow a discontinuous relay of fibers, including numerous new ones that originate in the OSVZ from oRG cells (Fig. 4). Discontinuity in the radial scaffold therefore provides ample opportunity for horizontal dispersion as neurons migrate from fiber to fiber. Studies that directly examine the extent to which the basal fibers of oRG cells support neuronal migration will be an important first step toward testing these concepts. The mature patterns of neocortical folding are likely the combined effect of these early mechanisms and others associated with neuronal differentiation and circuit formation that occur later, including the physical tension exerted by axonal fibers connecting closely associated cortical regions (Van Essen, 1997).

Increased neurogenesis and progenitor cell diversity

We propose that increases in neuron number in the human neocortex were achieved through three stages of progenitor cell expansion: 1) the population of founder cells increased in number in the form of nonventricular RG (oRG cells), 2) oRG cells undergo multiple rounds of asymmetric divisions to generate IP cells, and 3) IP cells acquired increased proliferative capacity to further amplify neuron production. Because the lineage from RG cell to immature neuron in the human OSVZ is punctuated by a greater number of intermediate steps than in the rodent, there may be considerable diversity in IP cell types (Hansen et al., 2010). Cells that constitute the OSVZ lineage of neurons (Fig. 1E) can therefore be subdivided into: 1) oRG cells that either have pial contact and were initially derived from ventricular RG or oRG cells that do not have pial contact and were derived locally via proliferative divisions of other oRG cells, 2) IP cells that are bipolar and no longer have oRG cell morphology but still express markers of the undifferentiated state and Notch activation or more mature IP cells that are bipolar or multipolar but no longer have active Notch signaling, and 3) immature neurons that account for ~45% of the OSVZ cell population. Presumably, these neurons are derived both locally and from the VZ/ISVZ and are in the process of migrating to the cortical plate. This revises the radial unit hypothesis by highlighting the role of an important neurogenic region interposed between the ventricle and the cortical mantle. Neurogenesis in the human neocortex involves multiple stem and transit-amplifying cell divisions in two distinct locations.

Previous concepts about asymmetric versus symmetric divisions in neocortical development proposed that asymmetric divisions of RG generate neuronal diversity through the sequential production of distinct neuronal subtypes fated to occupy different laminar positions. Symmetric divisions of IP cells, on the other hand, act as the workhorse for increasing cell number by expanding the number of neurons produced per asymmetric RG division (Noctor et al., 2004; Kriegstein et al., 2006). These concepts are now extended to the OSVZ, as both RG and IP cell

types are represented there. The major contribution of OSVZ progenitor cells to neurogenesis,

distinct from neurogenesis in the VZ/ISVZ, could allow for differential ontogeny related to

location of origin as a potential avenue for increased neuronal diversity. To begin testing this, it

will be important to analyze the extent to which VZ/ISVZ proliferation contributes to

neurogenesis independently of the OSVZ. Furthermore, because the number of neural progenitor

cells in late versus early neurogenesis is so disparate due to OSVZ expansion, proliferation in this

region may also be a mechanism to increase the number of later-born neurons, a feature that is

consistent with observations that the upper cortical layers are particularly cell dense in the

primate cerebral cortex (Marín-Padilla, 1992).

Future directions and challenges

Our new understanding of human neurogenesis describes the proliferative events within the

OSVZ but leaves major questions unanswered, including: 1) the cell types generated from this

region, 2) how the OSVZ is formed, and 3) how molecular regulators control OSVZ proliferation

and distinguish it from what is observed in the rodent.

The significant overlap of cells expressing SOX2 with TBR2, a marker for commitment to the

excitatory neuron lineage (Sessa et al., 2008), suggests that the human OSVZ contributes mostly

to the generation of excitatory neurons. However, given that cell fate analysis of mature oRG cell

progeny has not been performed in the human or ferret, the possibility remains that other cell

lineages, including inhibitory neuron and glial precursor cells (Letinic et al., 2002; Jakovcevski

and Zecevic, 2005; Reillo et al., 2010), may also be present. In particular, it has been suggested

that, in contrast to the rodent neocortex, where inhibitory neurons are primarily derived from

ventral sources (Anderson et al., 1997; Wonders and Anderson, 2006), the primate neocortex

utilizes an additional dorsal source of inhibitory neuron progenitor cells to proportionately

balance the increase in excitatory neurons (Letinic et al., 2002; Petanjek et al., 2009; Jakovcevski

et al., 2010; Zecevic et al., 2011; Yu and Zecevic, 2011). These conclusions are primarily based on observations of proliferating cells in the dorsal VZ and SVZ that express ventral-associated markers relevant for the generation of inhibitory neurons, such as MASH1 (ASCL1), DLX2, NKX2-1, and calretinin (CALB2).

These concepts remain controversial, however, as human infants with severe ventral forebrain hypoplasia suffer almost complete depletion of NOS1-, NPY-, and SST-expressing inhibitory neuron subtypes, suggesting that these cell populations are unlikely to have a dorsal source (Fertuzinhos et al., 2009). The population of CALB2-positive inhibitory neurons was relatively spared in these patients, but the subpallial progenitor cells that are responsible for generating this subtype were also not dramatically affected by the disease. Inhibitory neuron lineage markers in the rodent may also not have the same significance in humans. ASCL1 expression, for example, has been observed at low levels in the dorsal proliferative zones of humans, where it appears to be associated with the production of excitatory neurons (Hansen et al., 2010). It is also possible that putative inhibitory neuron progenitor cells observed in the dorsal cortex are transit-amplifying cell types migrating from the ventral telencephalon. The notion that dorsal progenitor cells in primate neocortex generate most inhibitory neurons requires further investigation.

Our understanding of gyrencephalic brain development has greatly improved in recent years because of observations in human, nonhuman primate, and ferret tissues. However, the ethical and technical limitations of working in primate species continue to pose challenges in understanding the origin and progeny of OSVZ proliferation as well as other unexplored aspects of human corticogenesis. Future efforts to address these questions will benefit from a combination of new lineage tracing techniques and the employment of a model system that is more amenable to genetic manipulation, such as the ferret.

The OSVZ as a site of human disease

The appreciation that OSVZ proliferation could be responsible for generating the majority of cortical neurons invites a re-interpretation of the mechanisms behind a wide range of neurodevelopmental diseases. Particularly relevant are those diseases that broadly affect neuronal number and brain size such as lissencephaly and microcephaly. Some of the genes shown to cause these disorders in humans have now been studied in model systems, and appear to be frequently involved in maintaining the proper structure and function of the mitotic spindle and centrosome. In the context of the mouse neocortex, these proteins tightly regulate RG divisions and neuronal migration (Wynshaw-Boris, 2007; Bond et al., 2002; 2005; Lizarraga et al., 2010; Buchman et al., 2010). However, in the context of the human neocortex, the function of these genes must also extend to oRG cells, since their mitotic somal translocation, division, and derivation from ventricular RG cells are likely to utilize related microtubule-based mechanisms. Pursuing a cell biological understanding of oRG cell behavior will be an exciting future direction that may reveal unexpected links to other neurodevelopmental disorders such as autism and schizophrenia.

A full understanding of OSVZ neurogenesis will also be critical for the proper generation of specific neuronal subtypes for cell replacement therapies, where potential differences between neurons derived from ventricular and outer subventricular regions may have to be recapitulated *in vitro*. Since OSVZ proliferation may be responsible for production of most neurons in the human neocortex, it is possible that derivation of neuron subtypes from human embryonic stem (hES) cells or induced pluripotent stem (iPS) cells could require a transitional oRG-like progenitor state. Supporting this, recent studies have shown that neuroepithelial "rosette" structures resembling VZ progenitor cells can be derived *in vitro* from hES cells. In contrast to the rosettes derived from mouse ES cells that generate both deep and upper layer neurons in correct laminar positions, rosettes from hES cells only succeed in producing deep layer neurons (Eiraku et al., 2008). Although these observations could be a reflection of limitations in the time frame or conditions of culture, they may suggest that even *in vitro*, OSVZ progenitor cell identity is distinct and

particularly important for generating upper layer neurons. An appreciation of the OSVZ in

neurogenesis and an understanding of the regulators that control its development will be critical

for deriving a full repertoire of human neurons for therapeutic ends (for discussion, see Hansen et

al., 2011).

MOLECULAR REGULATION OF NEOCORTICAL EXPANSION

Understanding the molecular basis behind the cellular mechanisms in human corticogenesis is key to identifying the evolutionary changes that resulted in neocortical expansion. This section aims to bridge the gap from cellular to molecular mechanisms, drawing heavily on examples in rodent literature that inform how human RG cells may be regulated. We use two related perspectives to organize these studies.

First, we can infer that human corticogenesis involves: 1) the production of oRG cells from the VZ, 2) the maintenance of RG identity outside of the VZ, and 3) extensive transit amplification of oRG daughter cells before neuronal differentiation. These features depend critically on the production and maintenance of RG cells outside of the ventricular epithelium, so how might this be achieved at the molecular level? The manipulation of regulators involved in progenitor cell polarity, signaling, and cell-cell interaction reveal the factors and signaling pathways that are most important for maintaining the RG state in rodents. If these signaling requirements are conserved in humans, RG maintenance in the OSVZ must either rely more heavily on mechanisms that act through shared features of vRG cells and oRG cells, such as the basal fiber, or through novel forms of regulation that are specific to the OSVZ. In either case, knowing the molecular complexities of the RG state is essential as a starting point for understanding how oRG cells are maintained.

Second, loss- and gain-of-function studies in mice already recapitulate some of the features of human corticogenesis. Although it is unlikely that human evolution precisely recapitulated these changes at the molecular level, these results nevertheless highlight the types of pathways and mechanistic variations that could lead to formation of an OSVZ.

Regulation by Notch signaling

The Notch signaling pathway is a highly conserved mechanism to create different signaling states between cells that make physical contact. This is achieved through lateral inhibition (Heitzler and Simpson, 1991; reviewed by Kageyama et al., 2008), whereby feedback loops that control gene expression levels operate in adjacent cells to amplify small, sometimes stochastic differences into larger ones. In the standard model, Notch ligands (Delta/DLL) are initially expressed at slightly different levels in a population of cells. Cells with higher expression levels stimulate Notch more potently in neighboring cells to induce downstream effectors such as HES1 and HES5, which repress the expression of Delta by transcriptional feedback, thereby diminishing the neighboring cell's ability to stimulate Notch in the initiating cell. Over a number of iterations, cells are thought to stabilize into a salt and pepper pattern of mutually exclusive high and low signaling states.

In the context of neural development, HES1 and HES5 act as transcriptional repressors of proneural basic helix-loop-helix (bHLH) transcription factors such as NEUROG2 and ASCL1 (Ishibashi et al., 1995), therefore associating low Notch signaling with neuronal differentiation. However, the basic model of lateral inhibition is significantly complicated by the developmental dynamics of the neocortex, as cells enter the system through asymmetric division and leave through neuronal migration. In addition, RG cells also undergo interkinetic nuclear oscillations, and the extensive surface of their basal fibers that traverse the radial dimension of the developing neocortex could facilitate reception of Notch signals from distant sources and diverse cell types (Fig. 5A). These observations suggest that the maintenance of Notch signaling in RG may be highly regulated in both space and time.

Overexpression of the activated Notch intracellular domain (NICD) results in increased numbers of cells expressing RG markers, showing functionally that Notch activation is associated with the RG state (Gaiano et al., 2000). Loss-of-function studies showed the requirement of Notch

signaling effectors HES1, HES3, and HES5 (Hatakeyama et al., 2004), either singly or in combination, as well as of the NICD signaling mediator CBF1 (RBPJ) (Mizutani et al., 2007; Imayoshi et al., 2010). Loss of these factors, in particular CBF1, promotes the depletion and premature differentiation of RG toward the neuronal lineage.

The expression patterns of Delta ligand (Campos et al., 2001) and Notch effector (Ohtsuka et al., 2006) suggested a scheme whereby Delta expressed on neuronally committed cells in the SVZ signals back to Notch receptors expressed on RG. This idea was tested by the removal of Mind-bomb1 (MIB1) (Yoon et al., 2008), an E3 ubiquitin ligase that is essential for generating functional Notch ligands (Itoh et al., 2003; Koo et al., 2005). MIB1 was expressed in neuronally committed TBR2-positive cells, and similar to studies of CBF1 deletion, its conditional knockdown in the neocortex also results in premature neuronal differentiation and depletion of RG cells. That isolated IP cells and postmitotic neurons stimulate HES1 activity in Notch-expressing neighboring cells in vitro further supports this idea. This study also raised the interesting possibility that the amount of time an IP cell pauses in the VZ before dividing or migrating away, a behavior that has been described as "sojourning" (Bayer and Altman, 1991; Noctor et al., 2004), could be related to its role in sustaining Notch activity in local RG cells.

Role of Notch signaling oscillations

In contrast to the standard model of Notch lateral inhibition, whereby cells are locked into high and low signaling states, Notch activation levels in rodent RG are dynamic and exhibit an oscillatory pattern (reviewed by Kageyama et al., 2008). An important insight came when HES1 expression was found to oscillate at 2–3 hr intervals in cultured cells due to negative autoregulation of *Hes1* transcription (Hirata et al., 2002). Shimojo et al., 2008 discovered that HES1 control in RG is multifaceted, with the autonomous HES1 oscillatory circuit layered into a more pronounced level of regulation. HES1 protein was detected only during the phases of the

cell cycle (late G1 through G2) when the cells were in the basal part of the VZ, but not during mitosis through early G1, when the cells were immediately adjacent to the ventricle. Furthermore, the oscillatory expression of HES1 in RG controls NEUROG2 and DLL1 expression and leads to their oscillation with inverse correlation. Therefore, RG are poised to generate neuronal progeny during periods of low HES1 expression. Consistent with previous reports, sustained overexpression of HES1 blocks expression of proneural genes, Notch ligands, and cell-cycle regulators—presumably locking the cells into a RG state but rendering them incapable of generating more differentiated progeny. Blockade of Notch signaling in RG has the opposite effect, whereby NEUROG2 and DLL1 switched from oscillatory to sustained expression, caused neuronal differentiation, and depleted the progenitor pool. These results show that, within the RG population, oscillatory expression of Notch-controlled genes is required for the simultaneous maintenance of progenitor identity and generation of neuronal progeny.

How might Notch oscillations be coordinated with asymmetric division? One possibility is that periods of low HES1 expression (M and early G1 phases) are permissive windows for neuronal differentiation. Directly after RG cell division, both daughter cells start with the same ground state of Notch activity and still possess neuroepithelial cell-cell interactions, having short apical fibers that contact the ventricle (Miyata et al., 2004). Why then does the self-renewed RG cell remain undifferentiated, whereas the daughter cell becomes neuronally committed? Because RG cells have long basal fibers, this could facilitate cell-cell interactions outside of the neuroepithelium. Retention of the basal fiber following division could be a critical determinant of a cell's ability to sense signals from the SVZ and more basal cell types. In this case, because Notch ligands are highly expressed in the SVZ, the daughter cell in the VZ without the basal fiber will be predisposed toward sustained NEUROG2 expression and neuronal differentiation, whereas the cell with the basal fiber quickly receives Notch signal and preserves RG identity (Fig. 5A and 5B).

Basal fiber inheritance

Inheritance of the basal fiber could also be a general mechanism that allows oRG and vRG cells to be regulated similarly. The Notch effector HES1 is expressed in oRG as well as vRG cells in fetal human neocortex, and pharmacological inhibition of Notch signaling in slice cultures induces neuronal differentiation of progenitor cells (Hansen et al., 2010). Therefore, Notch signaling restrains both types of RG from neuronal differentiation. The epithelial architecture in the VZ may facilitate Notch signaling from redundant sources, but oRG cells could rely more exclusively on neurons or IP cells attached to their basal fibers for Notch-dependent maintenance of the RG state (Fig. 3B).

It has also been proposed that integrin signaling maintains oRG status in cells contacting the basal lamina via their basal fiber (Fig. 3B) (Fietz et al., 2010; Fietz and Huttner, 2011). β3-integrin (ITGB3) expression has been observed in the basal fiber of oRG cells, and chemical or antibody-based inhibition of integrin-mediated signaling in ferret slice cultures causes a loss of PAX6-positive OSVZ cells, which include oRG cells. However, RG contact with the basal lamina in the rodent neocortex has been suggested to be dispensable for regulating cell fate and proliferation (Haubst et al., 2006), and not all oRG cells may contact the basal lamina. Therefore, further characterization of the precise requirements for integrin-mediated signaling in oRG cells will be important to substantiate this concept. Regulation of RG via the basal fiber is nevertheless an emerging idea that could be highly relevant to OSVZ proliferation.

Regulation by β-Catenin signaling

β-catenin (CTNNB1) has also been established as a central regulator of proliferation versus differentiation in rodent neural progenitor cells. β-catenin protein lies functionally at a crossroad between tissue architecture and regulation of the transcriptional activity that modifies cell fate, having dual roles as a component in the adherens junctions that link neuroepithelial/RG cells and

as a transcriptional coactivator in the presence of Wnt signal. Early studies using genetic deletion in the forebrain established a requirement for β-catenin in specifying dorsal telencephalic fate (Gunhaga et al., 2003; Backman et al., 2005), maintaining the structural integrity of the neuroepithelium and preventing progenitor cell apoptosis (Machon et al., 2003; Junghans et al., 2005), but did not distinguish whether the adhesive or transcriptional roles of β-catenin were primarily responsible for these effects. A later study tested the cell-autonomous role of β-catenin transcriptional activation by expressing ICAT or a dominant-negative version of TCF4, either of which blocks transcriptional activity by interfering with β-catenin/TCF4 complex formation (Woodhead et al., 2006). In this context, whereby neighboring cells provided a relatively normal radial scaffold, RG differentiated into neurons and migrated to the cortical plate, implying that β-catenin signaling suppresses neuronal differentiation and maintains progenitor cell proliferation independently of its role in adhesion. Observed increases in neuronal differentiation caused by β-catenin loss of function were preceded by increases in IP cell number, suggesting that β-catenin signaling restrains the development of IP cells from RG (Mutch et al., 2010).

Stabilizing β-Catenin increases the progenitor pool

Consistent with these findings, transgenic mice expressing stabilized β-catenin in neural progenitor cells exhibited gross defects in neocortical development. Neuroepithelial cells in this mouse have a higher propensity to re-enter the cell cycle and undergo symmetric self-renewing divisions, resulting in a massively expanded population of VZ progenitors leading to folding of the cortical anlage (Chenn and Walsh, 2002). This study was the first experimental suggestion that expansion of the ventricular founder population could be the cellular basis for developing gyrencephaly, thus serving as an example of how progenitor cell expansion can underlie neocortical expansion (Chapter 1: Fig. 1A) (Rakic, 1995; 2009). However, this mode of expansion does not mimic the development of naturally gyrencephalic animals, which display

vast increases in neocortical surface area without a proportional increase in ventricular surface area (for discussion, see Kriegstein et al., 2006).

Because the transgenic mice in this initial study did not live past birth, it was not possible to determine whether expansion of the neuroepithelial population would have lasting effects on neuronal number and neocortical size. Further work with mice that expressed lower amounts of stabilized β-catenin (Chenn and Walsh, 2003) indeed resulted in adult mice with enlarged forebrains and an increased number of neurons. However, the brains of these mice were disrupted in other ways, including an arrest of neuronal migration and disruption of cortical lamination. Thus, the example of stabilized β-catenin in neuroepithelial cells highlights how a relatively small genetic change can greatly enlarge the neocortex but also reveals that, unless such changes integrate with other developmental processes, the consequences will be deleterious.

How β-catenin functions in the developing human neocortex is an unexplored but interesting future direction. The ventricular epithelium in humans is capable of RG self-renewal and neurogenesis but also generates self-renewing oRG cells that presumably do not express adherens junction components. Therefore, understanding the relative roles of β-catenin expression in adherens junctions and in the nucleus in both proliferative zones of the human neocortex will be highly informative.

Regulation by polarity proteins

Adherens junction components

The participation of β-catenin in adherens junctions illustrates how proteins that are involved with RG polarity can regulate the progression of neurogenesis. Recent studies have highlighted that β-catenin signaling is affected by the expression of other adherens junction components such as cadherins and α-catenins, although not necessarily through mechanisms of β-catenin sequestration at cell-cell junctions. Reduction of N-cadherin (*Cdh2*) leads to a decrease in β-catenin signaling

and results in a phenotype that is similar to direct removal of β-catenin—whereby knockdown cells exit the cell cycle and prematurely differentiate into neurons (Zhang et al., 2010). Remarkably, this effect is independent of the canonical Wnt pathway, as reducing N-cadherin did not alter the ability of Wnt to stimulate β-catenin signaling. Instead, N-cadherin function was linked to AKT activity, with AKT stimulating β-catenin activity through direct phosphorylation and perhaps also indirectly through GSK3 inhibition (Fig. 5C).

Conditional genetic deletion of αE-catenin (*Ctnna1*) in the cortex disrupts the polarity of the epithelium, shortens cell-cycle length, and decreases neural progenitor cell apoptosis. Together, this results in a severely dysplastic phenotype, whereby progenitor cells disperse about the cortex and overproliferate, eventually giving rise to a larger mature brain (Lien et al., 2006). Global gene expression comparisons of normal versus αE-catenin-deleted brains showed that targets of Sonic hedgehog (Shh) signaling were expressed at higher levels in mutants (Fig. 5C). Chemical inhibition of Shh signaling rescues the overproliferation, but not the loss of cell polarity, in αE-catenin-deleted brains, implying a role for αE-catenin in suppressing Shh signaling in the developing cortex. Whether αE-catenin also regulates β-catenin signaling in RG has been controversial. A further study using αE-catenin conditional deleted mice found no evidence for changes in β-catenin nuclear activity using a number of assays, including quantification of protein levels, in vivo reporter activity, or quantification of downstream targets (Lien et al., 2008). However, another group reported that focal knockdown of αE-catenin phenocopied the removal of β-catenin signaling and promoted neuronal differentiation (Stocker and Chenn, 2009). The disparate findings between universal versus focal deletion of αE-catenin illustrate how tissue architecture can alter a cell-autonomous mutant phenotype and underscore how the RG intracellular signaling state is defined by both extrinsic and intrinsic factors.

NUMB and Par3 link cell polarity with Notch signaling

NUMB is a classic determinant of cell fate in dividing fly neuroblasts, where it localizes asymmetrically to the basal pole and promotes differentiation of the basal daughter cell by inhibiting the Notch pathway (Rhyu et al., 1994). In the context of vertebrate neural development, however, NUMB plays multiple roles in regulating RG cell polarity and differentiation. Though initially a matter of controversy (Zhong et al., 1996), mounting evidence supports the conserved role of NUMB as a determinant of neuronal fate in asymmetric RG cell divisions (Wakamatsu et al., 1999; Shen et al., 2002; Rasin et al., 2007). However, NUMB has an additional role in preserving apical-basal polarity within the mouse neuroepithelium (Rasin et al., 2007). NUMB, a known modulator of endocytosis, interacts and colocalizes with cadherins on the basolateral side of adherens junctions and with RAB11-positive endocytic vesicles. Combined loss-of-function experiments for NUMB and its homolog NUMBL showed disruption of epithelial integrity and RG that were displaced basally, implying a critical role for NUMB/NUMBL in regulating RG cell adhesion in the VZ. Although this displacement of RG resulted in the abnormal location of resulting neurons, the timing and sequence of neurogenesis was reasonably normal. Thus, RG can undergo the correct sequence of neurogenesis even in a disrupted tissue microenvironment.

In addition to the proteins that directly make up adherens junctions, other proteins that define the apical "identity" of RG are also critical for regulating the balance between proliferation and neurogenesis. Overexpression of Par3 (PARD3) or Par6 (PARD6A), core members of an apical protein complex that is important for epithelial polarity, increases the frequency of symmetric, proliferative RG cell divisions at the expense of asymmetric, neurogenic divisions, whereas small hairpin RNA-mediated knockdown has the opposite effect and promotes neuronal differentiation (Costa et al., 2008). Moreover, Par3 is segregated asymmetrically in RG cell divisions and has been found to exert its effects on neurogenesis through the Notch/Numb pathway (Bultje et al., 2009). Combined knockdown of NUMB and Par3 rescues the effects of loss of Par3 on

neurogenesis, placing NUMB activity downstream of Par3. This effect depends on the physical interaction of Par3 and NUMB.

These studies point to cooperative roles for Par3 and NUMB in maintaining epithelial polarity but antagonistic roles in regulating Notch signaling and neurogenesis. Both proteins localize to the lateral membrane domain in ventricular endfeet during interphase and promote apical-basal polarity (Rasin et al., 2007; Bultje et al., 2009). However, the direct interaction of Par3 with NUMB is required for Par3 to potentiate Notch signaling, possibly through preventing NUMB from interacting with Notch. Asymmetric distribution of Par3 in RG divisions could therefore bias the amount of Notch signaling in each daughter by controlling the level of active NUMB in the next cell cycle. The daughter cell that does not inherit the apical complex will receive less Par3, have higher active NUMB levels, and better inhibit Notch activation, resulting in the upregulation of proneural bHLH transcription factors (Fig. 5B). This scheme also explains the surprising observation that, when NUMB was knocked down, RG cells displaced outside of the ventricular epithelium remained functional as primary progenitor cells (Rasin et al., 2007). Loss of NUMB causes delamination of RG because of its polarity role but permits high enough levels of Notch signaling to maintain RG in their progenitor state outside of the VZ. Furthermore, these observations are consistent with the idea that oRG cells do not express apical constituents but are able to receive Notch signaling in the OSVZ.

Regulation by multiple integrated pathways

The examples shown serve to highlight the tightly controlled balance of pathway activation and repression that is required for proper RG cell function. An important future direction will be to fully describe the mechanistic steps leading to aberrant pathway activity, as it is often not obvious why a particular pathway is downstream of a particular protein. We have emphasized the roles of Notch and β-catenin signaling for maintaining the RG progenitor state, but clearly, regulation by

other pathways is also important. For example, FGF10 is expressed in neuroepithelial cells, and its loss extends the period of symmetric progenitor cell expansion and delays the onset of neurogenesis in the rostral cortex. However, RG cells in this mutant eventually differentiate in excess to overproduce neurons and IP cells, resulting in the tangential expansion of frontal areas and increased laminar thickness (Sahara and O'Leary, 2009). The RG signaling state is further complemented by signals from outside of the neuroepithelium. Mutant mice with disrupted meningeal development have increased self-renewing neuroepithelial divisions and decreased production of neurons and IP cells, resulting in a "gyrencephalic" appearance similar to that of the stabilized β-catenin mouse (Siegenthaler et al., 2009). This effect is rescued in vitro by meninges-derived conditioned media, suggesting the requirement of secreted factors from the meninges, most notably retinoic acid (RA), for normal neurogenesis. Although the importance of RA in this context has recently been called into question (Chatzi et al., 2011), this nevertheless underscores how regulation of the neuroepithelium could be due to the proximity of RG basal fibers with the meninges and other cell types (Fig. 5A).

A recent study testing the function of GSK3 in neocortical development (Kim et al., 2009) illustrates the view that the RG state is tightly controlled by the intersection of multiple pathways. GSK3 is the kinase responsible for phosphorylating β-catenin and targeting it for degradation. Conditional genetic deletion of GSK3 leads to a phenotype very similar to that of the stabilized β-catenin mouse, as expected because GSK3 loss should result in stabilization of cytoplasmic β-catenin and increased signaling. This included an expanded ventricular surface composed of more SOX2-expressing RG-like cells, increased cell-cycle re-entry, increased β-catenin nuclear signaling, and a decrease in neuronal differentiation. However, the authors found that the overproliferation phenotype could also be attributed to overactive Notch, Shh, and c-*Myc* (MYC) signaling (Fig. 5C). This demonstrates the widespread role of GSK3 in keeping multiple signaling

pathways in check but also highlights the importance of having a comprehensive set of assays to fully disclose the regulatory matrix that underlies a mutant phenotype.

Maintenance of radial glia outside of the neuroepithelium

Although the maintenance of RG is multifaceted, an emerging concept in rodent development is that the apical region is especially important because dysregulation most often leads to premature differentiation. However, this is not a rule, as neural progenitor cells isolated in culture recapitulate the proper timing and sequence of neuron production (Shen et al., 2006). Other studies have further substantiated the concept that RG can divide in a normal sequence despite having compromised polarity and location. In vivo studies show that loss of aPKCλ (PRKCI) (Imai et al., 2006) or its downstream substrate MARCKS (Weimer et al., 2009) disrupts RG polarity and placement in the cortical wall, but in neither case do they cause major defects in the sequence or degree of neurogenesis. Randomization of spindle orientation and cleavage plane angle by LGN (GPSM2) knockdown impairs the coinheritance of apical and basal contacts in RG, converting them to progenitor cells that are localized outside of the VZ/SVZ that still resemble RG in marker expression. Surprisingly, despite the aberrant location of these progenitor cells, the rate of neurogenesis and cell types produced were relatively normal (Konno et al., 2008). Further characterization of these LGN-deficient progenitor cells showed that they resemble oRG cells in morphology and are born in the VZ by RG divisions that have an oblique/horizontal cleavage plane. These divisions split the radial process into two daughter cells; the more basal daughter cell inherits the basal fiber, translocates to the SVZ, and remains undifferentiated (Fig. 5B) (Shitamukai et al., 2011). Importantly, small numbers of these cells were found to be present in normal mice (Wang et al., 2011) and also required Notch signaling for their maintenance (Shitamukai et al., 2011). These observations suggest that oRG cells, although infrequent in some species, are part of a conserved developmental mechanism that can be studied in mice.

These studies are highly reminiscent of what is seen in human development and suggest that, even in the rodent, correct neurogenesis is not necessarily tied to cell polarity or location. It will be important for future studies to describe the signaling state of displaced rodent RG cells compared to their ventricular counterparts. Further comparison with vRG and oRG cells in the human will help to refine our ideas about the requirements and mechanisms for oRG cell maintenance in the OSVZ. Do oRG cells have the same signaling requirements but have them met through OSVZ niche-specific means, or is there a higher degree of developmental cell autonomy that does not exist in the rodent?

In addition to the maintenance of oRG cells in the OSVZ, their production and expansion must also involve distinct modes of cell division such that the total number of RG cells is increased. Rodent studies that lead to overproduction of RG, for example by constitutive expression of β-catenin (Chenn and Walsh, 2002), *Fgf10* deletion (Sahara and O'Leary, 2009), or loss of meningeal secreted factors (Siegenthaler et al., 2009), could offer relevant insight. Alterations in one or more of these mechanisms could have biased the production of cells toward RG instead of neurons during the evolution of larger brains. For example, neocortical growth and the proposed discontinuity of oRG and vRG basal fibers in humans could negatively affect RA signaling from the meninges, thereby promoting RG cell expansion.

Analysis of gene expression in human brain

An understanding of the molecular basis of human brain development and function, although challenging, is beginning. Limitations in tissue collection have forced the majority of molecular studies of human brain development to use global profiling approaches to identify interesting distinguishing features. These efforts have proven to be effective, for instance, by the identification and correlation of brain development genes with regions of the genome that have undergone human-specific evolutionary acceleration (Pollard et al., 2006). Global transcriptome

analysis of the developing human brain has successfully identified and categorized expression patterns, alternative splicing, and differential regulation of genes in major brain regions (Johnson et al., 2009). Analysis of gene coexpression relationships in human brain has been effective at extracting cell type-specific expression patterns from unbiased data sets of whole-brain tissue (Oldham et al., 2008). These studies will undoubtedly build an enormous number of hypotheses and candidate regulators for the study of human brain development.

The next challenge will be to apply this information to the cellular mechanisms in our evolving understanding of fetal brain development, particularly that of OSVZ proliferation. Testing the importance of candidate genes identified from molecular studies of the human will be a critical first step. However, with the development of techniques that can acutely and robustly alter gene expression, the extension of these studies to both gyrencephalic and lissencephalic species, as well as multiple experimental platforms, will be worthwhile.

The success of these experimental approaches and validity of interspecies comparisons depends on whether evolution of brain size and shape in different species is based on related mechanisms. In the next sections, we will explore the generality of OSVZ proliferation and attempt to place these features in the context of neocortical evolution.

OSVZ PROLIFERATION IN THE CONTEXT OF EVOLUTION

Origins of the SVZ and six-layered neocortex

From the examination of multiple species, a rough correlation can be made between the generation of three-layered, six-layered, and gyrencephalic neocortex and specific features of progenitor cell organization during development. The cortex of reptiles consists of three layers (Ulinski, 1974; Goffinet, 1983; Cheung et al., 2007) comparable to layers I, V, and VI in mammals, which are generated by a reptile homolog of RG, an ependymoradial glial cell (Weissman et al., 2003). Ependymoradial glia form a ventricular neuroepithelium, and there is no SVZ in the developing reptile dorsal cortex (Cheung et al., 2007).

In contrast to reptiles, mammalian species have a six-layered neocortex, and all species examined so far appear to have a SVZ during embryonic neocortical development. However, the view that SVZ proliferation is necessary to generate a six-layered cortex has recently been called into question from studies in two metatherian (marsupial) species, *Monodelphis domestica* (opossum) and *Macropus eugenii* (tammar wallaby). These animals exhibit a distinctive SVZ layer, including cells that express TBR2 (a marker of neuronal commitment often associated with IP cells) as well as sparse labeling of the mitotic marker phospho-H3, suggesting the existence of SVZ neurogenesis (Cheung et al., 2010). However, a subsequent study found that these TBR2-expressing cells never incorporate BrdU, implying that they do not form a transit-amplifying progenitor cell class but are likely to be immature postmitotic neurons (Puzzolo and Mallamaci, 2010). These observations need to be reconciled, but they suggest that development of a proliferative SVZ may have occurred after the eutherian-metatherian split and that this feature may be more strictly correlated with eutherians (placental mammals) than mammals at large.

The human neocortex: a scaled-up primate brain

Studies of the human brain and comparisons of developmental proliferative zones between species may ultimately help to explain what makes the human brain unique. It is commonly thought that the exceptional cognitive abilities of humans are related to the large size of the neocortex. Recent evidence has shown that primates have greater neuronal density (neuron number/brain mass) compared to rodents of equal brain mass, a feature that is likely related to the topological differences in foldedness that could have been influenced by OSVZ proliferation. However, though the human brain is large by weight (1.5 kg) and neuron number (86 billion) (Azevedo et al., 2009; reviewed by Herculano-Houzel, 2009), this ratio does not deviate from what would be expected from a primate brain of similar mass, implying that, in terms of brain size and density, the human brain conforms to a scaled-up primate brain. Furthermore, developmental similarities between the human and ferret show that increased OSVZ proliferation and oRG cells are not primate-specific features (Fig. 6A). The percentage of progenitor cells in the SVZ/OSVZ of rodents, carnivores, ungulates, and primates shows a remarkable positive correlation with the degree of neocortical gyrification (Reillo et al., 2010). Thus, development of OSVZ proliferation appears to be an important general feature for increasing neuronal number and neocortical surface area throughout *Eutheria*.

Diversity of neocortical foldedness

Whether an OSVZ exists in the developing neocortex of different mammalian species is difficult to address without direct observation of embryonic tissues, but topological comparisons of adult brains (Fig. 6B) (Comparative Mammalian Brain Collections, http://brainmuseum.org) can be suggestive of developmental events. Interestingly, all eutherian superorders contain species that span the range of gyrencephalic to lissencephalic brains. For example, in the superorder *Euarchontoglires*, most members of *Rodentia* are lissencephalic and most primates are

gyrencephalic. However, the capybara is a gyrencephalic rodent, and various primates, such as the marmoset, lemur, and particularly the Senegal bushbaby, are almost entirely lissencephalic. The next closest superorder, *Laurasiatheria*, includes a wide variety of lissencephalic (bats, shrews, and moles) and gyrencephalic (carnivores, ungulates, and cetaceans) species. Species within a third superorder, *Afrotheria*, also display a wide range of cortical configuration, from the extremely gyrencephalic elephant to its closest extant relative, the lissencephalic manatee.

These observations indicate that the development and evolution of gyrencephaly in *Eutheria* was not an isolated event but has occurred multiple times, probably with instances of both gain and loss of foldedness and likely through related cellular mechanisms that utilize SVZ proliferation in slightly different ways during development. For example, in ferret, the contiguous ISVZ and OSVZ contain similar proportions of progenitor cell types (~40% PAX6-positive cells and 45%–50% TBR2-positive cells) and are distinguished mainly by their cell density (Fietz et al., 2010; Reillo et al., 2010). By contrast, the human ISVZ consists mainly of TBR2-positive IP cells, with a limited number of new oRG cells en route to the OSVZ, which is separated from the ISVZ by an inner fiber layer (Smart et al., 2002; Bayatti et al., 2008; Hansen et al., 2010).

Beyond these anatomical differences, even the function of oRG cells has been proposed to be different between human and ferret. Evidence in human tissue suggests that oRG cells serve to augment both of the primary roles of ventricular RG—increasing neurogenesis and expanding the radial scaffolding for neuronal migration—and demonstrates a lineage relationship between oRG cells and neurogenic TBR2-expressing transit-amplifying cells (Hansen et al., 2010). In contrast, experiments in the ferret show little evidence for this neurogenic lineage in the OSVZ. Instead, oRG (or IRG) cells served mainly to expand the radial scaffold for neuronal migration and mostly gave rise to astrocytes (Reillo et al., 2010). If these observations are confirmed, the neurogenic and scaffolding roles of RG may need to be considered separately when connecting OSVZ proliferation with neocortical expansion in various species.

Despite potential differences in their function, the presence of oRG cells in the ferret, which is evolutionarily more distant from primates than are rodents, argues that this could be an ancestral feature that exists across different species, being utilized to facilitate neocortical expansion to variable extents. Indeed, the developing mouse neocortex contains rare instances of oRG cells (Shitamukai et al., 2011; Wang et al., 2011), which divide asymmetrically to generate neurons without transit amplification (Wang et al., 2011). Although these cells do not constitute a distinct proliferative zone, their sparse observation in a lissencephalic species supports the idea that oRG cells existed in the common ancestor of eutherians but that only in gyrencephalic species has the expansion of oRG cells and OSVZ proliferation been appreciably utilized as a means to generate bigger, more complex brains. That oRG cells appear to generate neurons directly in the mouse but indirectly through daughter IP cells in the human underscores how the evolutionary increase in neuron number is determined by a contribution of both these cell types.

Whether the common ancestor of eutherians possessed relatively abundant or rare numbers of oRG cells is unknown, but it is interesting to consider how evolution could have selected for either large or small brain size and that contexts wherein a smaller neocortex was beneficial could have led to an evolutionary loss of gyrencephaly. The degree to which oRG cells in different species undergo neurogenic versus gliogenic programs and the extent to which they support neuronal migration are therefore ways in which neural development can be finely tuned to achieve the diversity in brain size and shape that we observe today.

ACKNOWLEDGMENTS

Figure 1. Features of human neocortical development.

Cellular behaviors observed in the outer subventricular zone (OSVZ) show that the human neocortex uses expanded numbers of both stem and transit-amplifying cell types (radial glia [RG] and intermediate progenitor [IP] cells, respectively).
(A) Cells expressing the neuronal markers NeuN (RBFOX3, red) and CTIP2 (BCL11B, green) make up ~45% of the OSVZ population (gestational week [GW] 15.5) but never colabel with the progenitor cell marker SOX2 (blue, inset).
(B) The cell division and behavior of OSVZ radial glia-like (oRG) cells is illustrated.
(C) The RG population increases through the generation of oRG cells from the ventricular zone (VZ) and their expansion in the OSVZ. Dashed lines indicate the unknown length of newborn radial fibers.
(D) oRG daughter cells exhibit protracted differentiation and have an increased capacity for transit amplification.
(E) The differentiation of oRG daughter cells is marked by the loss of SOX2 expression and Notch activation (HES1), with a gain in TBR2 expression. Together, these observations explain how the combination of oRG proliferation and differentiation expands the OSVZ over the course of midgestation and gives rise to an increased number of neurons. The lineage and molecular signatures of cells that form the OSVZ are shown (inset).
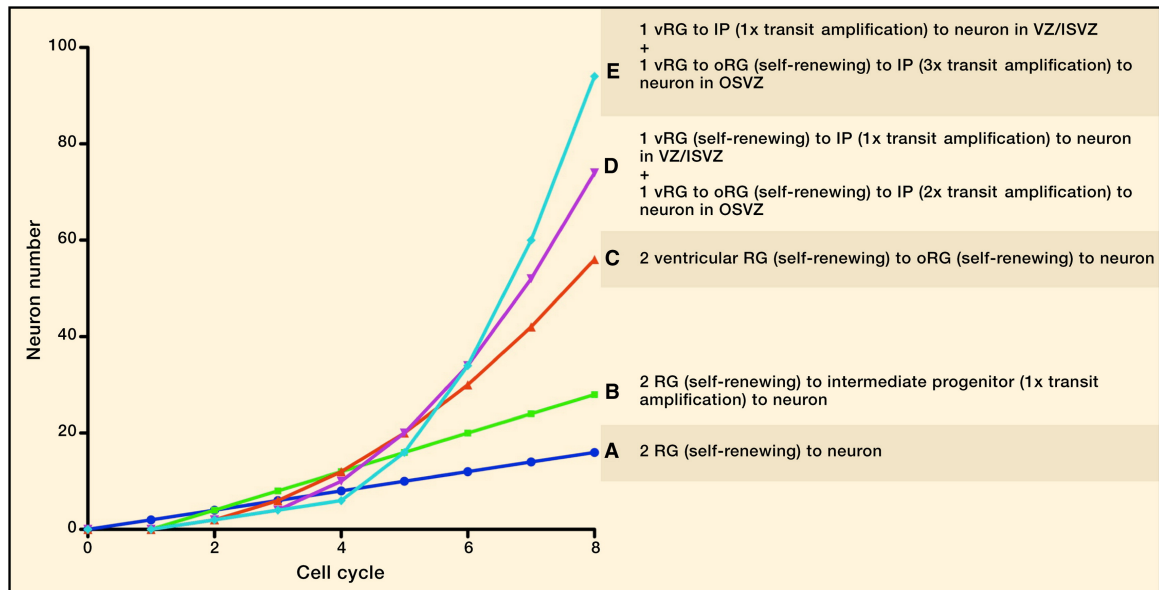
Figure 2. Different rates of neuron accumulation as a result of different modes of progenitor cell division.

The cellular mechanisms of human corticogenesis suggest that the outer subventricular zone (OSVZ) contains OSVZ radial glia-like (oRG) cells and an extended lineage of transit-amplifying intermediate progenitor (IP) cells. To illustrate the effect of these progenitor cells on the rate of neurogenesis, we model and contrast the outcomes in neuronal number from developmental schemes that utilize OSVZ proliferation versus ones that do not. In every case, we start with two radial glial (RG) cells and plot neuron number over the course of eight cell cycles. We also assume no cell death.

(A) Neurons are directly born from RG through repeated rounds of asymmetric division. The rate of accumulation is linear at one neuron/cell cycle/RG cell (Rakic, 1988; Rakic, 2009; Noctor et al., 2001).

(B) We take into account how RG cells give rise to IP cells that undergo one transit-amplifying division. This delays birth of the first neuron by one cycle but thereafter accumulates cells linearly at a rate of two neurons/cell cycle/RG cell. This is the model for rodent corticogenesis (Noctor et al., 2004; Noctor et al., 2008; Haubensak et al., 2004).

(C) Transit amplification by IP cells is not taken into account, but ventricular RG (vRG) cells in the human are assumed to generate oRG cells by repeated rounds of asymmetric division. Once born, oRG cells divide repeatedly to generate one neuron per cell cycle. Because the number of oRG cells increases every cell cycle, this results in exponential growth of neuron number (Fietz et al., 2010; Fietz and Huttner, 2011).

(D and E) One vRG cell undergoes a developmental scheme resembling the rodent (B), whereas the other generates oRG cells over repeated cell cycles. In addition to the exponential growth attributed to oRG cell accumulation, neuronal production is further amplified by two (D) or three (E) transit-amplifying cycles by each oRG-derived IP cell (Hansen et al., 2010). These plots highlight the differential effects of stem cell accumulation and extended transit amplification. We hypothesize that (E) is the most accurate model thus far, although there are several unknown parameters that should change the model. First, the number of transit-amplifying divisions in humans is unknown. Based on how the proportion of oRG cells to IP cells is ∼2:3, we predict that the number of IP divisions does not exceed 3–4, as IP cells would be observed to greatly outnumber oRG cells. Second, the rate of oRG generation is a combined effect of generation from the VZ and expansion in the OSVZ. These parameters are not understood but presumably dictate the relative amount of linear versus exponential neuron production in the human.
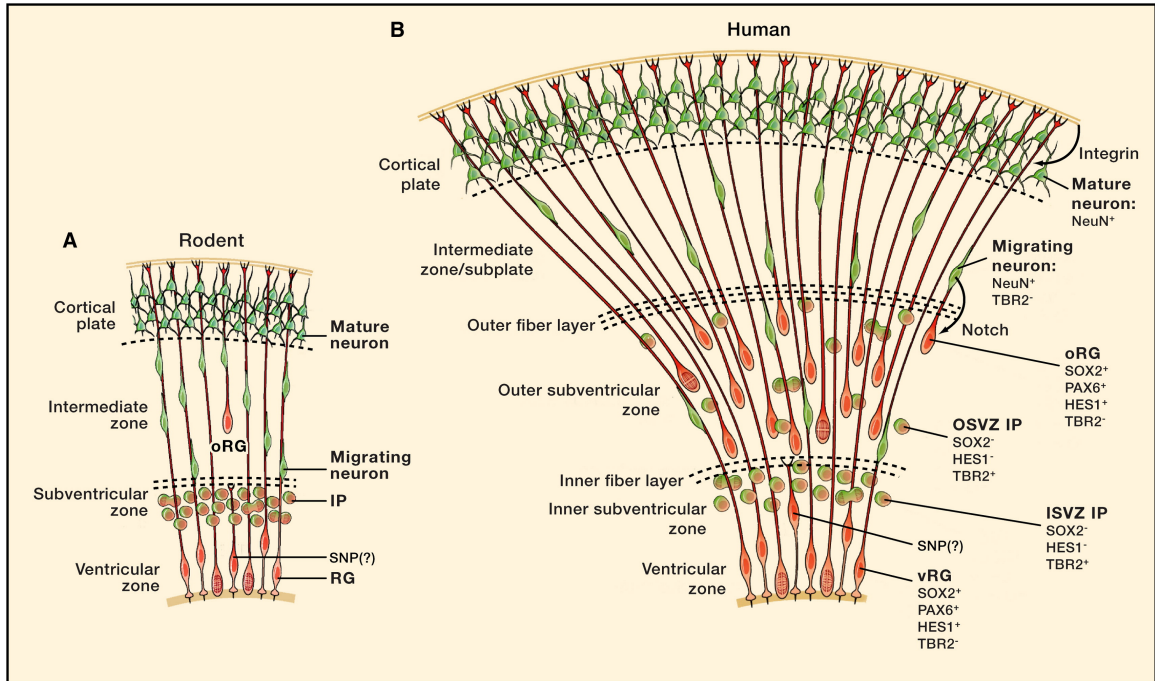
Figure 3. Contrasting rodent and human neocortical development.

(A) Current views of rodent corticogenesis are illustrated. Radial glial (RG) cells most often generate intermediate progenitor (IP) cells that divide to produce pairs of neurons. These neurons use RG fibers to migrate to the cortical plate. The historical view of neocortical development was that RG and neuronal progenitor cells were lineally distinct and that RG did not have a role in neurogenesis. Our current appreciation of the lineage relationship between RG cells, IP cells, and neurons has revised this view. The recent observation that small numbers of outer subventricular zone radial glia-like (oRG) cells exist in the mouse is also illustrated.

(B) We highlight the lineage of oRG cells, IP cells, and migrating neurons (red to green) present in the human outer subventricular zone (OSVZ) and the increased number of radial fibers that neurons can use to migrate to the cortical plate. The number of ontogenetic "units" is significantly increased with the addition of oRG cells over ventricular RG (vRG) cells. Maintenance of oRG cells by Notch and integrin signaling is shown. Short neural precursors (SNP), a transitional cell form between RG and IP cells, are also depicted in (A) and (B). For simplicity, we do not illustrate all of the cell types described in Figure 1E.
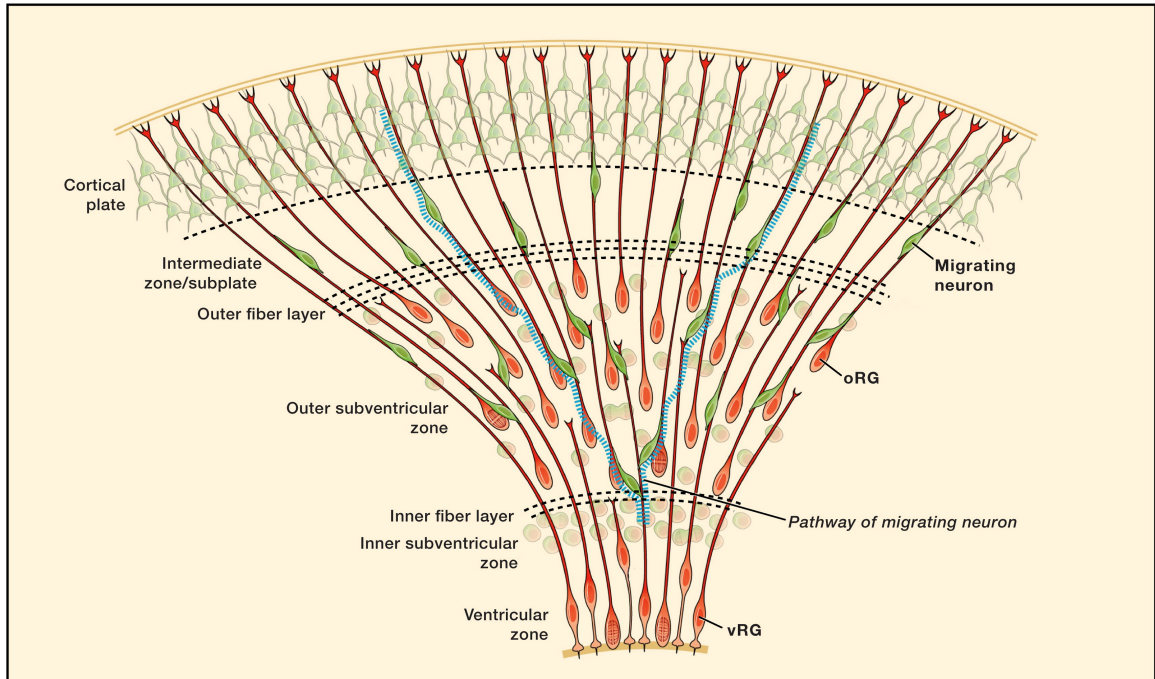
Figure 4. Remodeling of the radial migration scaffold in the OSVZ.

We hypothesize that development of the outer subventricular zone (OSVZ) results in dramatic remodeling of the migration scaffold, where fibers no longer span the apical and basal surfaces. Radial glia (RG) fibers originate from both the ventricular zone (VZ) and OSVZ but may only extend part of the way to the pial surface, therefore forcing migrating neurons to switch fibers and disperse tangentially en route to the cortical plate. This mechanism may be important in the expansion of neocortical surface area observed in gyrencephalic species.
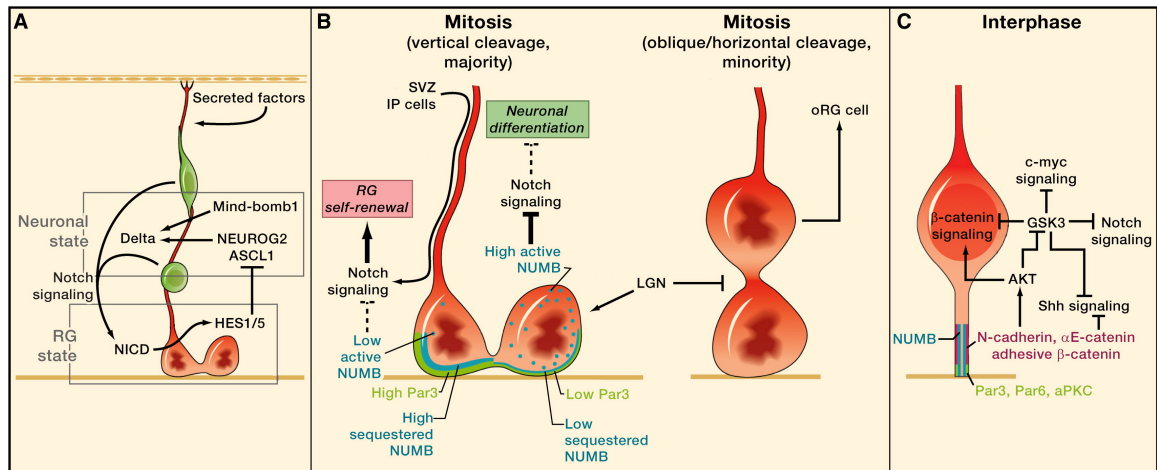
Figure 5. Molecular mechanisms of radial glia maintenance.

(A) The basal fiber of radial glia (RG) cells (red) is important for the reception of Notch signaling from neuronally committed cells in the subventricular zone (SVZ) and secreted factors such as retinoic acid from the meninges. In particular, we show how the reception of Notch signaling in RG results in activity of the Notch intracellular domain (NICD), which promotes HES1/5 expression and leads to repression of the neuronal state.

(B) We hypothesize that asymmetric distribution of Par3 (PARD3) and asymmetric inheritance of the basal fiber during RG mitosis result in differential Notch signaling and cell fate in the two daughters. Par3, a component of the apical complex, is distributed asymmetrically during mitosis and may contribute to asymmetric sequestration of NUMB, an inhibitor of Notch signaling, at cell-cell junctions. The daughter cell with less Par3 has higher levels of active NUMB that inhibits Notch signal, resulting in neuronal differentiation. Inheritance of the basal fiber may also help to enforce Notch signaling in only one of the daughter cells. We also highlight how removal of LGN (GPSM2) shifts vertical cleavages toward more oblique/horizontal ones, resulting in the production of outer subventricular zone radial glia-like (oRG) cells.

(C) Adherens junction components (pink) are critical for controlling multiple pathways that define the intracellular signaling state of RG cells.
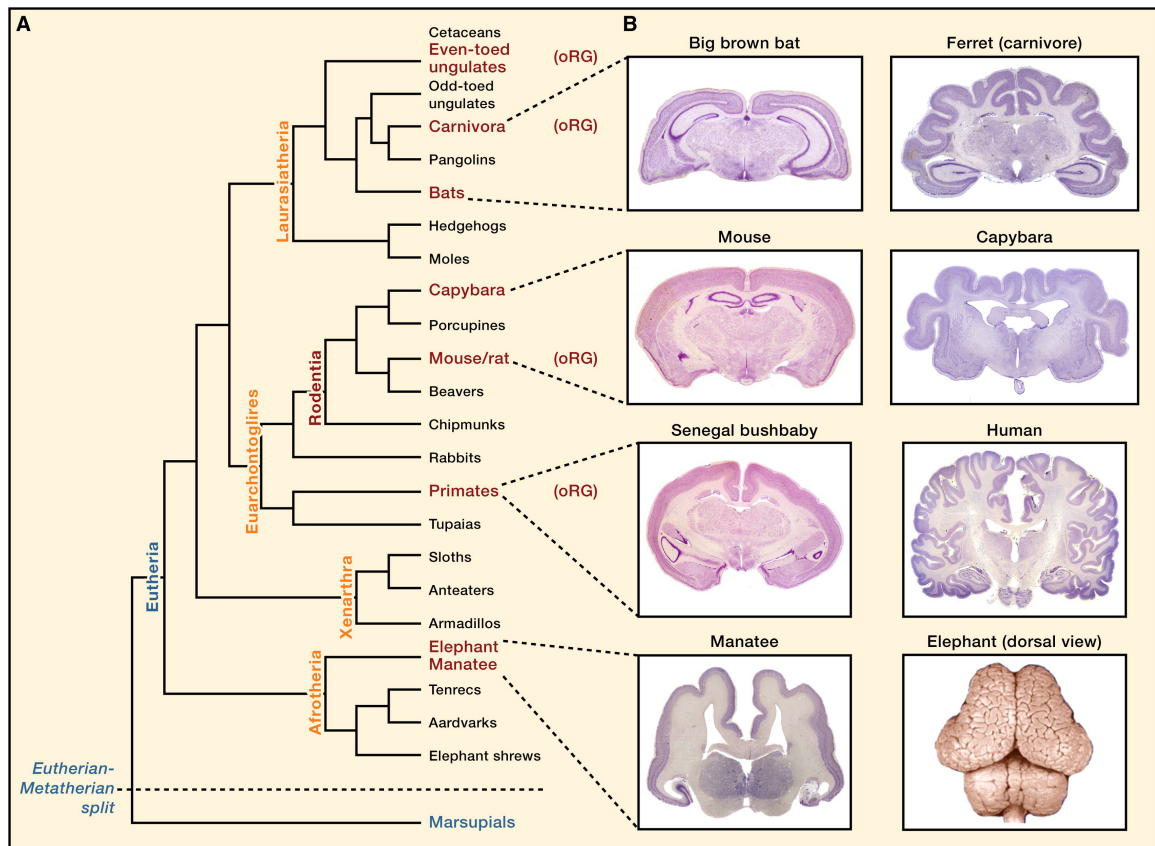
Figure 6. OSVZ proliferation in the context of evolution.

(A and B) A phylogenetic tree (adapted from the Tree of Life project [http://tolweb.org] and WhoZoo Project [http://whozoo.org]) is shown to illustrate the diversity of brain size/shape in an evolutionary context. Eutherian (placental mammals) and metatherian (marsupial) species, the two major infraclasses of mammals, are included, whereas monotremes (egg-laying mammals), the other major order of extant mammals, are not. Species in which outer subventricular zone radial glia-like cells have been observed in embryonic tissues are labeled (oRG). Species that lack the oRG label have not yet been examined for the presence of these cells. Each eutherian superorder illustrated (A, orange) contains species that have lissencephalic (left) and gyrencephalic (right) brains (B, from the Comparative Mammalian Brain Collections [http://brainmuseum.org]). Examples of both lissencephaly (armadillo) and gyrencephaly (sloth) also exist in the Xenarthra superorder (not shown). Thus, the evolution of gyrencephaly (or lissencephaly, as the case may be) was not an isolated event. oRG cells are present across multiple superorders, indicating that these features are not specific to a particular lineage of mammals. The degree of oRG-related proliferation and that of oRG-derived IP cells varies in different species and likely gives rise to diversity in neuronal number and brain shape. Images shown (B) are all coronal sections (not to scale) except for the elephant, which is a dorsal view.

CHAPTER 4

Towards a molecular understanding of the developing

human neocortex

This chapter is a work in progress by:

Lui, J.H., Bedolli, M.A., Kriegstein, A.R*, and Oldham, M.C.*

*co-mentors

SUMMARY

The large size and folded shape of the human neocortex is caused by proliferative events in the outer subventricular zone (OSVZ) during development. Inferring how these cellular processes are controlled mechanistically is a challenge, since our current molecular understanding of neocortex development is mostly derived from genetic studies of the mouse, which do not have an OSVZ. To begin understanding the molecular basis of OSVZ development, we systematically analyzed gene co-expression relationships in the developing human neocortex from microarray data of serially sectioned tissue, and generated an unbiased framework for grouping co-expressed genes into modules. Bioinformatic and anatomical annotation of the genes constituting these groups identified modules that correspond to gradients of gene expression, subcellular processes represented at different stages of neuronal maturation, and radial glia—the neural stem cells of the human brain. Because OSVZ development is likely the result of evolutionary changes to radial glia regulation, we focused on human radial glia modules and identified genes that have undergone functionally significant change in the human lineage. These data provide a compelling set of candidate regulators for interrogating human-specific radial glia biology and OSVZ development.

INTRODUCTION

Rationale

The large size, folded shape, and superior cognitive function of the human neocortex are all results of a finite set of instructions encoded in the human genome. Our recent characterization of progenitor cells in the developing human neocortex provides a new biological context for understanding how these molecular instructions unfold into developmental events that anticipate gyrencephaly and large brain size. These events involve the generation and massive proliferation of a progenitor cell lineage that begins with an outer radial glial (oRG) cell, ends after multiple rounds of transit-amplifying divisions with postmitotic neurons, and is located outside of the ventricular epithelium in the outer subventricular zone (OSVZ) (Hansen et al., 2010). OSVZ proliferation is present across mammalian species, but the amount observed in development correlates with neocortical size and folding, with mice and humans at two opposite extremes (Lui et al., 2011). Therefore, in order to understand how mammalian evolution has resulted in brains of different size and shape, it is critical to determine the molecular controls that initiate and maintain OSVZ proliferation.

There are a number of challenges in understanding the molecular controls of OSVZ proliferation. Genetic studies have identified important control mechanisms of mouse radial glia (RG), and while it is possible to infer how these mechanisms are translated to the human, this cannot be done with certainty without first understanding how RG are molecularly different between human and mouse. Second, because the observed variability in OSVZ proliferation across species is fundamentally caused by discrete genomic differences introduced by evolution, it is important to understand the relationship between the molecular controls of development and the species-specific genomic features that drive them. Studies in comparative genomics have identified many unique features of the human genome that could be responsible for human-specific features of

brain development (Pollard et al., 2006; McLean et al., 2011). However, this information has never been placed into the context of human RG cells and OSVZ proliferation.

Direct characterization of gene expression patterns present in the developing human neocortex is therefore a prerequisite for understanding how the known molecular mechanisms of mouse RG and the unique features of the human genome relate to OSVZ proliferation and neocortical expansion. Because of this, we aimed to describe the patterns of gene expression in the developing human neocortex, focusing on gene expression signatures of human RG. We further aimed to uncover molecular differences between ventricular RG (vRG) cells and oRG cells, as we hypothesized that these differences would give important clues towards understanding the evolution of OSVZ proliferation. Collectively, these data would allow for direct molecular comparisons to be made between human and mouse, and help refine hypotheses about human-specific gene regulation in neocortical development.

This chapter reports our effort to describe and analyze the gene co-expression patterns in the developing human neocortex.

Network analysis of gene co-expression relationships

Traditional methods of gene expression profiling have relied mostly on comparing mRNA levels derived from bulk tissue samples. Although these types of studies were useful for discovering broad gene expression differences between tissue samples, it was not possible to attribute the observed differences to the biology of a particular cell type, since each sample contained a heterogeneous population of cells. Because of this, technologies such as fluorescence activated cell sorting, laser-capture microdissection, and immunopanning have been developed to first isolate specific cell populations before profiling their gene expression (reviewed by Nelson et al., 2006; Okaty et al., 2011). These differential expression approaches are clearly an improvement over those using bulk tissue, but their usefulness still depends on the feasibility of accurately

isolating cell populations, which usually requires prior knowledge of distinguishing features between the populations of interest.

Because of this strategic limitation, where one needs to know something about the cell type before being able to isolate it, a complementary approach known as co-expression analysis has emerged to address the problem of describing cell type specific information from samples with cellular heterogeneity. Gene co-expression network analysis simply aims to identify groups of genes that have highly correlated expression in a tissue, by comparing how expression levels of individual genes change across many samples (Zhang and Horvath, 2005). This method assumes that if the transcript levels of two genes consistently move together across many samples (are highly correlated), then they are likely to be co-expressed in the tissue from where the RNA was derived. This concept can be expanded to include all genes, providing a comprehensive framework that groups genes into co-expression modules. Because the robustness of gene expression correlation in a tissue is likely the consequence of transcriptional co-regulation or cell type specific expression, these modules are expected to be functionally or anatomically significant. Importantly, this approach uncovers co-expression relationships using bulk tissue, and does not require knowledge of distinguishing features that delineate cell types.

When applied to microarray data generated from distinct adult human brain regions of many individuals, this type of network analysis identified large gene co-expression modules corresponding to neurons, astrocytes, and oligodendrocytes in every brain region. Other modules of co-expressed genes corresponded to region-specific cell types, such as Purkinje neurons in the cerebellum (Oldham et al., 2008). This demonstrated that it was possible to isolate the molecular signatures of specific cell types using microarray data from bulk tissue samples. These results followed from two basic premises: 1) cell types are distinguished by the genes that they express, and 2) the absolute number of each cell type will vary from sample to sample. Therefore, the

genes most specifically and consistently expressed in a given cell type should appear highly correlated in microarray data derived from bulk tissue samples.

Because the gene expression signatures of cells in the developing human neocortex are not well-defined, and oRG cells and vRG cells are virtually identical in their known gene expression—with any of the hypothesized differences not useful for cell sorting, we took this alternative approach for the characterization of gene expression patterns. Due to technical limitations, it would be difficult to collect enough samples from different fetal human brains to replicate the experimental design used in the adult human brain. However, we reasoned that if there were differences in the ratios of cell constituents among the sectioned samples of one piece of tissue, the same principles described above would apply, and the resultant co-expression network would show co-expression relationships present within the single piece of tissue. Specifically, we hypothesized that this approach would reveal the co-expression signatures contributed by human RG cells, as this is an abundant cell type in fetal neocortex. We further hoped that the signatures of vRG and oRG cells could be identified as highly related but distinct modules.

A co-expression network of the developing human neocortex from one individual

To generate a gene co-expression network from the developing human brain, we began with an almost intact cortical hemisphere from a donated gestational week (GW) 14.5 fetal specimen. The ventral telencephalon containing the ganglionic eminences was separated from the dorsal cortex, and a sliver of cortical tissue was removed and fixed for staining. Both of the larger fragments were then flash-frozen for RNA analysis. Total RNA was extracted and purified from 150μm serial coronal sections (cut along the rostral-caudal axis) of the neocortical fragment (Fig. 1). Because of the orientation of sectioning, each sample contained RNA contributed by every cell type in the cortical wall ranging from vRG cell to oRG cell to neuron. However, because the

stoichiometry of each cell type was expected to differ slightly in each section, the changes in expression across samples could be leveraged to reveal correlations between genes.

We profiled the described RNA samples from GW14.5 human neocortex using Illumina HumanHT12-v4 microarrays. Following data pre-processing (see methods), a gene expression signature of 89 observations along the rostral-caudal axis could be generated for each probe/gene present on the microarray. Patterns derived from the 30,425 probes of highest quality were selected for constructing a co-expression network. The matrix of Pearson correlation coefficients for every combination of these probes was generated to quantify the level of similarity between genes. Based on this, highly correlated genes were then grouped into co-expression modules (see methods for description of similarity criteria used for module generation).

The general structure of the co-expression network is as follows: Each module is a group of genes that are highly correlated with each other. Although similar, the pattern of expression of each gene within a module is not exactly the same, and thus an important summarizing measurement of each module is the "average" expression pattern of its gene constituents, which we refer to as the module eigengene (defined as the first principal component obtained by singular value decomposition of a module gene expression matrix). To assess similarities between modules, Pearson correlation coefficients were further calculated between every module eigengene pair to additionally group similar modules with each other.

Module eigengenes describe the most salient gene expression "patterns" within a given dataset. However, it is often of interest to relate the expression of individual genes of interest to these identified patterns. We therefore quantified the strength of "module membership" for each gene with respect to each module by calculating the Pearson correlation between each gene's expression pattern and each module eigengene. We refer to this quantity as a gene's "kME value", which loosely translates as the connectivity of the gene (k) with respect to the module eigengene

(ME) (Horvath and Dong, 2008). Reciprocally, for each module we can generate a list that ranks all genes in order of their correlation with the module eigengene. This allows the module definition to be expanded to include all genes with module membership within a p-value threshold. Given these methods of analysis, we predicted that genes with robust co-expression relationships in the developing human neocortex would be captured by the data and that modules corresponding to RG cells could be identified.

RESULTS

A co-expression network of 55 modules

We generated a co-expression network from the GW14.5 human neocortex dataset that contained 55 modules, which we labeled by colors (Fig. 2A). Module eigengenes represent major patterns of gene expression, and we observed that two groups of modules had expression patterns that exhibited clear and opposing gradients across the 89 measured samples. One gradient, represented best by the *turquoise* module (which was the largest module in the network), increased in expression in the caudal to rostral direction, whereas the other gradient, represented by the *blue* module (which was the second largest module in the network), increased in the rostral to caudal direction (Fig. 2A). We further found that a number of genes (*DLX1*, *GAD1*, *CALB2*) expressed in inhibitory neurons had very high module memberships (kME values) in the modules exhibiting the high rostral-low caudal gradient. This finding suggested that inhibitory neurons are present in greater abundance in the rostral aspect of the neocortex than in the caudal aspect.

Observed gradients of gene expression in the rostral-caudal axis could be explained by differences in the amount of a cell type, differences in the amount of gene expression within a cell type, or both. To verify that the bioinformatically identified gradient genes were expressed physiologically in the same manner, we immunostained GW14.5 tissue sections from the most rostral and caudal aspects of the neocortex of an age-matched but unrelated individual, and compared the expression of TOX, a strong member of the turquoise (high rostral-low caudal) module. As predicted, the level of TOX was higher rostrally, and its expression was restricted to the cortical plate (Fig. 2B). This suggested that genes expressed by neurons in the cortical plate make a contribution to the high rostral-low caudal expression gradient captured by the turquoise module. To investigate whether cells in the cortical plate were also contributing to the opposite gradient, we performed *in situ* hybridization for *CPNE4*, a member of the blue (high caudal-low

rostral) gradient. Although the expression of *CPNE4* was much more sparse than TOX, it was also restricted to the cortical plate (Fig. 2C). Together, these results suggest that neurons in the cortical plate are contributing most to the observed gradients of gene expression in the neocortex. Further analysis will be required to determine whether the genes in these opposing gradients are expressed by mutually exclusive cell types.

Bioinformatic and anatomical annotation of the 5-block network structure

Previous work has shown that the presence of very large gene co-expression modules in a network can obscure the presence of smaller, yet biologically meaningful, gene co-expression modules (Oldham et al., 2006). Because the effects of the two observed gradients were so strong (contained nearly 20% of all genes that showed significant module memberships), we generated a second dataset that subtracted the observed gradient effects through linear regression analysis. We then constructed another gene co-expression network using the same module detection parameters.

The resultant network contained 45 modules, which when clustered on the basis of correlation between module eigengenes, resulted in 5 major blocks of modules (Fig. 3). Thus, our network analysis of transcriptome organization in fetal neocortex, beginning from the level of the gene, to groupings of genes into modules, and finally groupings of modules into blocks, highlights the utility of this approach for the simplification of a very complex system. We hypothesized that each block would correspond to either a major cell type or biological process present within the tissue, with each module representing nuances and heterogeneity within the general theme of the block. More generally, gene co-expression modules provide a natural framework in which to search for the enrichment of informative gene sets, where such sets can be defined according to any number of biologically meaningful criteria, including ontological classification, chromosomal location, the presence of regulatory motifs, and cell type-specific expression patterns.

To characterize the biological significance of each block, we used several bioinformatic strategies. At the level of single genes, we took two approaches. First, we examined the lists of genes ranked by module membership for each module, seeking out genes of well-known function that also had high memberships for the block as a whole. We then took the reciprocal approach, beginning with well-characterized genes in neocortical development, and then determining which modules/blocks these genes had a high membership for.

Using these methods, we found that Block 1 contained genes such as *TBR1* and *POU3F2* (*BRN2*), known transcriptional regulators in the specification of excitatory neuron layer subtypes (Molyneaux et al., 2007). Block 1 also contained cell surface proteins such as *NCAM1* and *CD24*, both of which are involved in neuronal cell adhesion (Fig. 4). Further enrichment analyses of these modules with other published gene sets from the Gene Ontology Project (Ashburner et al., 2000), Molecular Signatures Database (Subramanian et al., 2005), and Ingenuity Pathway Analysis (Ingenuity® Systems, www.ingenuity.com), suggested that the co-expression patterns of Block 1 are most relevant in the molecular processes of migrating and/or immature neurons.

We took similar approaches with Blocks 3 and 4 and found that both blocks were also highly related to neurons. Block 3 contained genes in the Robo and Semaphorin families, well known to be important in axon guidance, whereas Block 4 contained genes such as *SHANK3*, *STX1A* (syntaxin), and *NMDA-R1*, known to be important in mechanisms of synaptic transmission. Further enrichment analyses with published gene sets confirmed that these biological processes were important in the modules. The genes present in Block 5, meanwhile, are enriched with processes involving the ribosome, mitochondria, and energy metabolism. Since the processes enriched in Block 5 are likely ubiquitous to all cells in the cortical wall, it is unclear whether the gene activity patterns in these modules are driven by all cells in the tissue or a subset of cells for which these processes are likely to be particularly pronounced (for example, actively dividing cells).

We also sought to characterize the significance of each block anatomically. Although the co-expression network quantifies gene expression at the level of mRNA, we took the initial approach of immunohistochemistry, which qualitatively describes the location and level of protein expression in a tissue. Although we expected some discordance between the location of mRNA vs. protein expression in the tissue because of factors such as post-transcriptional regulations and antibody specificity, we anticipated that this approach would give an anatomical approximation of the bioinformatic data. Importantly, this approach did not require new reagents to be generated.

As a first experiment, we performed immunostaining of several nuclear genes present in Blocks 1 and 3 and assessed their expression patterns (Fig. 5). We found that all of the genes exhibited widespread expression throughout the cortical wall, making it unlikely that any one gene or small combination of genes would define a specific cell subtype. In comparison to TBR1 as a reference, which is expressed only in postmitotic neurons and absent from the ventricular zone (Fig. 5A; Bayatti et al., 2008), the other proteins were either expressed uniformly through the entire cortical wall or expressed at higher levels in the cortical plate and at lower levels elsewhere. Although we have not yet been able to formally test for the co-expression of these genes in the tissue, the abundance of stained cells supported the original prediction that genes in Blocks 1 (Fig. 5A) and 3 (Fig. 5B) were co-expressed with each other. However, while these genes were certainly co-expressed in many of the same cells, it is also possible that their co-expression relationships reflect regulatory processes that are shared among different cellular populations.

Identification of putative RG modules and novel RG genes

To identify the modules within the 5-block structure corresponding to RG cells, we first selected genes known to be expressed in RG cells, and then asked whether they showed strong association with any modules in particular. Although none of these selected genes are truly specific to RG cells, we reasoned that with enough markers, commonalities between module memberships

would emerge. Although there were some exceptions to the rule, we found that the majority of selected genes had high levels of membership for the *mediumorchid3*, *lightcyan1*, *white*, *orange*, and *violet* modules (Fig. 6A). To expand this analysis, we identified other gene sets related to RG cells and quantified their extent of enrichment in the 45 modules. We found that the same five modules were most consistently enriched, suggesting that these modules correspond to RG cells (Fig. 6B). Additional enrichment analyses of these modules with other gene sets from the Gene Ontology Project (Ashburner et al., 2000), Molecular Signatures Database (Subramanian et al., 2005), and Ingenuity Pathway Analysis (Ingenuity® Systems, www.ingenuity.com) showed their association with the cell cycle and proliferation at large.

The first four of these modules formed Block 2, but the *violet* module, although highly correlated with Block 2, was clustered with Block 5 (Block 2b, Fig. 7A). We were intrigued by the natural separation of these modules, and predicted that they would correspond to a level of heterogeneity within the RG cell population. To verify that the members of these modules were indeed expressed in RG cells, and to determine whether the separation of these modules corresponded to differences in ventricular vs. outer subventricular gene expression, we performed immunostaining for strong members of these modules.

Since the initial selection of RG-related genes tended to correlate well with all five of these modules (Fig. 6A), we identified a set of RG "contrast" genes that were significantly more correlated (difference in p-value for module membership $> 10^3$) with one of the five modules than with any of the other four. We predicted that these genes would reveal the distinguishing features of one module vs. the others.

We stained for two of such RG contrast genes, ATAD2 and ZBTB20 (Fig. 7B and D), which were predicted to be expressed in the nucleus and were highly correlated with Block 2a, but less so with Block 2b (*violet*). ATAD2 is an E2F-dependent transcriptional co-factor for c-myc (Ciro

et al., 2009), whereas ZBTB20 is a transcription factor implicated in the specification of CA1 neurons of the mouse hippocampus (Xie et al., 2010). Neither of these genes had been previously associated with human RG cells, but when immunostained in GW14.5 neocortical sections, were indeed expressed throughout the dorsal VZ and OSVZ (Fig. 7D). When compared with SOX2, a gene expressed generally in primary progenitor cells of the neocortex, both ATAD2 and ZBTB20 had similar but slightly different expression patterns. ATAD2 was co-expressed in a large subset of SOX2-positive cells, but not at the ventricular surface where mitosis occurs. Based on this expression pattern and the association of ATAD2 with proliferation-related transcription, we suggest that ATAD2 expression is cell cycle phase-specific.

ZBTB20 expression was extremely similar to that of SOX2 in the VZ/OSVZ, but was not expressed beyond the boundary of the OSVZ (Fig. 7D). This pattern of expression was identical to another marker of RG cells, PAX6. Interestingly, the role of ZBTB20 in the hippocampus does not extend to the neocortex in mouse, suggesting that neocortical ZBTB20 expression in the human is a species-specific feature. Reciprocally, we also stained for two genes with higher module membership in the *violet* module than in Block 2, CDC20 and SOX3 (Fig. 7C). Both CDC20 and SOX3 labeled cells throughout the VZ/OSVZ, with significant co-labeling with SOX2 and Ki67, a marker for S/G2/M phases, indicating that they are also progenitor cells (Fig. 7E). In particular, CDC20 labeled only a small subset (<10%) of the SOX2-positive population, suggesting that while this subset does not delineate VZ vs. OSVZ expression, subsets of primary progenitor cells can be defined by this method.

Together, these data show that co-expression network analysis can successfully identify novel genes expressed in RG cells such as ATAD2 and ZBTB20, as well as others not discussed such as PALLD, VCL, and MDK. However, none of the gene expression patterns tested thus far were specific for either the VZ or OSVZ. Based on the numbers of labeled cells, these patterns were also not entirely specific for RG cells and likely include slightly more differentiated cell types,

similar to other known markers of RG cells such as SOX2 and PAX6. Nevertheless, this method has allowed us to focus on a defined gene set that is expressed by primary progenitor cells of the neocortex, many of which are RG cells. These unexplored genetic regulators of human RG cells could be very relevant to OSVZ generation.

Connecting RG modules with evolutionarily relevant genes

We aimed to find gene expression signatures of human RG cells to provide a better context for understanding the evolutionary changes that gave rise to the OSVZ. Our identification of the *mediumorchid3*, *lightcyan1*, *white*, *orange*, and *violet* modules as RG-related allowed us to investigate whether the genes in these groups have been relevant in evolution. We used PolyPhen-2 (Adzhubei et al., 2010), a bioinformatic tool that identifies genes with damaging mutations (human-specific amino acid changes predicted to cause functional change), to determine the genes in our dataset likely to have undergone such changes in evolution. We determined the module membership for each of these genes in our 45 modules, and identified only a small number that correlate highly to the 5 RG-related modules. Examples of such genes include STIL, PRC1, and DTL (Fig. 8), all of which have not specifically been implicated in RG cells, but are key regulators of the mechanics in mitosis and cytokinesis. Together, this approach has helped focus our efforts toward a small number of genes that are likely expressed in human RG cells and may have evolved uniquely human functions. Further work to manipulate the expression of these genes will elucidate their functional significance in the context of OSVZ proliferation.

DISCUSSION

Using co-expression network analysis, we have comprehensively described and grouped the gene expression patterns of GW14.5 neocortex into modules. Using well-characterized genes and gene sets as a handle to interrogate the function of these groups, we identified modules that correspond to cellular processes of neurons at various stages of maturation, including migration, axon guidance, and synaptic transmission. Because the utility of this approach is that for every "known" gene, we can easily identify novel genes in closest correlation with it, these data now serve as a rich starting point for understanding more about these biological processes.

The studies described in this chapter were aimed as a first step towards identifying and testing the molecular mechanisms that drive OSVZ proliferation, and thus we focused our efforts on finding genes that were expressed in human RG cells. We were successful in identifying five modules that had high association with known RG genes and were functionally important in cell proliferation. These modules also contained many genes never before associated with RG cells, some of which may have human-specific functions. An exciting future direction for understanding these genes will be to confirm their expression physiologically and test their function in the context of OSVZ proliferation.

While we hoped to identify specific markers for different subtypes of RG cells, including oRG cells, we learned that this was challenge given the nature of gene expression patterns in developing tissues. Our implicit assumption was that oRG cells could be designated as a cell type distinct from other RG cells, and that its different location in the cortical wall would have a molecular correlate at the level of the co-expression modules. However, this assumption may not be entirely justified, as even in the mouse where RG cells are relatively well characterized, no defined set of genetic markers exist to specifically define the cell type. Rather, RG cells are best defined by a combination of morphology, location, and a large set of co-expressed genes. More

generally, the categorization of cells into distinct "types" is conceptually useful for considering the organization and structure of a tissue. However, these categorizations can also be artificial in developing tissues, as cells are constantly in transition from one set of features to the next. For example, since RG cells are part of a developmental timeline of differentiation, their expressed genes are usually also present in overlapping cell types later in the timeline, making it a challenge to define a discrete molecular signature. In the context of human development, this effect may be especially pronounced since the differentiation of neurons from RG cells occurs over many cell cycles with multiple transitional cell forms (Lui et al., 2011).

Of the genes in both the neuronal modules and radial glial modules that we selected to immunostain, we found patterns of expression that almost certainly spanned more than one cell type. While "neuronal" genes were often expressed at highest levels in the cortical plate, they were also expressed at lower levels in most other cells of the cortical wall. Similarly, the genes expressed in RG cells were also expressed in a widespread manner throughout the proliferative zones, similar to known markers. While we predict that a more comprehensive anatomical analysis of the RG-related genes could reveal differences in OSVZ vs. VZ gene expression, our analysis has been most successful at identifying the strongest gene co-expression patterns. Because the mechanisms that control these co-expression relationships are likely important in a large time window of differentiation, it follows that the gene expression patterns we observed are also not limited to one cell type.

Because of these issues, an important future direction will be to utilize the information in the five RG cell modules to better analyze the similarities and differences in gene expression among RG cells. For example, it will now be possible to identify cell surface markers expressed broadly by human RG cells but not neurons. Combining this information with microdissection of the VZ vs. OSVZ could better allow us to identify distinguishing features of oRG cells and vRG cells.
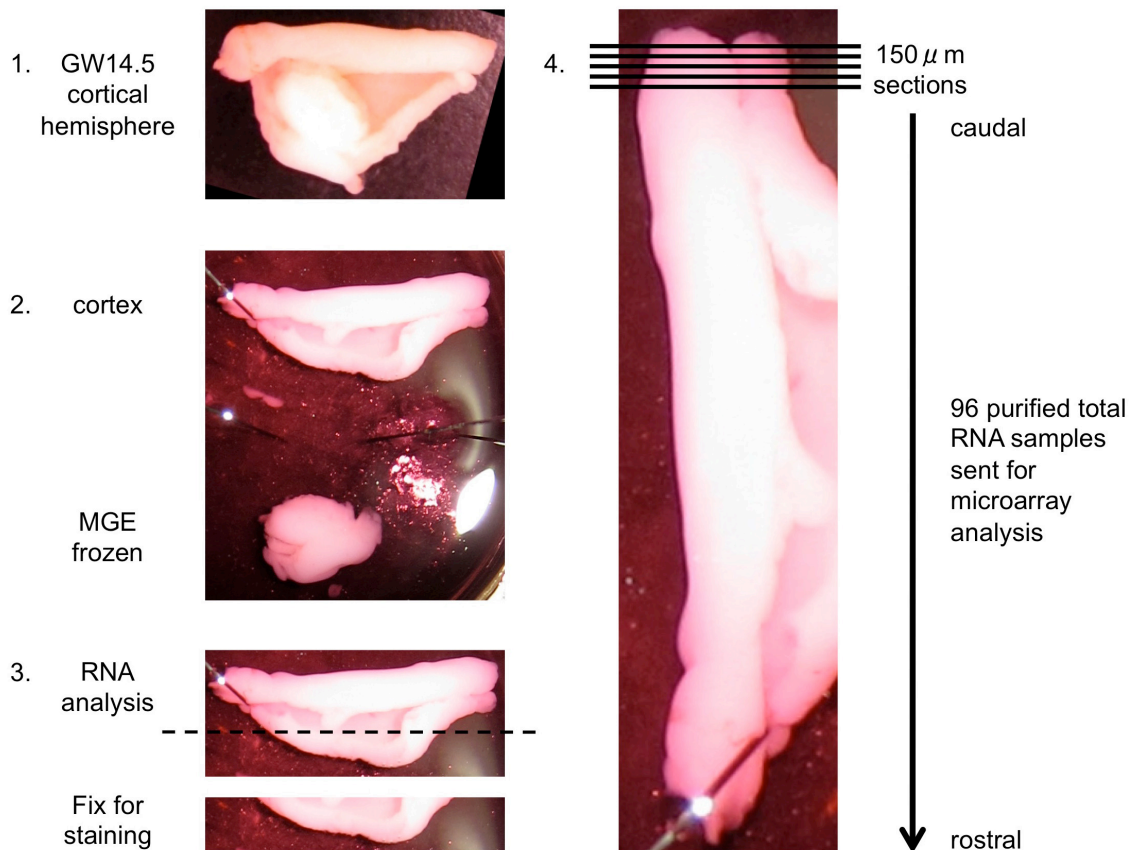
Figure 1. Strategy for generating a gene co-expression network from the developing human neocortex of one individual.

A mostly intact cortical hemisphere from a donated GW14.5 fetal specimen was used as the starting material (Step 1). The medial ganglionic eminence (MGE) was dissected away from the cortex for flash-freezing and future RNA analysis (Step 2). A small sliver of the lateral cortex was dissected and fixed in 4% paraformaldehyde for future sectioning and staining (Step 3). The remainder of the cortex was then flash-frozen and sectioned in the coronal plane (150μm) to generate ~100 tissue samples. Total RNA from each cortical sample was extracted using Trizol with strict quality control (Step 4). 96 purified RNA samples were analyzed using Illumina HumanHT12-v4 microarrays with 89 samples used for network construction. Highly correlated genes were grouped into 55 gene co-expression modules.
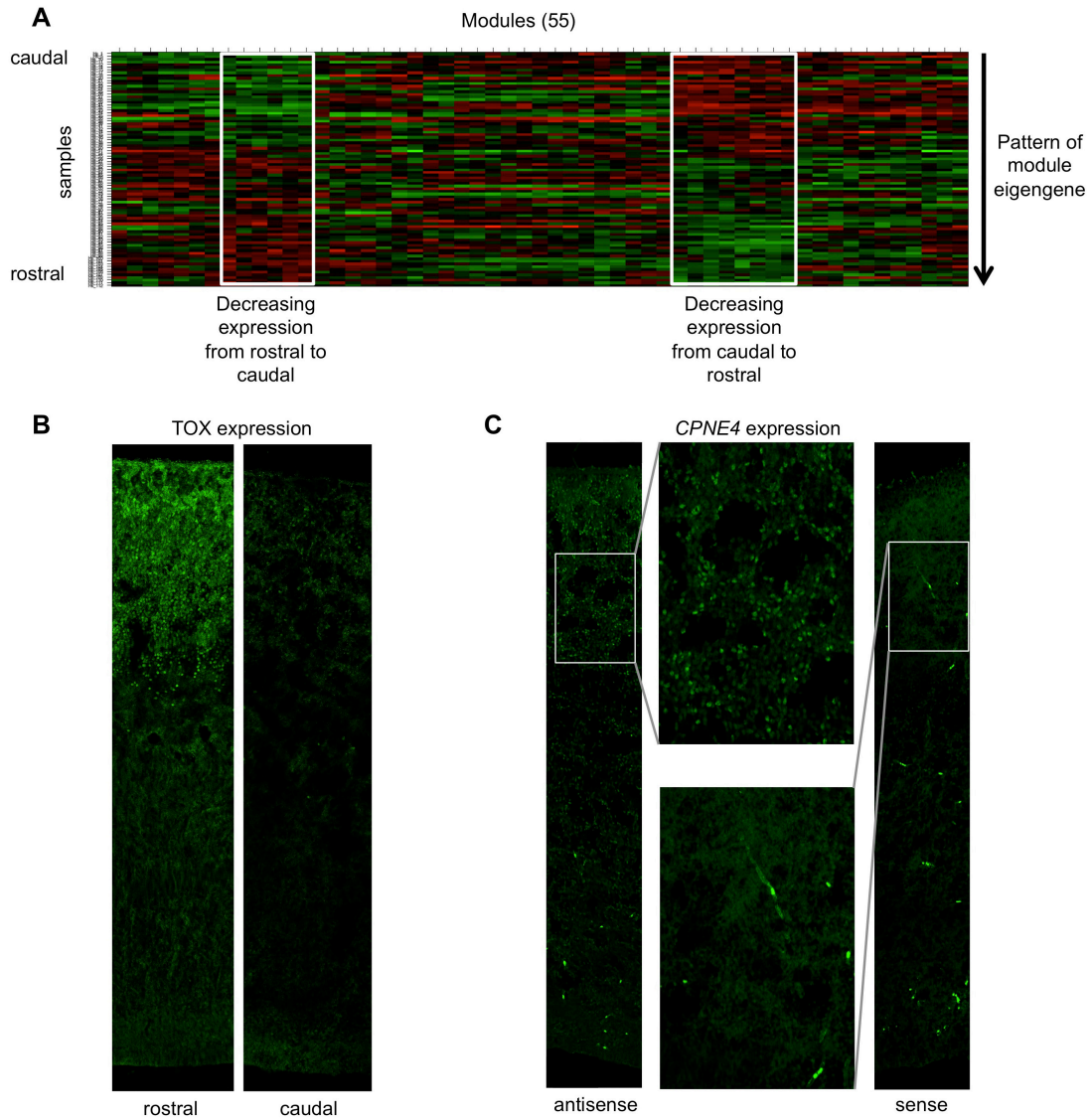
Figure 2. Gradients of gene expression are revealed in the GW14.5 human neocortex co-expression network.

A heat-map schematic (red-high expression, green-low expression) of the co-expression network is shown (A). Each column along the horizontal axis represents a summary of the characteristic expression pattern of genes constituting a module (a module eigengene). Module eigengenes (55 total) are clustered by similarity along the horizontal axis, with samples arranged on the vertical axis (caudal to rostral). Modules with rostral-caudal and caudal-rostral gene expression gradients are highlighted (white boxes).

(B) Immunostaining for TOX, a gene identified from the rostral-caudal gradient, in GW14.5 neocortical tissue. Sections from the rostral and caudal aspects of the cortex are shown.

(C) *In situ* hybridization for *CPNE4*, a gene identified from the caudal-rostral gradient, in GW14.5 neocortical tissue. The antisense probe is shown on the left with an inset over the cortical plate. The control sense probe is shown on the right.
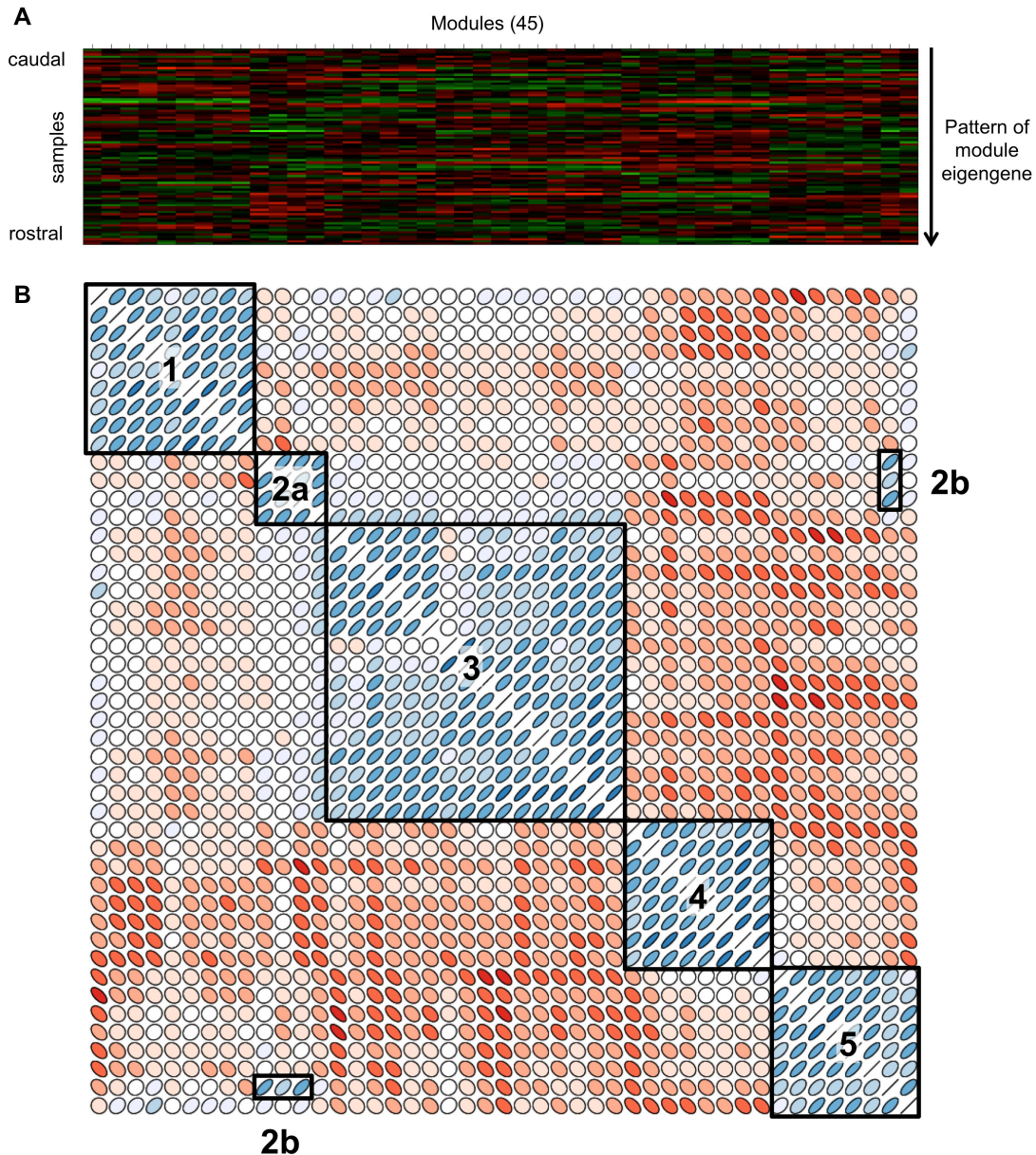
Figure 3. Exclusion of gradients reveals 5 meta-patterns of gene activity in GW14.5 human neocortex.

A recalculated network in which gradients have been subtracted from all gene expression patterns. A heat-map schematic of the resultant 45 modules is shown (A).

An alternative representation of module eigengene clustering is shown (B). Correlation coefficients between every combination of the 45 module eigengenes are represented by ellipses. Negative (positive) correlations are denoted by the strength of the red (blue) color and the width/direction of the ellipse. The higher the absolute value of the correlation coefficient, the more narrow the ellipse. This depiction reveals 5 major blocks of co-expression modules (labeled Blocks 1 to 5). Importantly, one module (*violet*, 2b) stands alone and is highly correlated with both Blocks 2a and 5.
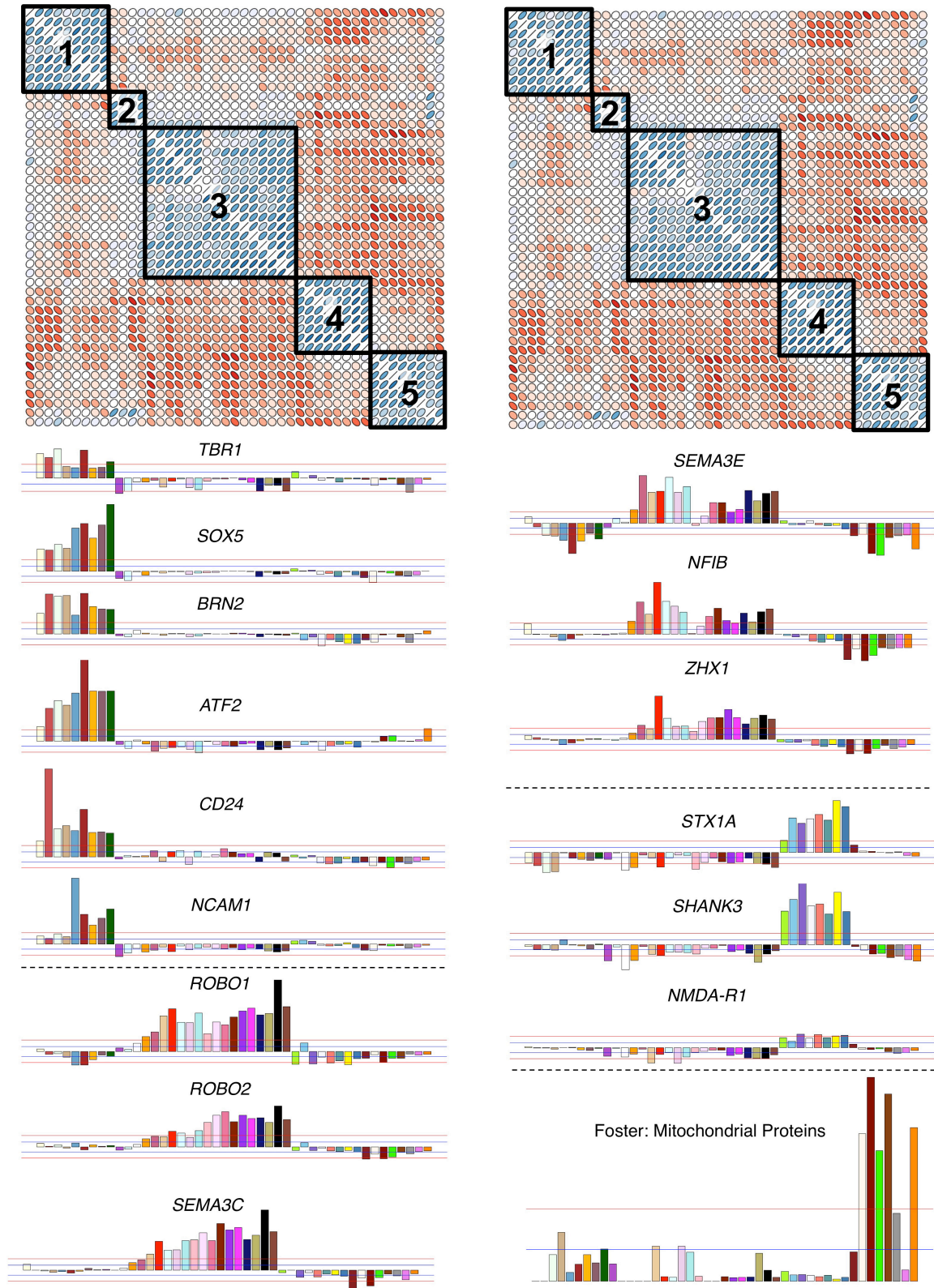
Figure 4. Module membership levels of well-characterized genes suggest different functions for each co-expression block.

Genes that show high levels of module membership for entire blocks of modules are shown to inform the function of individual blocks. The pattern of expression of a given gene is correlated with each of the 45 module eigengenes to determine a set of correlation coefficients (with associated p-values), known as module memberships. The significance of all module memberships (-$\log_{10}$ of the p-value) for a given gene are plotted along the horizontal axis to highlight the modules to which a gene most strongly associates (red lines denote the significance threshold based on the Bonferroni-corrected p-value for the number of modules (i.e. $\log_{10}(.05/45)$) in both positive and negative directions).

Enrichment analysis of the "Foster: Mitochondrial Proteins" gene set (PMID: 16615899) reveals that most modules in Block 5 are significantly enriched with genes encoding proteins that are enriched in mitochondria with every module eigengene is shown in a similar manner. Significance was assessed using Fisher's exact test.
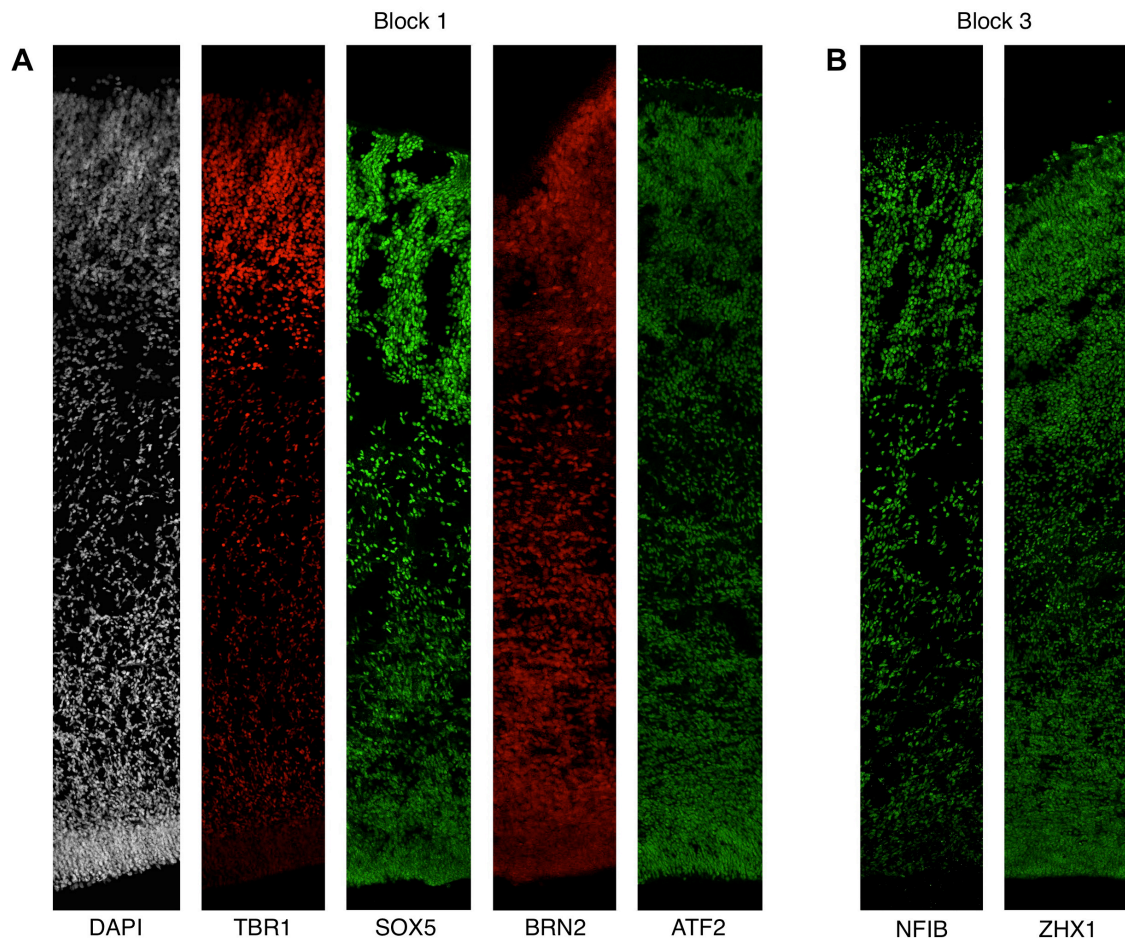
Figure 5. Immunostaining for module members of Blocks 1 and 3 show widespread expression in the neocortical wall.

Nuclear genes with high module memberships for Blocks 1 (A) and 3 (B) were selected for immunostaining in GW14.5 neocortical tissue.
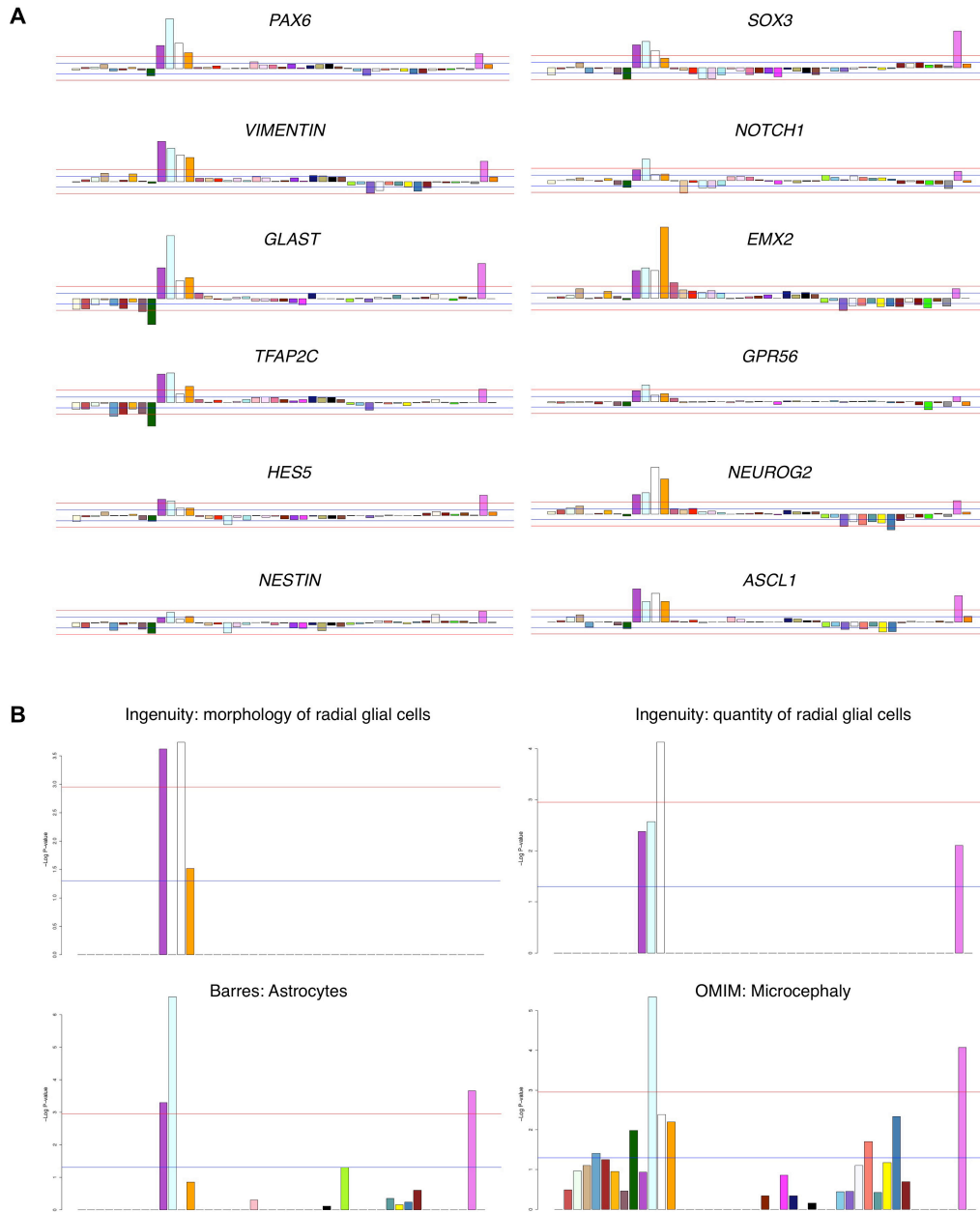
Figure 6. Module membership levels of known radial glia-related genes and gene sets identify five putative radial glia modules.

Module memberships of genes known to be expressed in radial glia are plotted along the horizontal axis (red lines denote the significance threshold based on the Bonferroni-corrected p-value for the number of modules (i.e. $\log_{10}(.05/45)$) in both positive and negative directions). This analysis identifies Blocks 2a and 2b as a group of five putative radial glia modules (A).

An enrichment analysis between gene sets associated with radial glia (Ingenuity® Systems, www.ingenuity.com; Cahoy et al., 2008; Online Mendelian Inheritance in Man ID: 607117) and the 45 modules is shown (B) in support of the classification of radial glia modules. Significance was assessed using Fisher's exact test.
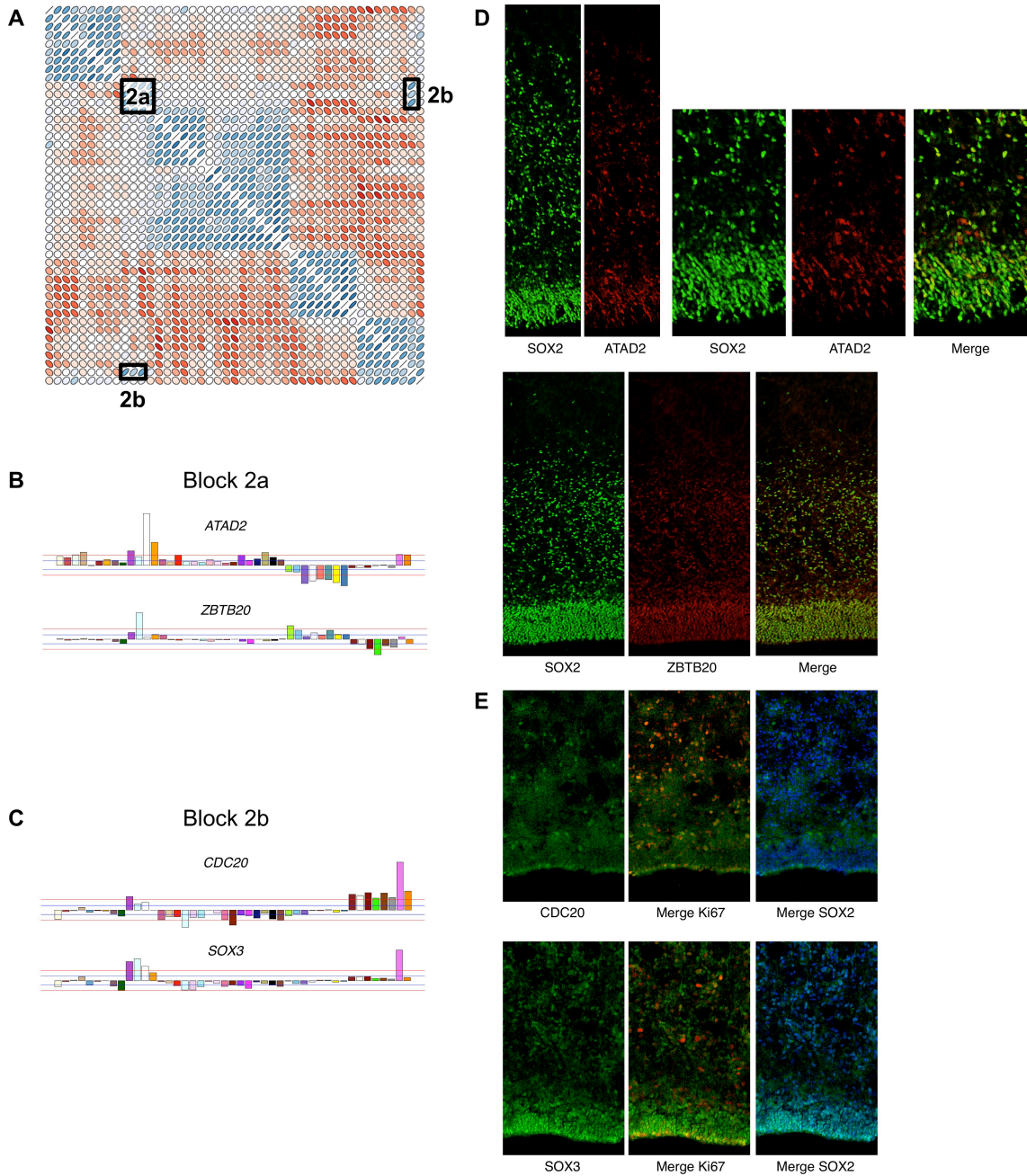
Figure 7. Immunostaining for novel radial glia genes confirms expression in radial glia.

Genes from the putative radial glia modules (A) that are distinguished in their module membership to Block 2a (ATAD2, ZBTB20) vs. Block 2b (CDC20, SOX3) were selected for immunostaining in GW14.5 tissue. Module membership levels for genes that distinguish Block 2a from 2b are shown (B). Module membership levels for genes that distinguish Block 2b from 2a are shown (C).

Immunostaining for ATAD2 and ZBTB20, both of which are novel radial glia genes from Block 2a, shows widespread expression throughout the ventricular and outer subventricular regions (D)

as compared with SOX2, a general marker for primary progenitor cells. These patterns are consistent with, but not limited to, the expression of these genes in radial glia.

Immunostaining for CDC20 and SOX3, both of which are radial glia genes from Block 2b, shows expression throughout the ventricular and outer subventricular regions and do not distinguish between the two (E). Significant co-labeling with Ki67 and SOX2 indicate that these are progenitor cell markers.

STIL

PRC1

DTL

Figure 8. Genes identified to have human-specific evolutionary change in radial glia modules.

Genes that have human-specific amino acid changes predicted to cause functional changes were identified using PolyPhen-2 (Adzhubei et al., 2010). Several genes that have both these features and high module memberships in the 5 radial glia modules are shown.

METHODS

Fetal tissue collection

Fetal cortical tissue was collected from elective pregnancy termination specimens at San Francisco General Hospital, usually within 2 hours of the procedure. Tissues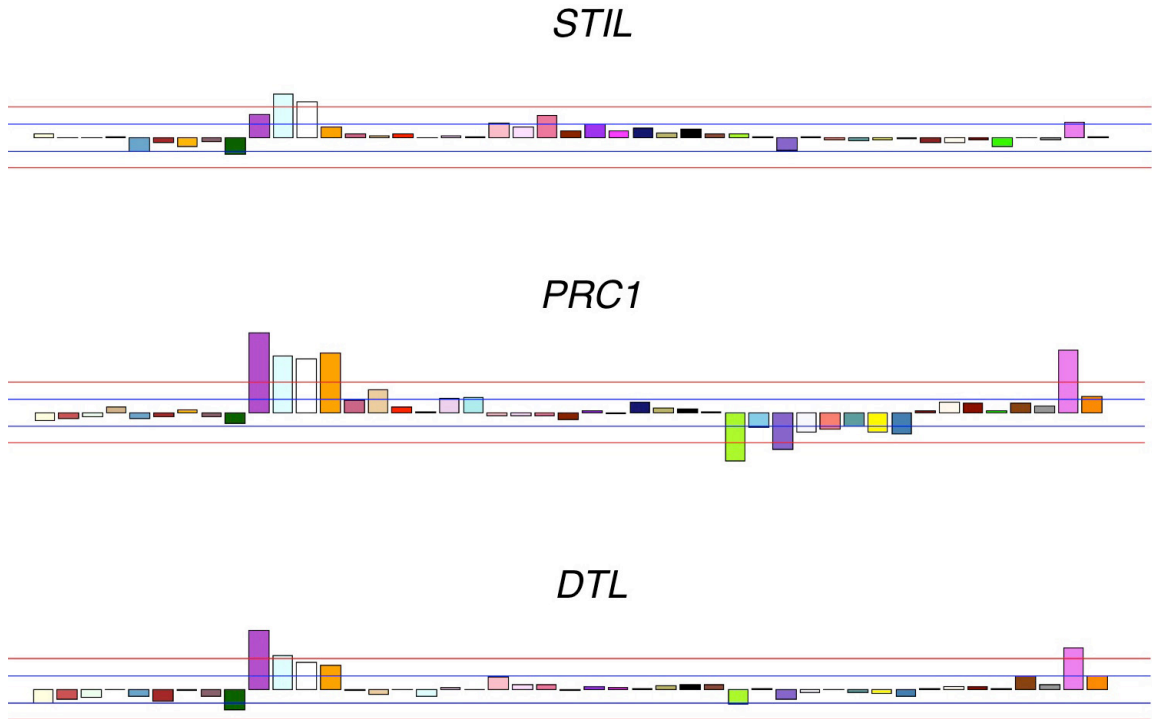 were examined only with previous patient consent and in strict observance of legal and institutional ethical regulations. Research protocols were approved by the Committee on Human Research (institutional review board) at University of California, San Francisco. Gestational age was determined using fetal foot length. Brain tissue was transported in L-15 medium on ice to the laboratory for further processing. The sample used to generate the co-expression network was a mostly intact hemisphere removed from the calvarium of a GW14.5 specimen.

RNA extraction and microarray analysis

The GW14.5 hemisphere was first microdissected to separate the ventral from the dorsal telencephalon. Both fragments were flash-frozen to preserve RNA quality. The dorsal neocortical fragment was cryosectioned along the rostral-caudal axis at 150μm thickness, and the total RNA from each section was extracted using Trizol (Invitrogen). RNA quality was measured using the Agilent Bioanalyzer 2100. 96 samples with RNA Integrity Number > 7 were sent to the Southern California Genotyping Consortium for amplification (Ambion: Illumina TotalPrep RNA Amplification), hybridization, and analysis on Illumina HT12-v4 Expression Beadchips.

Microarray data pre-processing

Following quantile normalization (Bolstad et al., 2003) of the raw microarray data, a significant batch effect associated with the Illumina microarrays was detected (each microarray can hybridize mRNA for up to 12 samples). We used the ComBat algorithm (Johnson et al., 2007) to correct this effect, revealing a much weaker batch effect associated with the RNA extraction date,

which was also corrected via ComBat. Following these steps, the resulting dataset consisted of ~47,000 gene expression measurements for 89 observations along the rostral-caudal axis of GW14.5 developing human neocortex.

Definition of modules

Gene co-expression modules were identified using custom R software as follows. First, a Pearson correlation matrix (PCM) was constructed using only those probes that have been independently validated as being of "perfect" or "good" quality (n = 30,425 probes; Barbosa-Morais et al., 2010). Second, all groups of at least 10 probes that were inter-correlated with one another above a threshold (corresponding to the top 2% of correlations in the PCM) were identified. Each of these initial groups was summarized by the first principal component (obtained via singular value decomposition), which we refer to as the module eigengene, or ME (Horvath and Dong, 2008). MEs were then correlated with one another and highly similar modules (Pearson correlation > 0.85) were merged until no pairs of modules met this merging criterion. MEs were then recalculated for the merged modules as described above.

Subtraction of gradients

To subtract the pronounced gene expression gradients from the microarray data (i.e. the gene expression patterns represented by the turquoise and blue modules from the initial network construction), expression values for all probes were redefined using a linear regression model. Specifically, the expression values for each probe were modeled as the residuals resulting from linear regression of the probe's original expression values on the turquoise ME from the initial network construction (i.e. the caudal-rostral expression gradient). Because the caudal-rostral (turquoise) and rostro-caudal (blue) expression patterns were nearly perfectly anti-correlated (r ~= –0.97), the residuals obtained with this approach effectively eliminate gradients in both

directions. After eliminating the gradients, modules of co-expressed genes were again identified, using the same algorithm and parameters described above.

Module annotation and enrichment analysis

For analysis at the level of single genes (known radial glial genes, genes identified using PolyPhen-2, Adzhubei et al., 2010), the kME p-value of a gene/module eigengene pair (based on the co-expression network) was used to quantify module membership. To determine whether modules of co-expressed genes were significantly enriched with informative gene sets, modules were redefined using the kME table and a significance threshold, as described in Oldham et al., 2008. Here, we identified all probes that were positively correlated with each ME above a significance threshold corresponding to a Bonferroni-corrected p-value (i.e. .05 / (# modules * # probes)). Manually curated gene sets or gene sets from the Molecular Signatures Database (http://www.broadinstitute.org/gsea/msigdb/index.jsp) were cross-referenced with all module definitions using unique gene symbols. The statistical significance of gene set enrichment was calculated using Fisher's exact test. A gene set was deemed nominally significant if the resulting p-values were < .05 for any module after applying a Bonferroni correction for the number of modules.

Immunostaining

GW14.5 neocortical tissue was fixed in 4% PFA in PBS at 4 °C for 3 days, dehydrated in 30% sucrose in PBS, embedded and frozen at -80 °C in O.C.T. compound (Tissue-Tek), sectioned on a Leica CM3050S (50 or 20 μm) and stored at -80 °C. Cryosections were subjected to heat/citrate-based antigen retrieval for 5 min and permeablized and blocked overnight in PBS plus 0.1% Triton X-100, 10% serum, 0.2% gelatin. Primary incubations were 3 hours at room temperature or 4 °C overnight. Washes and secondary incubations were standard procedures. Images were

acquired on a Leica TCS SP5 broadband laser confocal microscope with detection settings normalized to a secondary only control.

Primary antibodies were: goat anti-SOX2 (Santa Cruz sc-17320, 1:250), mouse anti-Ki67 (Dako F7268, 1:150), rabbit anti-TOX (Sigma HPA018322, 1:250), rabbit anti-TBR1 (Abcam ab31940, 1:500), rabbit anti-SOX5 (Abcam ab26041, 1:500), goat anti-BRN2 (Santa Cruz sc-31983, 1:100), rabbit anti-ATF2 (Abcam ab32160, 1:250), rabbit anti-NFIB (Abcam ab11989, 1:500), rabbit anti-ZHX1 (Abcam ab84506, 1:200), rabbit anti-ATAD2 (Sigma HPA029424, 1:150), rabbit anti-ZBTB20 (Sigma HPA016815, 1:50), rabbit anti-CDC20 (Abcam ab26483, 1:500), rabbit anti-SOX3 (Abcam ab42471, 1:200). Secondary antibodies were: AlexaFluor 488 (1:1,000), 546 (1:500), or 647 (1:500)-conjugated donkey anti-goat, -rabbit or -mouse IgG (Invitrogen).

In situ hybridization

Antisense and sense RNA probes were generated for human *CPNE4* (bp: 1623-2113) from a cDNA clone (Open Biosystems Clone 3162881). The 490bp PCR product was cloned into the TOPO-TA vector (Invitrogen) and linearized. T7 RNA polymerase was used to transcribe the probes incorporating DIG (digoxygenin)-conjugated UTP (Roche). Standard protocols were used for the preparation of paraformaldehyde fixed cryosections from GW14.5 human neocortex and the probe was hybridized overnight at 65°C followed by stringency washes at the same temperature. Tissues were incubated for 1 hour at room temperature with anti-DIG FITC antibody (Roche) for fluorescent visualization. Fluorescent images were collected on a Leica TCS SP5 broadband confocal microscope.

CONCLUDING REMARKS

In this dissertation, we present experimental evidence that subventricular neurogenic divisions underlie the increase in neuron number in the evolutionary path to the human cerebral neocortex. We define oRG cells as the self-renewing building blocks of human OSVZ proliferation and show that they function to enhance both traditional roles of RG cells. They generate daughter transit-amplifying IP cells that expand neuron number, and they provide additional radial fiber guides for neuronal migration. We further examine the generality of these features throughout different species in evolution. From this, we find that the mechanisms of OSVZ proliferation are likely evolutionarily conserved amongst placental mammals, but function to variable extent in different species to control neocortical size and folding.

Because evolutionary differences between genomes are ultimately what underlie the observed diversity in neocortical size and shape, we end with a characterization of the gene expression signatures in the developing human brain, particularly of radial glial cells. We identify genes expressed in human radial glia that are likely to have undergone human-specific evolutionary changes, and plan to use these genes to interrogate the mechanisms of OSVZ proliferation. We anticipate that these new perspectives on human neocortical development will shed further light on brain evolution and provide a substrate for understanding the mechanisms of neurodevelopmental diseases.

REFERENCES

Abdel-Mannan, O., Cheung, A.F., and Molnar, Z. (2008). Evolution of cortical neurogenesis. Brain Res Bull *75*, 398-404.

Adzhubei, I.A., Schmidt, S., Peshkin, L., Ramensky, V.E., Gerasimova, A., Bork, P., Kondrashov, A.S., and Sunyaev, S.R. (2010). A method and server for predicting damaging missense mutations. Nat Methods *7*, 248-249.

Alvarez-Buylla, A., Theelen, M., and Nottebohm, F. (1988). Mapping of radial glia and of a new cell type in adult canary brain. J Neurosci *8*, 2707-2712.

Alvarez-Buylla, A., Theelen, M., and Nottebohm, F. (1990). Proliferation "hot spots" in adult avian ventricular zone reveal radial cell division. Neuron *5*, 101-109.

Anderson, S.A., Eisenstat, D.D., Shi, L., and Rubenstein, J.L. (1997). Interneuron migration from basal forebrain to neocortex: dependence on Dlx genes. Science *278*, 474-476.

Arnold, S.J., Huang, G.J., Cheung, A.F., Era, T., Nishikawa, S., Bikoff, E.K., Molnar, Z., Robertson, E.J., and Groszer, M. (2008). The T-box transcription factor Eomes/Tbr2 regulates neurogenesis in the cortical subventricular zone. Genes Dev *22*, 2479-2484.

Ashburner, M., Ball, C.A., Blake, J.A., Botstein, D., Butler, H., Cherry, J.M., Davis, A.P., Dolinski, K., Dwight, S.S., Eppig, J.T.*, et al.* (2000). Gene ontology: tool for the unification of biology. The Gene Ontology Consortium. Nat Genet *25*, 25-29.

Austin, C.P., and Cepko, C.L. (1990). Cellular migration patterns in the developing mouse cerebral cortex. Development *110*, 713-732.

Azevedo, F.A., Carvalho, L.R., Grinberg, L.T., Farfel, J.M., Ferretti, R.E., Leite, R.E., Jacob Filho, W., Lent, R., and Herculano-Houzel, S. (2009). Equal numbers of neuronal and nonneuronal cells make the human brain an isometrically scaled-up primate brain. J Comp Neurol *513*, 532-541.

Baala, L., Briault, S., Etchevers, H.C., Laumonnier, F., Natiq, A., Amiel, J., Boddaert, N., Picard, C., Sbiti, A., Asermouh, A.*, et al.* (2007). Homozygous silencing of T-box transcription factor EOMES leads to microcephaly with polymicrogyria and corpus callosum agenesis. Nat Genet *39*, 454-456.

Backman, M., Machon, O., Mygland, L., van den Bout, C.J., Zhong, W., Taketo, M.M., and Krauss, S. (2005). Effects of canonical Wnt signaling on dorso-ventral specification of the mouse telencephalon. Dev Biol *279*, 155-168.

Baek, J.H., Hatakeyama, J., Sakamoto, S., Ohtsuka, T., and Kageyama, R. (2006). Persistent and high levels of Hes1 expression regulate boundary formation in the developing central nervous system. Development *133*, 2467-2476.

Barbosa-Morais, N.L., Dunning, M.J., Samarajiwa, S.A., Darot, J.F., Ritchie, M.E., Lynch, A.G., and Tavare, S. (2010). A re-annotation pipeline for Illumina BeadArrays: improving the interpretation of gene expression data. Nucleic Acids Res *38*, e17.

Bayatti, N., Moss, J.A., Sun, L., Ambrose, P., Ward, J.F., Lindsay, S., and Clowry, G.J. (2008). A molecular neuroanatomical study of the developing human neocortex from 8 to 17 postconceptional weeks revealing the early differentiation of the subplate and subventricular zone. Cereb Cortex *18*, 1536-1548.

Bayer, S.A., and Altman, J. (1991). Neocortical Development (New York: Raven Press).

Bentivoglio, M., and Mazzarello, P. (1999). The history of radial glia. Brain Res Bull *49*, 305-315.

Bolstad, B.M., Irizarry, R.A., Astrand, M., and Speed, T.P. (2003). A comparison of normalization methods for high density oligonucleotide array data based on variance and bias. Bioinformatics *19*, 185-193.

Bond, J., Roberts, E., Mochida, G.H., Hampshire, D.J., Scott, S., Askham, J.M., Springell, K., Mahadevan, M., Crow, Y.J., Markham, A.F.*, et al.* (2002). ASPM is a major determinant of cerebral cortical size. Nat Genet *32*, 316-320.

Bond, J., Roberts, E., Springell, K., Lizarraga, S.B., Scott, S., Higgins, J., Hampshire, D.J., Morrison, E.E., Leal, G.F., Silva, E.O.*, et al.* (2005). A centrosomal mechanism involving CDK5RAP2 and CENPJ controls brain size. Nat Genet *37*, 353-355.

Borrell, V., Kaspar, B.K., Gage, F.H., and Callaway, E.M. (2006). In vivo evidence for radial migration of neurons by long-distance somal translocation in the developing ferret visual cortex. Cereb Cortex *16*, 1571-1583.

Buchman, J.J., Tseng, H.C., Zhou, Y., Frank, C.L., Xie, Z., and Tsai, L.H. (2010). Cdk5rap2 interacts with pericentrin to maintain the neural progenitor pool in the developing neocortex. Neuron *66*, 386-402.

Bultje, R.S., Castaneda-Castellanos, D.R., Jan, L.Y., Jan, Y.N., Kriegstein, A.R., and Shi, S.H. (2009). Mammalian Par3 regulates progenitor cell asymmetric division via notch signaling in the developing neocortex. Neuron *63*, 189-202.

Cahoy, J.D., Emery, B., Kaushal, A., Foo, L.C., Zamanian, J.L., Christopherson, K.S., Xing, Y., Lubischer, J.L., Krieg, P.A., Krupenko, S.A.*, et al.* (2008). A transcriptome database for astrocytes, neurons, and oligodendrocytes: a new resource for understanding brain development and function. J Neurosci *28*, 264-278.

Cajal, S.R. (1911). Histologie du système nerveux de l'homme et des vertébrés (Paris: Maloine).

Campos, L.S., Duarte, A.J., Branco, T., and Henrique, D. (2001). mDll1 and mDll3 expression in the developing mouse brain: role in the establishment of the early cortex. J Neurosci Res *64*, 590-598.

Chatzi, C., Brade, T., and Duester, G. (2011). Retinoic acid functions as a key GABAergic differentiation signal in the basal ganglia. PLoS Biol *9*, e1000609.

Chenn, A., and Walsh, C.A. (2002). Regulation of cerebral cortical size by control of cell cycle exit in neural precursors. Science *297*, 365-369.

Chenn, A., and Walsh, C.A. (2003). Increased neuronal production, enlarged forebrains and cytoarchitectural distortions in beta-catenin overexpressing transgenic mice. Cereb Cortex *13*, 599-606.

Chenn, A., Zhang, Y.A., Chang, B.T., and McConnell, S.K. (1998). Intrinsic polarity of mammalian neuroepithelial cells. Mol Cell Neurosci *11*, 183-193.

Cheung, A.F., Kondo, S., Abdel-Mannan, O., Chodroff, R.A., Sirey, T.M., Bluy, L.E., Webber, N., DeProto, J., Karlen, S.J., Krubitzer, L.*, et al.* (2010). The subventricular zone is the developmental milestone of a 6-layered neocortex: comparisons in metatherian and eutherian mammals. Cereb Cortex *20*, 1071-1081.

Cheung, A.F., Pollen, A.A., Tavare, A., DeProto, J., and Molnar, Z. (2007). Comparative aspects of cortical neurogenesis in vertebrates. J Anat *211*, 164-176.

Choi, B.H. (1986). Glial fibrillary acidic protein in radial glia of early human fetal cerebrum: a light and electron microscopic immunoperoxidase study. J Neuropathol Exp Neurol *45*, 408-418.

Ciro, M., Prosperini, E., Quarto, M., Grazini, U., Walfridsson, J., McBlane, F., Nucifero, P., Pacchiana, G., Capra, M., Christensen, J.*, et al.* (2009). ATAD2 is a novel cofactor for MYC, overexpressed and amplified in aggressive tumors. Cancer Res *69*, 8491-8498.

Costa, M.R., Wen, G., Lepier, A., Schroeder, T., and Gotz, M. (2008). Par-complex proteins promote proliferative progenitor divisions in the developing mouse cerebral cortex. Development *135*, 11-22.

Eiraku, M., Watanabe, K., Matsuo-Takasaki, M., Kawada, M., Yonemura, S., Matsumura, M., Wataya, T., Nishiyama, A., Muguruma, K., and Sasai, Y. (2008). Self-organized formation of polarized cortical tissues from ESCs and its active manipulation by extrinsic signals. Cell Stem Cell *3*, 519-532.

Englund, C., Fink, A., Lau, C., Pham, D., Daza, R.A., Bulfone, A., Kowalczyk, T., and Hevner, R.F. (2005). Pax6, Tbr2, and Tbr1 are expressed sequentially by radial glia, intermediate progenitor cells, and postmitotic neurons in developing neocortex. J Neurosci *25*, 247-251.

Fawcett, D.W., and Jensh, R.P. (2002). Bloom & Fawcett: Concise Histology, Second Edition (London: Hodder Arnold).

Fertuzinhos, S., Krsnik, Z., Kawasawa, Y.I., Rasin, M.R., Kwan, K.Y., Chen, J.G., Judas, M., Hayashi, M., and Sestan, N. (2009). Selective depletion of molecularly defined cortical interneurons in human holoprosencephaly with severe striatal hypoplasia. Cereb Cortex *19*, 2196-2207.

Fietz, S.A., and Huttner, W.B. (2011). Cortical progenitor expansion, self-renewal and neurogenesis-a polarized perspective. Curr Opin Neurobiol *21*, 23-35.

Fietz, S.A., Kelava, I., Vogt, J., Wilsch-Brauninger, M., Stenzel, D., Fish, J.L., Corbeil, D., Riehn, A., Distler, W., Nitsch, R., *et al.* (2010). OSVZ progenitors of human and ferret neocortex are epithelial-like and expand by integrin signaling. Nat Neurosci *13*, 690-699.

Fish, J.L., Dehay, C., Kennedy, H., and Huttner, W.B. (2008). Making bigger brains-the evolution of neural-progenitor-cell division. J Cell Sci *121*, 2783-2793.

Gaiano, N., Nye, J.S., and Fishell, G. (2000). Radial glial identity is promoted by Notch1 signaling in the murine forebrain. Neuron *26*, 395-404.

Gal, J.S., Morozov, Y.M., Ayoub, A.E., Chatterjee, M., Rakic, P., and Haydar, T.F. (2006). Molecular and morphological heterogeneity of neural precursors in the mouse neocortical proliferative zones. J Neurosci *26*, 1045-1056.

Gan, W.B., Grutzendler, J., Wong, W.T., Wong, R.O., and Lichtman, J.W. (2000). Multicolor "DiOlistic" labeling of the nervous system using lipophilic dye combinations. Neuron *27*, 219-225.

Goffinet, A.M. (1983). The embryonic development of the cortical plate in reptiles: a comparative study in Emys orbicularis and Lacerta agilis. J Comp Neurol *215*, 437-452.

Gohlke, J.M., Griffith, W.C., and Faustman, E.M. (2007). Computational models of neocortical neuronogenesis and programmed cell death in the developing mouse, monkey, and human. Cereb Cortex *17*, 2433-2442.

Gotz, M., and Huttner, W.B. (2005). The cell biology of neurogenesis. Nat Rev Mol Cell Biol *6*, 777-788.

Gotz, M., Stoykova, A., and Gruss, P. (1998). Pax6 controls radial glia differentiation in the cerebral cortex. Neuron *21*, 1031-1044.

Gould, S.J. (1977). Ontogeny and Phylogeny (Cambridge: Harvard University Press).

Gunhaga, L., Marklund, M., Sjodal, M., Hsieh, J.C., Jessell, T.M., and Edlund, T. (2003). Specification of dorsal telencephalic character by sequential Wnt and FGF signaling. Nat Neurosci *6*, 701-707.

Haas, K., Sin, W.C., Javaherian, A., Li, Z., and Cline, H.T. (2001). Single-cell electroporation for gene transfer in vivo. Neuron *29*, 583-591.

Hansen, D.V., Lui, J.H., Parker, P.R., and Kriegstein, A.R. (2010). Neurogenic radial glia in the outer subventricular zone of human neocortex. Nature *464*, 554-561.

Hansen, D.V., Rubenstein, J.L., and Kriegstein, A.R. (2011). Deriving excitatory neurons of the neocortex from pluripotent stem cells. Neuron *70*, 645-660.

Hartfuss, E., Galli, R., Heins, N., and Gotz, M. (2001). Characterization of CNS precursor subtypes and radial glia. Dev Biol *229*, 15-30.

Hatakeyama, J., Bessho, Y., Katoh, K., Ookawara, S., Fujioka, M., Guillemot, F., and Kageyama, R. (2004). Hes genes regulate size, shape and histogenesis of the nervous system by control of the timing of neural stem cell differentiation. Development *131*, 5539-5550.

Haubensak, W., Attardo, A., Denk, W., and Huttner, W.B. (2004). Neurons arise in the basal neuroepithelium of the early mammalian telencephalon: a major site of neurogenesis. Proc Natl Acad Sci U S A *101*, 3196-3201.

Haubst, N., Georges-Labouesse, E., De Arcangelis, A., Mayer, U., and Gotz, M. (2006). Basement membrane attachment is dispensable for radial glial cell fate and for proliferation, but affects positioning of neuronal subtypes. Development *133*, 3245-3254.

Heitzler, P., and Simpson, P. (1991). The choice of cell fate in the epidermis of Drosophila. Cell *64*, 1083-1092.

Herculano-Houzel, S. (2009). The human brain in numbers: a linearly scaled-up primate brain. Front Hum Neurosci *3*, 31.

Hirata, H., Yoshiura, S., Ohtsuka, T., Bessho, Y., Harada, T., Yoshikawa, K., and Kageyama, R. (2002). Oscillatory expression of the bHLH factor Hes1 regulated by a negative feedback loop. Science *298*, 840-843.

Horvath, S., and Dong, J. (2008). Geometric interpretation of gene coexpression network analysis. PLoS Comput Biol *4*, e1000117.

Imai, F., Hirai, S., Akimoto, K., Koyama, H., Miyata, T., Ogawa, M., Noguchi, S., Sasaoka, T., Noda, T., and Ohno, S. (2006). Inactivation of aPKClambda results in the loss of adherens junctions in neuroepithelial cells without affecting neurogenesis in mouse neocortex.

Development *133*, 1735-1744.

Imayoshi, I., Sakamoto, M., Yamaguchi, M., Mori, K., and Kageyama, R. (2010). Essential roles of Notch signaling in maintenance of neural stem cells in developing and adult brains. J Neurosci *30*, 3489-3498.

Ishibashi, M., Ang, S.L., Shiota, K., Nakanishi, S., Kageyama, R., and Guillemot, F. (1995). Targeted disruption of mammalian hairy and Enhancer of split homolog-1 (HES-1) leads to up-regulation of neural helix-loop-helix factors, premature neurogenesis, and severe neural tube defects. Genes Dev *9*, 3136-3148.

Itoh, M., Kim, C.H., Palardy, G., Oda, T., Jiang, Y.J., Maust, D., Yeo, S.Y., Lorick, K., Wright, G.J., Ariza-McNaughton, L.*, et al.* (2003). Mind bomb is a ubiquitin ligase that is essential for efficient activation of Notch signaling by Delta. Dev Cell *4*, 67-82.

Jakovcevski, I., Mayer, N., and Zecevic, N. (2010). Multiple Origins of Human Neocortical Interneurons Are Supported by Distinct Expression of Transcription Factors. Cereb Cortex *21*, 1771-1782.

Jakovcevski, I., and Zecevic, N. (2005). Olig transcription factors are expressed in oligodendrocyte and neuronal cells in human fetal CNS. J Neurosci *25*, 10064-10073.

Johnson, M.B., Kawasawa, Y.I., Mason, C.E., Krsnik, Z., Coppola, G., Bogdanovic, D., Geschwind, D.H., Mane, S.M., State, M.W., and Sestan, N. (2009). Functional and evolutionary insights into human brain development through global transcriptome analysis. Neuron *62*, 494-509.

Johnson, W.E., Li, C., and Rabinovic, A. (2007). Adjusting batch effects in microarray expression data using empirical Bayes methods. Biostatistics *8*, 118-127.

Junghans, D., Hack, I., Frotscher, M., Taylor, V., and Kemler, R. (2005). Beta-catenin-mediated cell-adhesion is vital for embryonic forebrain development. Dev Dyn *233*, 528-539.

Kageyama, R., Ohtsuka, T., Shimojo, H., and Imayoshi, I. (2008). Dynamic Notch signaling in neural progenitor cells and a revised view of lateral inhibition. Nat Neurosci *11*, 1247-1251.

Kim, W.Y., Wang, X., Wu, Y., Doble, B.W., Patel, S., Woodgett, J.R., and Snider, W.D. (2009). GSK-3 is a master regulator of neural progenitor homeostasis. Nat Neurosci *12*, 1390-1397.

Konno, D., Shioi, G., Shitamukai, A., Mori, A., Kiyonari, H., Miyata, T., and Matsuzaki, F. (2008). Neuroepithelial progenitors undergo LGN-dependent planar divisions to maintain self-renewability during mammalian neurogenesis. Nat Cell Biol *10*, 93-101.

Koo, B.K., Lim, H.S., Song, R., Yoon, M.J., Yoon, K.J., Moon, J.S., Kim, Y.W., Kwon, M.C.,

Yoo, K.W., Kong, M.P., *et al.* (2005). Mind bomb 1 is essential for generating functional Notch ligands to activate Notch. Development *132*, 3459-3470.

Kornack, D.R., and Rakic, P. (1995). Radial and horizontal deployment of clonally related cells in the primate neocortex: relationship to distinct mitotic lineages. Neuron *15*, 311-321.

Kowalczyk, T., Pontious, A., Englund, C., Daza, R.A., Bedogni, F., Hodge, R., Attardo, A., Bell, C., Huttner, W.B., and Hevner, R.F. (2009). Intermediate neuronal progenitors (basal progenitors) produce pyramidal-projection neurons for all layers of cerebral cortex. Cereb Cortex *19*, 2439-2450.

Kriegstein, A., Noctor, S., and Martinez-Cerdeno, V. (2006). Patterns of neural stem and progenitor cell division may underlie evolutionary cortical expansion. Nat Rev Neurosci *7*, 883-890.

Kuan, C.Y., Roth, K.A., Flavell, R.A., and Rakic, P. (2000). Mechanisms of programmed cell death in the developing brain. Trends Neurosci *23*, 291-297.

Letinic, K., Zoncu, R., and Rakic, P. (2002). Origin of GABAergic neurons in the human neocortex. Nature *417*, 645-649.

Levitt, P., Cooper, M.L., and Rakic, P. (1981). Coexistence of neuronal and glial precursor cells in the cerebral ventricular zone of the fetal monkey: an ultrastructural immunoperoxidase analysis. J Neurosci *1*, 27-39.

Lien, W.H., Klezovitch, O., Fernandez, T.E., Delrow, J., and Vasioukhin, V. (2006). alphaE-catenin controls cerebral cortical size by regulating the hedgehog signaling pathway. Science *311*, 1609-1612.

Lien, W.H., Klezovitch, O., Null, M., and Vasioukhin, V. (2008). alphaE-catenin is not a significant regulator of beta-catenin signaling in the developing mammalian brain. J Cell Sci *121*, 1357-1362.

Lizarraga, S.B., Margossian, S.P., Harris, M.H., Campagna, D.R., Han, A.P., Blevins, S., Mudbhary, R., Barker, J.E., Walsh, C.A., and Fleming, M.D. (2010). Cdk5rap2 regulates centrosome function and chromosome segregation in neuronal progenitors. Development *137*, 1907-1917.

Lui, J.H., Hansen, D.V., and Kriegstein, A.R. (2011). Development and evolution of the human neocortex. Cell *146*, 18-36.

Lukaszewicz, A., Savatier, P., Cortay, V., Giroud, P., Huissoud, C., Berland, M., Kennedy, H., and Dehay, C. (2005). G1 phase regulation, area-specific cell cycle control, and cytoarchitectonics in the primate cortex. Neuron *47*, 353-364.

Machon, O., van den Bout, C.J., Backman, M., Kemler, R., and Krauss, S. (2003). Role of beta-catenin in the developing cortical and hippocampal neuroepithelium. Neuroscience *122*, 129-143.

Malatesta, P., Hartfuss, E., and Gotz, M. (2000). Isolation of radial glial cells by fluorescent-activated cell sorting reveals a neuronal lineage. Development *127*, 5253-5263.

Marin-Padilla, M. (1992). Ontogenesis of the pyramidal cell of the mammalian neocortex and developmental cytoarchitectonics: a unifying theory. J Comp Neurol *321*, 223-240.

McLean, C.Y., Reno, P.L., Pollen, A.A., Bassan, A.I., Capellini, T.D., Guenther, C., Indjeian, V.B., Lim, X., Menke, D.B., Schaar, B.T.*, et al.* (2011). Human-specific loss of regulatory DNA and the evolution of human-specific traits. Nature *471*, 216-219.

Miyata, T., Kawaguchi, A., Okano, H., and Ogawa, M. (2001). Asymmetric inheritance of radial glial fibers by cortical neurons. Neuron *31*, 727-741.

Miyata, T., Kawaguchi, A., Saito, K., Kawano, M., Muto, T., and Ogawa, M. (2004). Asymmetric production of surface-dividing and non-surface-dividing cortical progenitor cells. Development *131*, 3133-3145.

Mizutani, K., Yoon, K., Dang, L., Tokunaga, A., and Gaiano, N. (2007). Differential Notch signalling distinguishes neural stem cells from intermediate progenitors. Nature *449*, 351-355.

Mo, Z., and Zecevic, N. (2008). Is Pax6 critical for neurogenesis in the human fetal brain? Cereb Cortex *18*, 1455-1465.

Molyneaux, B.J., Arlotta, P., Menezes, J.R., and Macklis, J.D. (2007). Neuronal subtype specification in the cerebral cortex. Nat Rev Neurosci *8*, 427-437.

Mutch, C.A., Schulte, J.D., Olson, E., and Chenn, A. (2010). Beta-catenin signaling negatively regulates intermediate progenitor population numbers in the developing cortex. PLoS One *5* e12376.

Nelson, S.B., Hempel, C., and Sugino, K. (2006). Probing the transcriptome of neuronal cell types. Curr Opin Neurobiol *16*, 571-576.

Noctor, S.C., Flint, A.C., Weissman, T.A., Dammerman, R.S., and Kriegstein, A.R. (2001). Neurons derived from radial glial cells establish radial units in neocortex. Nature *409*, 714-720.

Noctor, S.C., Flint, A.C., Weissman, T.A., Wong, W.S., Clinton, B.K., and Kriegstein, A.R. (2002). Dividing precursor cells of the embryonic cortical ventricular zone have morphological and molecular characteristics of radial glia. J Neurosci *22*, 3161-3173.

Noctor, S.C., Martinez-Cerdeno, V., Ivic, L., and Kriegstein, A.R. (2004). Cortical neurons arise in symmetric and asymmetric division zones and migrate through specific phases. Nat Neurosci *7*, 136-144.

Noctor, S.C., Martinez-Cerdeno, V., and Kriegstein, A.R. (2008). Distinct behaviors of neural stem and progenitor cells underlie cortical neurogenesis. J Comp Neurol *508*, 28-44.

Ochiai, W., Nakatani, S., Takahara, T., Kainuma, M., Masaoka, M., Minobe, S., Namihira, M., Nakashima, K., Sakakibara, A., Ogawa, M.*, et al.* (2009). Periventricular notch activation and asymmetric Ngn2 and Tbr2 expression in pair-generated neocortical daughter cells. Mol Cell Neurosci *40*, 225-233.

Ohtsuka, T., Imayoshi, I., Shimojo, H., Nishi, E., Kageyama, R., and McConnell, S.K. (2006). Visualization of embryonic neural stem cells using Hes promoters in transgenic mice. Mol Cell Neurosci *31*, 109-122.

Okaty, B.W., Sugino, K., and Nelson, S.B. (2011). Cell type-specific transcriptomics in the brain. J Neurosci *31*, 6939-6943.

Oldham, M.C., Horvath, S., and Geschwind, D.H. (2006). Conservation and evolution of gene coexpression networks in human and chimpanzee brains. Proc Natl Acad Sci U S A *103*, 17973-17978.

Oldham, M.C., Konopka, G., Iwamoto, K., Langfelder, P., Kato, T., Horvath, S., and Geschwind, D.H. (2008). Functional organization of the transcriptome in human brain. Nat Neurosci *11*, 1271-1282.

Petanjek, Z., Berger, B., and Esclapez, M. (2009). Origins of cortical GABAergic neurons in the cynomolgus monkey. Cereb Cortex *19*, 249-262.

Pollard, K.S., Salama, S.R., Lambert, N., Lambot, M.A., Coppens, S., Pedersen, J.S., Katzman, S., King, B., Onodera, C., Siepel, A.*, et al.* (2006). An RNA gene expressed during cortical development evolved rapidly in humans. Nature *443*, 167-172.

Puzzolo, E., and Mallamaci, A. (2010). Cortico-cerebral histogenesis in the opossum Monodelphis domestica: generation of a hexalaminar neocortex in the absence of a basal proliferative compartment. Neural Dev *5*, 8.

Rakic, P. (1971). Guidance of neurons migrating to the fetal monkey neocortex. Brain Res *33*, 471-476.

Rakic, P. (1972). Mode of cell migration to the superficial layers of fetal monkey neocortex. J Comp Neurol *145*, 61-83.

Rakic, P. (1974). Neurons in rhesus monkey visual cortex: systematic relation between time of origin and eventual disposition. Science *183*, 425-427.

Rakic, P. (1988). Specification of cerebral cortical areas. Science *241*, 170-176.

Rakic, P. (1995). A small step for the cell, a giant leap for mankind: a hypothesis of neocortical expansion during evolution. Trends Neurosci *18*, 383-388.

Rakic, P. (2003). Developmental and evolutionary adaptations of cortical radial glia. Cereb Cortex *13*, 541-549.

Rakic, P. (2009). Evolution of the neocortex: a perspective from developmental biology. Nat Rev Neurosci *10*, 724-735.

Rakic, P., and Sidman, R.L. (1968). Supravital DNA synthesis in the developing human and mouse brain. J Neuropathol Exp Neurol *27*, 246-276.

Rasin, M.R., Gazula, V.R., Breunig, J.J., Kwan, K.Y., Johnson, M.B., Liu-Chen, S., Li, H.S., Jan, L.Y., Jan, Y.N., Rakic, P.*, et al.* (2007). Numb and Numbl are required for maintenance of cadherin-based adhesion and polarity of neural progenitors. Nat Neurosci *10*, 819-827.

Reid, C.B., Tavazoie, S.F., and Walsh, C.A. (1997). Clonal dispersion and evidence for asymmetric cell division in ferret cortex. Development *124*, 2441-2450.

Reillo, I., de Juan Romero, C., Garcia-Cabezas, M.A., and Borrell, V. (2010). A Role for Intermediate Radial Glia in the Tangential Expansion of the Mammalian Cerebral Cortex. Cereb Cortex *21*, 1674-1694.

Rhyu, M.S., Jan, L.Y., and Jan, Y.N. (1994). Asymmetric distribution of numb protein during division of the sensory organ precursor cell confers distinct fates to daughter cells. Cell *76*, 477-491.

Sahara, S., and O'Leary, D.D. (2009). Fgf10 regulates transition period of cortical stem cell differentiation to radial glia controlling generation of neurons and basal progenitors. Neuron *63*, 48-62.

Sauer, F.C. (1935). Mitosis in the neural tube. J Comp Neurol *62*, 377-405.

Schmechel, D.E., and Rakic, P. (1979a). A Golgi study of radial glial cells in developing monkey telencephalon: morphogenesis and transformation into astrocytes. Anat Embryol (Berl) *156*, 115-152.

Schmechel, D.E., and Rakic, P. (1979b). Arrested proliferation of radial glial cells during

midgestation in rhesus monkey. Nature *277*, 303-305.

Sessa, A., Mao, C.A., Hadjantonakis, A.K., Klein, W.H., and Broccoli, V. (2008). Tbr2 directs conversion of radial glia into basal precursors and guides neuronal amplification by indirect neurogenesis in the developing neocortex. Neuron *60*, 56-69.

Shen, Q., Wang, Y., Dimos, J.T., Fasano, C.A., Phoenix, T.N., Lemischka, I.R., Ivanova, N.B., Stifani, S., Morrisey, E.E., and Temple, S. (2006). The timing of cortical neurogenesis is encoded within lineages of individual progenitor cells. Nat Neurosci *9*, 743-751.

Shen, Q., Zhong, W., Jan, Y.N., and Temple, S. (2002). Asymmetric Numb distribution is critical for asymmetric cell division of mouse cerebral cortical stem cells and neuroblasts. Development *129*, 4843-4853.

Shimojo, H., Ohtsuka, T., and Kageyama, R. (2008). Oscillations in notch signaling regulate maintenance of neural progenitors. Neuron *58*, 52-64.

Shitamukai, A., Konno, D., and Matsuzaki, F. (2011). Oblique Radial Glial Divisions in the Developing Mouse Neocortex Induce Self-Renewing Progenitors outside the Germinal Zone That Resemble Primate Outer Subventricular Zone Progenitors. J Neurosci *31*, 3683-3695.

Siegenthaler, J.A., Ashique, A.M., Zarbalis, K., Patterson, K.P., Hecht, J.H., Kane, M.A., Folias, A.E., Choe, Y., May, S.R., Kume, T.*, et al.* (2009). Retinoic acid from the meninges regulates cortical neuron generation. Cell *139*, 597-609.

Smart, I.H. (1973). Proliferative characteristics of the ependymal layer during the early development of the mouse neocortex: a pilot study based on recording the number, location and plane of cleavage of mitotic figures. J Anat *116*, 67-91.

Smart, I.H., Dehay, C., Giroud, P., Berland, M., and Kennedy, H. (2002). Unique morphological features of the proliferative zones and postmitotic compartments of the neural epithelium giving rise to striate and extrastriate cortex in the monkey. Cereb Cortex *12*, 37-53.

Smart, I.H., and McSherry, G.M. (1986a). Gyrus formation in the cerebral cortex in the ferret. I. Description of the external changes. J Anat *146*, 141-152.

Smart, I.H., and McSherry, G.M. (1986b). Gyrus formation in the cerebral cortex of the ferret. II. Description of the internal histological changes. J Anat *147*, 27-43.

Stancik, E.K., Navarro-Quiroga, I., Sellke, R., and Haydar, T.F. (2010). Heterogeneity in ventricular zone neural precursors contributes to neuronal fate diversity in the postnatal neocortex. J Neurosci *30*, 7028-7036.

Stocker, A.M., and Chenn, A. (2009). Focal reduction of alphaE-catenin causes premature

differentiation and reduction of beta-catenin signaling during cortical development. Dev Biol *328*, 66-77.

Subramanian, A., Tamayo, P., Mootha, V.K., Mukherjee, S., Ebert, B.L., Gillette, M.A., Paulovich, A., Pomeroy, S.L., Golub, T.R., Lander, E.S*., et al.* (2005). Gene set enrichment analysis: a knowledge-based approach for interpreting genome-wide expression profiles. Proc Natl Acad Sci U S A *102*, 15545-15550.

Tan, S.S., and Breen, S. (1993). Radial mosaicism and tangential cell dispersion both contribute to mouse neocortical development. Nature *362*, 638-640.

Torii, M., Hashimoto-Torii, K., Levitt, P., and Rakic, P. (2009). Integration of neuronal clones in the radial cortical columns by EphA and ephrin-A signalling. Nature *461*, 524-528.

Ulinski, P.S. (1974). Cytoarchitecture of cerebral cortex in snakes. J Comp Neurol *158*, 243-266.

Van Essen, D.C. (1997). A tension-based theory of morphogenesis and compact wiring in the central nervous system. Nature *385*, 313-318.

Voigt, T. (1989). Development of glial cells in the cerebral wall of ferrets: direct tracing of their transformation from radial glia into astrocytes. J Comp Neurol *289*, 74-88.

Wakamatsu, Y., Maynard, T.M., Jones, S.U., and Weston, J.A. (1999). NUMB localizes in the basal cortex of mitotic avian neuroepithelial cells and modulates neuronal differentiation by binding to NOTCH-1. Neuron *23*, 71-81.

Walsh, C., and Cepko, C.L. (1988). Clonally related cortical cells show several migration patterns. Science *241*, 1342-1345.

Wang, X., Tsai, J.W., Lamonica, B., and Kriegstein, A.R. (2011). A new subtype of progenitor cell in the mouse embryonic neocortex. Nat Neurosci *14*, 555-561.

Ware, M.L., Tavazoie, S.F., Reid, C.B., and Walsh, C.A. (1999). Coexistence of widespread clones and large radial clones in early embryonic ferret cortex. Cereb Cortex *9*, 636-645.

Weimer, J.M., Yokota, Y., Stanco, A., Stumpo, D.J., Blackshear, P.J., and Anton, E.S. (2009). MARCKS modulates radial progenitor placement, proliferation and organization in the developing cerebral cortex. Development *136*, 2965-2975.

Weissman, T., Noctor, S.C., Clinton, B.K., Honig, L.S., and Kriegstein, A.R. (2003). Neurogenic radial glial cells in reptile, rodent and human: from mitosis to migration. Cereb Cortex *13*, 550-559.

Wonders, C.P., and Anderson, S.A. (2006). The origin and specification of cortical interneurons. Nat Rev Neurosci *7*, 687-696.

Woodhead, G.J., Mutch, C.A., Olson, E.C., and Chenn, A. (2006). Cell-autonomous beta-catenin signaling regulates cortical precursor proliferation. J Neurosci *26*, 12620-12630.

Wynshaw-Boris, A. (2007). Lissencephaly and LIS1: insights into the molecular mechanisms of neuronal migration and development. Clin Genet *72*, 296-304.

Xie, Z., Ma, X., Ji, W., Zhou, G., Lu, Y., Xiang, Z., Wang, Y.X., Zhang, L., Hu, Y., Ding, Y.Q., *et al.* (2010). Zbtb20 is essential for the specification of CA1 field identity in the developing hippocampus. Proc Natl Acad Sci U S A *107*, 6510-6515.

Yoon, K.J., Koo, B.K., Im, S.K., Jeong, H.W., Ghim, J., Kwon, M.C., Moon, J.S., Miyata, T., and Kong, Y.Y. (2008). Mind bomb 1-expressing intermediate progenitors generate notch signaling to maintain radial glial cells. Neuron *58*, 519-531.

Yu, X., and Zecevic, N. (2011). Dorsal radial glial cells have the potential to generate cortical interneurons in human but not in mouse brain. J Neurosci *31*, 2413-2420.

Zecevic, N., Chen, Y., and Filipovic, R. (2005). Contributions of cortical subventricular zone to the development of the human cerebral cortex. J Comp Neurol *491*, 109-122.

Zecevic, N., Hu, F., and Jakovcevski, I. (2011). Interneurons in the developing human neocortex. Dev Neurobiol *71*, 18-33.

Zhang, B., and Horvath, S. (2005). A general framework for weighted gene co-expression network analysis. Stat Appl Genet Mol Biol *4*, Article17.

Zhang, J., Woodhead, G.J., Swaminathan, S.K., Noles, S.R., McQuinn, E.R., Pisarek, A.J., Stocker, A.M., Mutch, C.A., Funatsu, N., and Chenn, A. (2010). Cortical neural precursors inhibit their own differentiation via N-cadherin maintenance of beta-catenin signaling. Dev Cell *18*, 472-479.

Zhong, W., Feder, J.N., Jiang, M.M., Jan, L.Y., and Jan, Y.N. (1996). Asymmetric localization of a mammalian numb homolog during mouse cortical neurogenesis. Neuron *17*, 43-53.
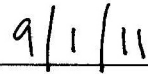
Publishing Agreement

It is the policy of the University to encourage the distribution of all theses, dissertations, and manuscripts. Copies of all UCSF theses, dissertations, and manuscripts will be routed to the library via the Graduate Division. The library will make all theses, dissertations, and manuscripts accessible to the public and will preserve these to the best of their abilities, in perpetuity.

Please sign the following statement:
I hereby grant permission to the Graduate Division of the University of California, San Francisco to release copies of my thesis, dissertation, or manuscript to the Campus Library to provide access and preservation, in whole or in part, in perpetuity.

_____   _____
Author Signature   Date

141